DIGITAL SIGNAL PROCESSING FOR RADAR RECOGNITION IN DENSE RADAR ENVIRONMENTS

by

Hemant Kumar Mardia

Submitted in accordance with the
requirements for the degree of Doctor of Philosophy

THE UNIVERSITY OF LEEDS
Department of Electrical and Electronic Engineering

November 1987

ABSTRACT

Radars are widely used in modern defence for surveillance and tracking. New signal processing techniques and architectures are required to enable the recognition of radars in high pulse density environments. Electronic Surveillance Measures (ESM) receivers are presented for automatic, real time identification of radars by measurement and digital processing.

The statistics of measurement errors and pulse measurement blocking rates as functions of pulse density, radar type and receiver measurement time are examined. The relative value of each of the measurable radar characteristics for sorting is examined and the processing requirements determined.

Architectures for high speed, real time processing of the measured data are presented. The processor is divided into the pulse grouping process and the pulse sequence deinterleaver. An efficient algorithm for n - dimensional grouping is given which uses metric techniques optimised for ESM, combined with conventional " pigeon-hole " sorting for high speed data manipulation. Processing is greatly reduced by adaptive feedback. The algorithm is applicable to stable or agile radars.

New algorithms for Time of Arrival (TOA) based recognition and extraction of repetitive pulse sequences are presented. Fast extraction of signals is achieved with low

false alarm rates by combining histogramming with interval extrapolation. Fuzzy logic is used to enhance detection of sequences in high pulse densities and a weighting function suppresses false alarms. The algorithm incorporates a learning process, giving increased efficiency as a function of time. The algorithm is applied to stable and agile repetition rate radars.

Simulation software is described, which allows testing of receiver systems with realistic, complex radar environments.

The design of two receivers is described. The complete design of a Radar Warning Receiver, using look-up table hardware for high speed operation, is presented with experimental results. An ESM receiver integrating the grouping and TOA pulse sequencer processes with adaptive feedback is designed and shown to be feasible in a small amount of hardware using parallel processing and VLSI circuits.

Results of simulations of the receiver designs demonstrate their expected performance.

ACKNOWLEDGEMENTS

I would like to thank Professor Rhodes and Dr. Lopes, whose support and guidance has been greatly appreciated.

I would like to thank Filtronic Components and the Electrical Engineering department of the University of Leeds for the opportunity to carry out this research.

I would also like to thank colleagues at Filtronic Components for their helpful advice.

CONTENTS

LIST OF TABLES AND ILLUSTRATIONS

LIST OF ABBREVIATIONS

AC	- Alternating Current
CPU	- Central Processing Unit
CW	- Continuous Wave
DAFM	- Digital Amplitude and Frequency Measurement
DC	- Direct Current
DIFM	- Digital IFM
DLVA	- Detector Log Video Amplifier
DOA	- Direction Of Arrival
DSP	- Digital Signal Processing
ECM	- Electronic Countermeasures
ESM	- Electronic Support Measures
EW	- Electronic Warfare
FAR	- False Alarm Rate
IC	- Integrated Circuit
IFM	- Instantaneous Frequency Measurement
MER	- Measurement Error Rate
MIP	- Millions of Instructions Per second
POI	- Probability Of Intercept
PPS	- Pulses per second
PRI	- Pulse Repetition Interval
PRF	- Pulse Repetition Rate
PW	- Pulse Width
RAM	- Random Access Memory
RF	- Radio Frequency
ROM	- Read Only Memory
RWR	- Radar Warning Receiver
RX	- Receiver

SI - Sampling Interval

SNR - Signal to Noise Ratio

TOA - Time Of Arrival

1.0 INTRODUCTION

Radar systems are used heavily in modern defence to provide surveillance and weapons guidance. Consequently the ability to detect and identify radars has become important, to allow protective measures to be taken.

A radar system transmits radio signals and by analysis of received reflections determines range and direction information. Simple radar signals are characterised by their carrier frequency, signal power, pulse width and pulse repetition rate (fig.1.1). The relative direction of arrival (DOA) can also be measured. The ESM receiver measures the signals received via antennas, processes the data and identifies the radars, allowing ECM to be employed to jam the radars.

Radar techniques have evolved to reduce the effectiveness of ESM and ECM. Modern radar systems can rapidly change one or more of their characteristics and are denoted "agile" e.g. frequency hopping, jittered PRI or staggered PRI. Doppler radars transmit continuous or high duty cycle signals. These have to be separated from the pulsed signals and are processed separately.

Radar systems are operated over a wide range of microwave frequencies and power levels. Projected radar environments are combinations of several radar types with total pulse densities in the order of millions per second [1]. The ESM reciver is required to

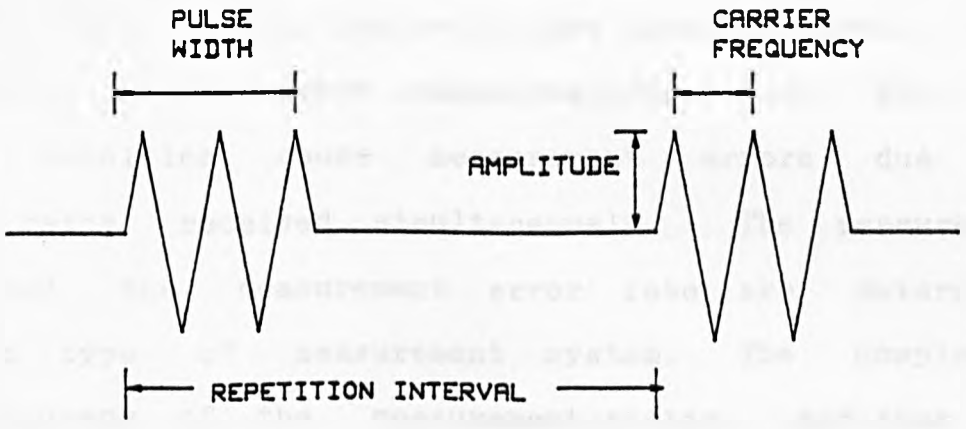

FIG. 1.1 RADAR CHARACTERISTICS

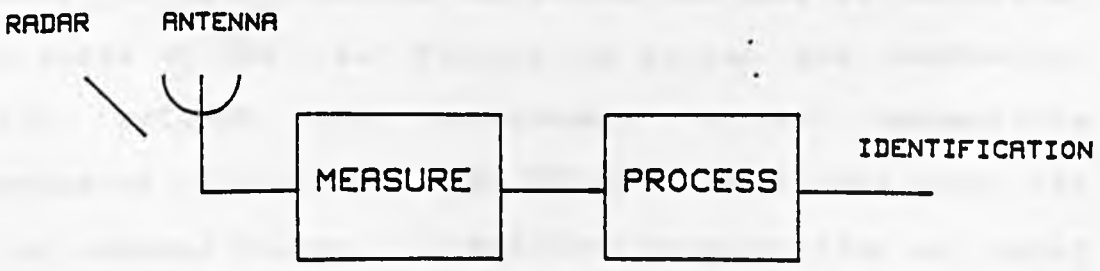

FIG. 1.2 ESM RECEIVER

separate multiple, concurrent radar signals quickly, with high POI. The false alarm rate must be low.

The ESM receiver can be divided into two parts - the measurement and processor subsystems (fig. 1.2). The high pulse densities cause measurement errors due to pulses being received simultaneously. The measurement rate and the measurement error rate are determined by the type of measurement system. The complexity and accuracy of the measurement system, and thus the processing requirement, is traded off against size and cost restraints.

The processor must recognise and separate each of the radar pulse sequences from the background of pulses, by analysis of the measurements. This would be trivial if one of the radar characteristics was unique to each radar. However, measurement errors and radar agility will cause a spread in the measurements of each radar and thus the pulse parameters of several radars to overlap. Thus grouping of pulses with similar parameter sets is required. Where the parameter set is not unique the pulses can only be separated on the basis of TOA i.e. fitting the pulses into sequences.

PRI agility and measurement errors necessitate sophisticated algorithms. The PRI must be derived from the TOAs of several pulses. In addition to separation of radar signals, the PRI provides important information about the radar, allows prediction of subsequent pulses and further analysis determines radar scan pattern for classification.

Two types of receiver exist - RWR and ESM. The RWR is required only to provide warning of specified threat radars which are normally in the form of a programmable emitter library. Consequently the sorting task is simplified, as signals not matching predefined library characterisitcs can be discarded. RWR can be used on small vehicles and aircraft where detailed ESM information is not required, but where detection of threat radars would be invaluable.

The ESM receiver analyses and attempts to identify every radar in the environment. These will include new radar signals. Detailed and accurate information is required to prime ECM systems and for library information. Thus the processing task is much greater than for the RWR, but the ESM receiver is of greater value when the radars are unknown or their characteristics are deliberately changed.

RWR/ESM receivers, especially for size constrained applications e.g. airborne, have employed crude sorting algorithms due to the limited measurement and processing abilities, and can only operate effectively in low pulse density environments. ESM receivers for naval applications use high resolution measurement and mini or mainframe computers to provide the necessary processing power [1]. Efficient software coupled with state of the art hardware can provide a substantially better solution.

The types of pulse measurement receivers are discussed in chapter 2. The measurement of each pulse parameter by

various techniques is discussed to determine the rate and quality of data to be processed. Statistics are presented which give an estimate of the probability of making a valid measurement of each parameter in high pulse densities, and the probability of corruption. This allows the relative value of each parameter for sorting to be calculated, and the processor to be designed accordingly.

The processor is discussed in chapter 3. Processing architectures and algorithms are proposed for real time sorting of the radar pulses. The sorting process is shown to be amenable to parallel processing, to gain greater processing power. Pulse grouping is applied first and adaptive pattern recognition algorithms are presented which provide efficient grouping. Following grouping is extraction of the sequences of pulses in time. The TOA deinterleaving task is very intensive and there is scope for higher efficiency. Thus fast, accurate algorithms capable of dealing with corrupted data are proposed, and again a learning process incorporated.

The processing architecture and sorting algorithms can be used as the basis of an advanced ESM receiver. In order to evaluate these algorithms, particularly in an adaptive receiver, simulation is necessary. The simulation software developed for this purpose is described in chapter 4. This allows the generation of a complex radar environment, and the testing of a receiver system with this environment.

Two receivers are presented in chapter 5. The first is a

simple RWR with fast hardware, which has been designed and built. An improvement on this RWR, incorporating a TOA sorting algorithm, is presented and evaluated using the simulation software. Finally, an ESM processor design is presented using ideas from chapter 3, combining grouping and TOA deinterleaving, with a front end measurement system described in chapter 2. This is simulated and the performance shown.

The conclusion of the thesis and suggestions for further work are given in chapter 6.

2.0 ESM MEASUREMENT

2.1 The measurement system

The measurement system detects and measures the parameters of incident radar emissions and passes the data to the processor for analysis. The type of measurement system determines the accuracy and rate of measurement and both are important factors in the sorting process.

The alternative architectures of measurement system can be classified as :

a) Wide open measurement

b) Scanning measurement

c) Channelised measurement

d) Hybrid

a) Wide open measurement gives fast response to any pulse within a large range. This type of measurement is preferred as it gives 100 percent POI to a pulse within the measurement range which is especially important as shorter pulses and transmission times are used for radar [2]. In practice the measurement unit has a "dead time " during which no new measurement can be made. If another pulse is received during this time an erroneous measurement can be made. The higher the pulse density, the higher the probability of an overlap and thus an error. For instantaneous measurement the unit is required to cover a large range of the measured parameter, which requires a compromise in accuracy.

b) Scanning measurement concentrates measurement on

one portion of the required range at a time. This allows high accuracy measurement and reduces the pulse density to the processor, thus reducing the processing task in high density environments. However, the POI is reduced as a function of the scan rate, with the risk of missing short burst emissions completely.

c) Channelised measurement has the advantages of both the two approaches above with a penalty in cost and size of hardware. The measurement range is divided into several parallel channels. An output is available from each of these channels simultaneously and instantaneously. This reduces the processing task by separating the pulses by this parameter and has higher integrity than a wide open system in a high pulse density environment where simultaneous pulses can occur. To obtain maximum advantage of this approach parallel processing is required, to operate on each of the individual channels with interaction between the processors to cope with radars whose parameters cross the channel boundaries.

d) A measurement system combining two of the above systems can provide better performance than any of the systems in isolation [3]. A wide open or channelised measurement unit combined with a scanning measurement provides instantaneous coverage with the ability to resolve selected difficult areas, determined by the processor. Thus where high pulse densities occur the scanning measurement can

be used to extract a small portion of the pulses with greater measurement accuracy for further analysis.

The use of hybrid architecture can increase the performance of the system without a significant increase in size and cost.

New technologies and devices will provide further options. SAW based channelisers and spectrum analysers, can be used to provide fine channelisation, in a small size. Acousto-optic spectrum analysers can provide fast, multiple signal frequency measurement, in a small size. Current limitations on both these technologies are the limited frequency coverage and dynamic range [4].

One or more CW radar will block the measurement system. CW radars use lower transmit powers than pulsed radars and these low level CW radars can be removed by AC coupled detection systems. High level CW radars must be filtered (tunable bandstop filters). POI is not a problem for CW radars and thus a narrowband superhet or similar device can be used, to give detection and high resolution frequency measurement. Thus sorting the radars is not a problem, with frequency and DOA giving unique identification.

The pulse parameters that can be measured are carrier frequency, pulse width (PW), Direction of Arrival (DOA), Time of Arrival (TOA) and signal power. Further pulse information such as carrier modulation and pulse shape can be measured to assist classification.

The ranges and accuracies of these measurements affect the complexity and type of sorting technique and are examined below.

2.1.1 Carrier frequency

The carrier frequency is a vital parameter in radar identification, as radar frequencies are known through intelligence and prior ESM reports. With sufficient accuracy, frequency is also a powerful sorting parameter. The active radar bands cover 1 to 18 GHz, 24 to 40 GHz and 90GHz upwards. The most active band for radar threats i.e. airborne or missile, is 6-18 GHz, due to the physical size of equipment being smaller with increasing frequency, and the availability of solid state devices covering this band.

The accuracy of the radar frequency is typically in the order of kHz with adjacent radars potentially within a few MHz. The frequency dispositions of radars show a clustering of radars at similar frequencies i.e certain sections of this band are densely populated [5]. This distribution means that the number of radars that can be resolved does not increase linearly with measurement resolution.

Radar signals now employ frequency agility. The carrier frequency can be scanned between two frequencies from pulse to pulse or "hopped" to several frequency steps. Chirped pulses are also used, where the effective carrier frequency rises during the pulse. Frequency agility is typically over a range of 200MHz. Missile guidance radars tend to use CW

illuminators and therefore it is desirable to detect these radars. However high power CW radars will prevent detection of any other radars in a wide open system unless the CW is removed (by filtering or the use of AC coupled detectors).

A scanning frequency measurement i.e. superhet receiver, would be required to cover an octave band with an acceptable POI. The POI is a function of scan rate and the Pulse Width distribution of the radars.

Threat radars have short pulses for high range resolution - ranging from 100ns to several microseconds. Thus a scan rate in the order of microseconds will be required to prevent missing an excessive proportion of pulses. This may be achieved by a high speed synthesiser or varactor tuned VCO and selective filter (fig. 2.1), however the speed is limited by the detected IF power required and the time resolution to calculate the detected frequencies to sufficient accuracy.

$$\text{scan time} = \frac{\text{frequency range}}{(\text{frequency step})^2} \qquad (2.1)$$

e.g. to cover 12GHz bandwidth with 10 MHz resolution would require 120 us, and therefore the scan time is not acceptable. Greater speed can only be achieved by using several superhet receivers covering sub-bands and wider filter bandwidths.

A channelised receiver would comprise of a filter bank with a detector and video amplifier on each channel (fig. 2.2). The channels will overlap to provide continuous

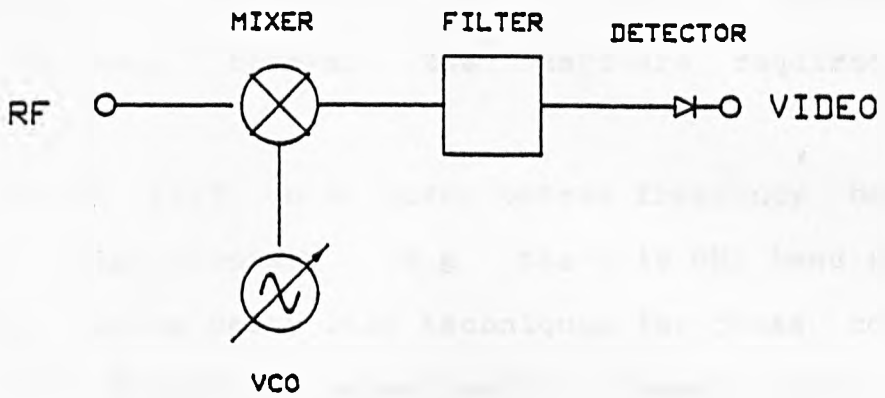

FIG. 2.1 SUPERHET RECEIVER

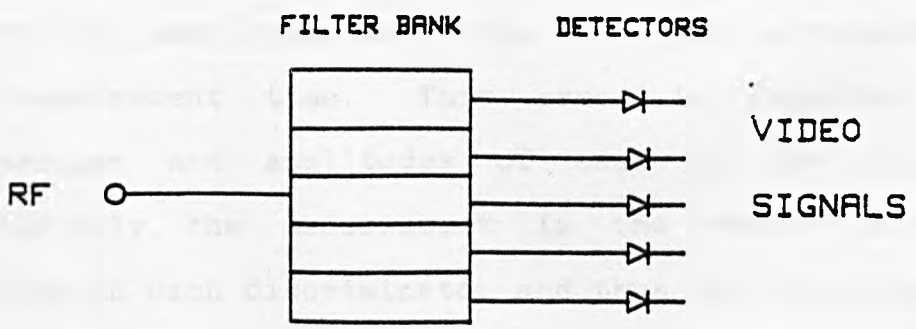

FIG. 2.2 CHANNELISED RECEIVER

coverage. This would provide coarse frequency measurement combined with good simultaneous signal performance. Frequency can be determined to a greater accuracy within each channel, however the hardware required can be prohibitive.

Compact DIFM units cover octave frequency bands with medium to high accuracy, (e.g. the 6-18 GHz band with 10MHz accuracy) using delay line techniques for phase comparison and thus frequency measurement. These units provide measurement across the whole band "instantaneously". This is currently the most cost effective solution and is therefore prevalent in ESM receivers.

The DIFM unit determines frequency by measuring phase differences across delay lines. The resolution of the IFM is limited by the length of delay lines used and the number of delay lines required to resolve ambiguity. Quantisation errors, signal strength and temperature variations determine the accuracy.

The greatest limitation of the DIFM is the measurement errors that occur when more than one pulse is received during the measurement time. This error is dependent on the frequencies and amplitudes of each of the pulses [6]. Specifically, the measurement is the vector sum of the carriers in each discriminator and thus the magnitude of the error is reduced for greater signal strength difference and close carrier frequencies. IFM units can measure correctly with simultaneous signal levels greater than 10

dB lower than the desired signal.

Processing required to operate with a DIFM unit has been examined, with methods of reducing the effect of the poor simultaneous signal performance. The simultaneous signal problem can be alleviated by dividing the frequency band into several sub bands each with an IFM (channelised). The processing techniques are still applicable to these configurations.

The measurement is normally made from the leading edge of the pulse, however by repeatedly sampling, complex frequency modulated signals can also be measured. This allows within pulse modulation to be measured [7]. This also gives greater POI to partially overlapped pulses. Measurement errors due to overlapping pulses can be minimised, by only measuring when the IFM detected voltages are stable.

2.1.2 Direction of Arrival

Measurement of the relative bearing of an emitter is required for two purposes. Firstly, for countermeasures to be taken against emitters and secondly, for pulse sorting. Greater reliance has to be placed on this parameter for sorting, as the other parameters become more agile. The directional information can only be changed by physical movement and therefore a high resolution is desirable. However DOA alone is not sufficient because radars tend to be clustered into the same physical sites rather than evenly spread over 360 degrees azimuth.

There are two main methods of determining the direction

of arrival of a pulse - phase comparison and amplitude comparison between antennae. The performance is compromised by the need for broadband frequency coverage, 360 degree azimuth direction coverage, and installation limitations. Phase comparison approaches are inherently frequency dependent therefore frequency compensation is required. Special broadband multielement antenna structures have been developed using interferometry for DOA i.e. the different time of arrival and thus phase at different elements. These devices can deliver accuracies in the order of 1 or 2 degrees r.m.s. [5].

Amplitude comparison exploits the gain characteristics of several antennas to calculate DOA. This is achieved by comparison of the signal power received from the antennae which are normally equispaced around 360 degrees. This can be achieved using broadband spiral antennae with detector log video amplifiers [8]. This approach has been investigated. The antennae are common to the complete measurement system thereby minimising hardware, and this is the basis of the low cost receiver.

The limitation on the accuracy of the DOA measurement is the signal gain tracking between the antennas, particularly gain ripples due to non-ideal mounting. The absolute gain and beamwidth vary from antenna to antenna. The gain and beamwidth also vary with frequency. Comparis on causes gain variations with frequency to be cancelled.

The four antennas are equispaced about 360 degrees i.e each antenna is orientated at 90 degrees from the adjacent antennas (fig. 2.3). The peak pulse amplitude is measured at each antenna using DLVAs followed by Analog to Digital converters (ADC). Assuming that a single pulse is received, a high power level will be measured in one antenna and smaller power levels will be measured in one or both of the adjacent antennas. By subtracting the power levels in decibels, an unambiguous power difference is given for any DOA. The spiral antenna pattern can be approximated by a Guassian function of direction, thus the difference of the logged amplitudes gives an approximately linear slope versus angle (fig. 2.4).

The accuracy of the amplitude measurement can be low due to variations with frequency, however providing the DLVAs outputs track closely with frequency and temperature, the relative accuracy can be much greater.

The accuracy of the DOA is also determined by the signal power level and the sensitivity of the DLVA. When the signal is at the boresight of one antenna the received power in the adjacent antenna can be 30 dB lower, where the power may not be detected. Thus maximum accuracy can only be attained where the signal is not attenuated below the sensitivity of the DLVA units. Therefore the dynamic range of the unit is reduced by the maximum attenuation required for the desired accuracy.

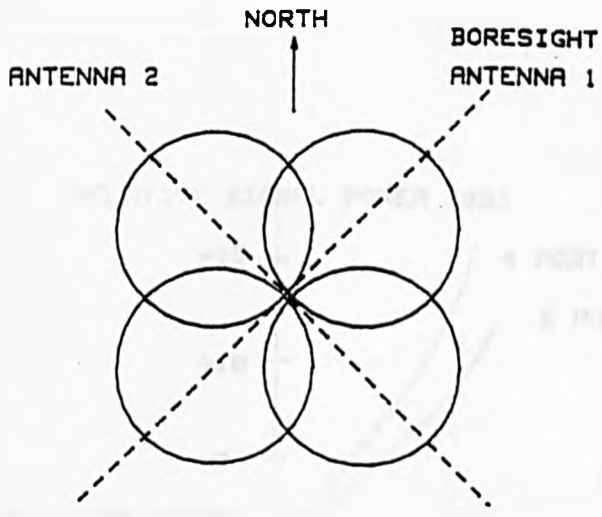

FIG. 2.3 SIGNAL STRENGTH PATTERNS

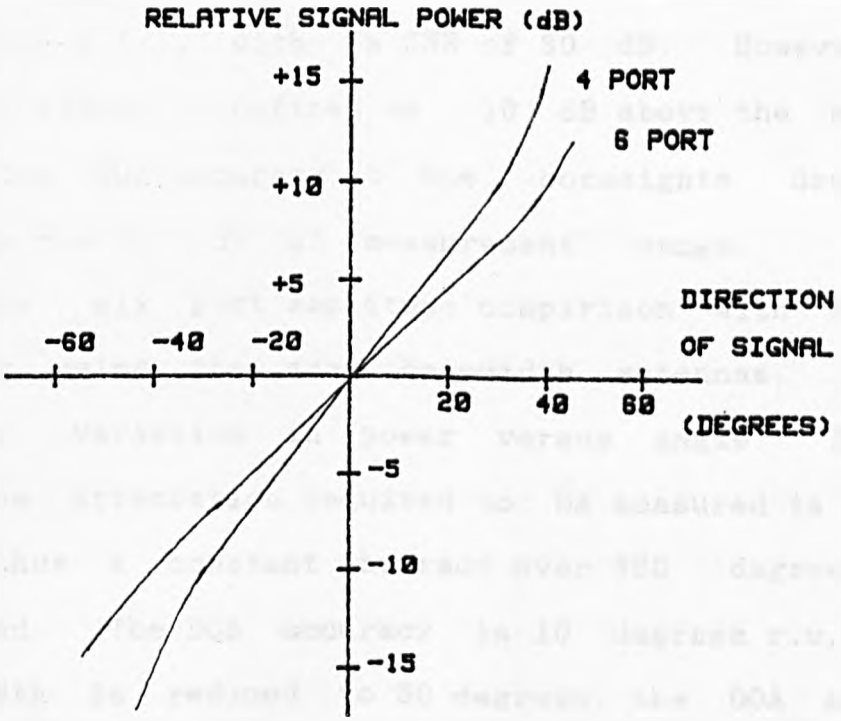

FIG. 2.4 POWER VS. DOA

A resolution of .5 dB is a typical performance figure for the amplitude measurement. This gives an accuracy of 8 degrees r.m.s. for the four port system (as calculated in appendix A.1), with a SNR of 30 dB. However, if the minimum signal is defined as 10 dB above the sensitivity, then the DOA accuracy at the boresights drops to 30 degrees due to lack of measurement range.

The six port amplitude comparison with 60 degree spacing using the same beamwidth antennas, produces a smaller variation in power versus angle. The highest relative attenuation required to be measured is 8 dB (fig. 2.4), thus a constant accuracy over 360 degrees can be achieved. The DOA accuracy is 10 degrees r.m.s. If the beamwidth is reduced to 50 degrees, the DOA accuracy is improved to 5 degrees r.m.s for 30 dB SNR (appendix A.1).

The availability of a site on an aircraft with a field of view of 360 degrees is very limited i.e the use of a single omnidirectional antenna for such a system is not normally an option. Therefore the frequency measurement system requires to share the antennas used for DOA, for frequency measurement from any direction.

A narrow beamwidth antenna can be scanned across the required range, thus determining DOA by the position of the antenna. The resolution is determined by the beamwidth of the antenna which can be a few degrees. However the disadvantages of missed pulses due to slow physical movement reduce the effectiveness of this

approach.

A similar system can be achieved electronically. Several antennas are orientated about 360 degrees and a multiway switch used to connect each antenna in turn, to a single measurement unit. The scan rate can be much higher than the mechanical equivalent.

The performance of the system is a compromise between a fast scan rate to maximise the POI to fleeting emissions [9], yet slow enough to allow measurement.

The measurement is again made from the leading edge of an incident pulse. Amplitude comparison systems are very susceptible to errors due to simultaneous pulses. Phase comparison systems are less susceptible . Again erroneous measurements can be reduced by only measuring when the detected voltages have stabilised.

2.1.3 Pulse Width

The pulse width of radar transmissions can be 100 ns to 100 us. The PW of the signal can be measured to a high resolution, however errors in this parameter can be large. Errors are caused by multipath reflections either adding to or subtracting from the pulse causing a shorter or longer pulse to be received. Errors can also occur due to pulse overlaps i.e. more than one pulse being received at the same time.

This has a greater probability of occuring in denser environments. The number and size of the pulse

width errors is dependent on the type of signals present in the environment and is greater in the wide open system than in channelised or superhet systems. A small proportion of radars are PW agile.

This parameter is best measured between the 3dB detected power points and can be measured to very high resolution (better than 50ns), to give the best result on poor pulse shapes. The rising edge of radar pulses is well defined but the trailing edge less well defined due to the above reasons. Pulse width can be used as a coarse deinterleaving parameter and average PW is useful for identification of radar type.

2.1.4 Amplitude

The sensitivity of the receiver is determined by the range and power of the radars to be detected. The ESM receiver has a range advantage over the transmitting radar as the signal is received direct, not reflected.

Therefore the sensitivity of the receiver can be made such that it can detect signals that are on the threshold of the radar's detection. The choice of sensitivity determines the received pulse density i.e a low sensitivity receiver only receives high power radar signals or close radars. The required sensitivity can be achieved by preceding the measurement unit by a broadband amplifier.

The radar range equation gives received power (P_R) at the radar as [10]:

$$P_R = \frac{P_T G_T^2 W^2 \sigma}{(4\pi)^3 R^4} \qquad (2.2)$$

where σ = radar cross section of target

and W = wavelength , R = range , P = power , G = gain

The received power (P_E) at the ESM receiver (the target) is [10]:

$$P_E = \frac{P_T G_T G_E W^2}{(4\pi)^2 R^2} \qquad (2.3)$$

The measured signal strength of each pulse can vary due to movement, multipath, pulse overlaps and scan patterns of scanning radar and therefore the absolute accuracy is poor and not useful for deinterleaving. As has been discussed, the relative signal strengths received by several antenna can be used to derive DOA. The absolute value is useful to the pilot/operator for an estimate of the range of a radar. The transmitted power of the radar is normally unknown thus the actual range can not be calculated. The time difference between amplitude peaks of pulses from a detected radar is useful for determining scan pattern.

The dynamic range of the system is required to be as large as possible. A range of 40 dB is a typical requirement [1]. Larger ranges are achieved with the use of limiting amplifiers which compress the large input power range to a small output power range. Limiting also produces a capture effect, causing the smaller of the simultaneous signals to be suppressed by

up to 6dB.

2.15 Pulse Repetition Interval

The PRI of a radar is normally very stable (better than 1 part in 1000 [11]). Long range radars have large PRI and pulse widths while short range radars have small PRI and pulse widths. The range of PRFs is from several hundred hertz to 30 kHz. PRI agile radars are increasingly used. The forms of agility are jittered PRI, multistage staggered PRI (fig. 2.5) and formatted frames. High duty cycle pulse doppler radars are also employed with PRFs of several hundred kilohertz, and unless filtered, these signals can cause severe problems in the ESM receiver.

The regularity of the PRI means that it can be a powerful pulse deinterleaving parameter. The individual pulse measurements can be sequenced and pulse to pulse variations examined to give more information e.g. amplitude variations show the scan type of the radar. The PRI is also needed for radar classification and prediction of subsequent pulses.

The PRI is unlike the previous parameters in that it is not available instantaneously with each pulse. The PRI is derived from the TOA differences between pulses. This can be achieved by analogue filtering however the large PRI range, high accuracy and agility can be better dealt with by digital signal processing.

Measurement accuracy of TOA can be to 100ns, however

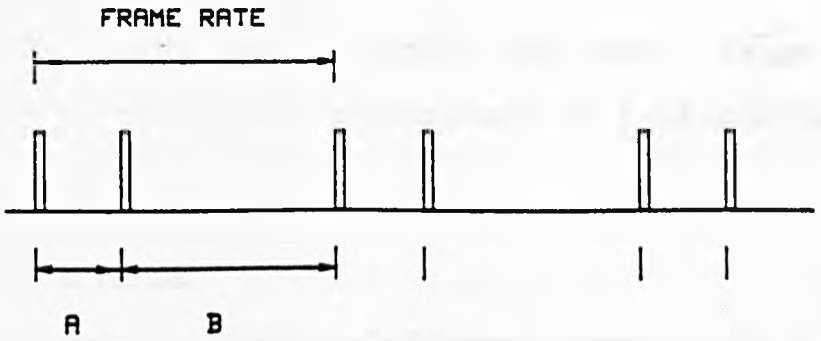

FIG. 2.5 STAGGERED PRI SIGNAL

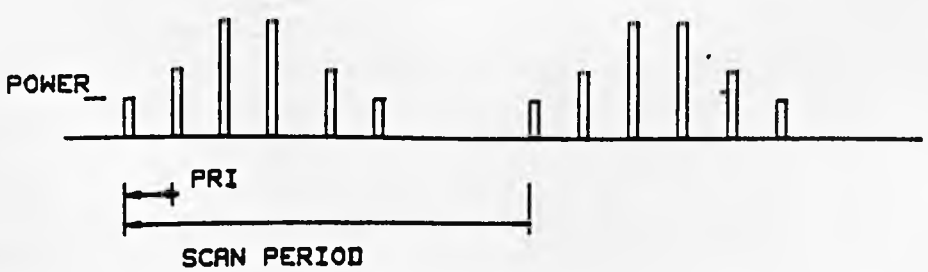

FIG 2.6 SCANNING RADAR SIGNAL

simultaneous pulses and multipath may cause large errors. For the typical PRI ranges measurement to 1 us resolution is sufficient.

2.1.6 Scan type

Search radars employ different scan patterns e.g. circular, sector, conical etc. The time for one scan can be one second to thirty seconds. The scan type and scan time of the radar can be derived by examination of the pulse amplitude variations (fig. 2.6) and is useful for ESM classification.

2.1.7 ESM measurement front-ends

Different configurations of receivers can be chosen towards a specification given the same set of constraints. A quantitative measure of the performance of a receiver from the deinterleaving aspect has been formulated.

The 'resolving power' of a measurement can be expressed by :-

$$\text{Resolving power} = \frac{\text{Measurement range}}{\text{Measurement variation}} \qquad (2.4)$$

where the measurement variation is equal to the sum of the variation of the radar parameter and the short term measurement error.

Long term error effects such as temperature variation though reducing the measurement accuracy, do not degrade the resolving power, and thus high resolution is desirable even where the accuracy is lower.

The sorting power is also dependent on the probability of correctly measuring the pulse characteristic in high pulse densities. This is determined by the measurement time and simultaneous signal performance for each measurement. The usefulness of each parameter when it is used for sorting is therefore dependent on the likelihood of corruption of that parameter.

Let R_f, R_d, R_i, R_p, be the resolving powers of the frequency, DOA, PRI and PW measurements respectively. The resolving power of the receiver is the total number of unique combinations of these parameters it can separate

pulses into i.e. the product of these values. Then the receiver sorting power can be expressed as the multiple of the resolving power of each parameter and the probability of measuring the pulse parameter :

$$\text{Receiver sorting power} = (R_f.p_f)(R_d.p_d)(R_i.p_i)(R_p.p_p) \quad (2.5)$$

The radar environment determines the type of ESM system required. The expected requirement for an ESM system [1] will be :-

Frequency range : 2 to 18 GHz
Pulse density : 1,000,000 pulses/s
Pulse widths : 100 ns to 100 us
PRI range : 10 us to 5 ms
Direction : 360 degrees coverage
Dynamic range : 60 dB

ESM measurement receivers to fulfil this requirement are also constrained by size and cost. High performance ESM front ends consist of broadband high resolution IFM and interferometer DOA measurement units (the frequency band is normally split into at least two bands of 2-6 and 6-18 GHz). A minicomputer is used to provide the processing power.

For typical radar parameter variations [11] and assuming an ideal receiver i.e. no measurement errors, then the best resolving powers that could be achieved realistically are :

$$R_f = \frac{12000}{2} = 6000 \qquad \text{(stable radars)}$$

$$= \frac{12000}{200} = 60 \qquad \text{(agile radars)}$$

$$R_d = \frac{360}{0.5} = 720$$

$$R_i = \frac{5000}{5} = 1000$$

$$R_p = \frac{100}{1} = 100$$

i.e

Ideal receiver sorting power = 6000x720x1000x100

$$= 4.3 \times 10^{11}$$

The RWR requirement is not as severe as the ESM requirement (though size and cost must be smaller). The required frequency range is 6 to 18 GHz and operating pulse density 100,000 pulses/s.

RWR measurement front ends consist of typically four spiral antennas connected to four DLVAs. This gives instantaneous DOA, PW, amplitude and TOA measurement. An alternative system switches between the four antenna to a single IFM and amplitude measurement unit. This gives frequency but not instantaneous DOA measurement.

The probability of measurement of each of the parameters is now discussed.

2.2 PULSE STATISTICS

The high pulse density environment must cause a significant measurement error rate and prevent pulse measurements (pulse blocking rate), especially in a wide open system. The quality of identification and the rate of false alarms are functions of these rates. The greater the measurement corruption, the more difficult reliable identification and thus the greater the loading on the processor.

The error rates are functions not only of the pulse density but also the Pulse width, PRI and amplitude distributions of the radars, the receiver measurement time and simultaneous signal capability.

Decision thresholds will be set within the processor to accept or reject postulated radar identifications. These would normally be preset, though the threshold must be lower for higher pulse densities to allow detection. It is shown that the decision thresholds can be adaptively matched to the environment by monitoring the average pulse rate and pulse width.

2.2.1 Leading edge measurement

A simple measurement system is assumed where measurements (frequency or DOA) are made from the leading edge and require the measurement time T_m of stable input for a valid measurement, and have a dead time T_d before the next measurement can be made.

A measurement error is assumed to occur only if two leading edges occur within the measurement time.

The PW is measured from leading edge to trailing edge crossing 3dB thresholds.

An estimate of the pulse blocking rate can be obtained by assuming that the background of pulses consists of a large number of radars combining to produce a random, Poisson distribution. The pulses are characterised by R pulses/s average density, average pulse width W_2, and with similar amplitude . If the time required for measurement by the receiver is T_m, then the probability that no part of any pulses occur in time T_m from the leading edge of the desired pulse is the probability p_m of a valid measurement. The desired pulse has an average pulse width of W_1. Figure 2.7 shows the condition of two pulses overlapping.

The Poisson distribution is such that the probability of k events occuring in unit time, given an average rate of R events per unit time is given by [12] :

$$p(k) = \frac{R^k}{k!} . \exp(-R) \qquad k = 0,1,2...n \qquad (2.6)$$

Thus the probability of no events in time T_m+W_2 (or T_m+T_d if the pulse width is less than the dead time) gives the probability of a valid measurement (of frequency or DOA) :

$$\begin{aligned} p_m &= \exp(-R(T_m+W_2)) && W_2 > T_d \\ &= \exp(-R(T_m+T_d)) && W_2 <= T_d \end{aligned} \qquad (2.7)$$

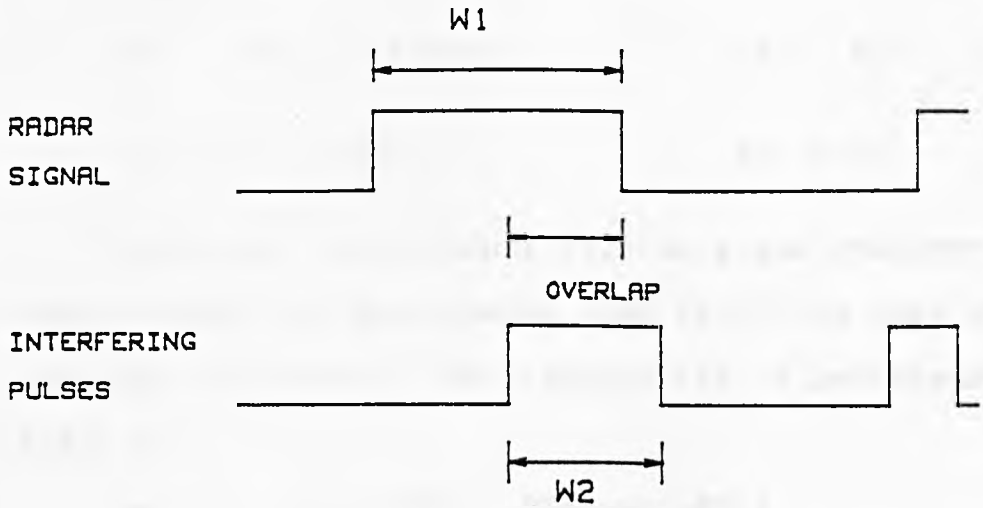

FIG. 2.7 RADAR PULSE OVERLAP

PW measurement differs from frequency and DOA measurement. For valid measurement of PW both edges of the desired pulse must not be overlapped.

$$pm = \exp(-R(W_1+W_2)) \qquad W_2 > W_1$$

$$pm = \exp(-2RW_2) \qquad W_2 <= W_1 \qquad (2.8)$$

Erroneous measurements will be given whenever two events occur within the measurement time Tm in the case of frequency and DOA measurement. The probability of measurement error is given by :

$$pe = 1 - \exp(-RTm) - RTm.\exp(-RTm) \qquad (2.9)$$

Erroneous PW measurements will be given when two events occur within the pulse width W2 (on average) :

$$pe = 1 - \exp(-RW_2) - RW_2.\exp(-RW_2) \qquad (2.10)$$

Figure 2.8 shows the probability of valid measurement of frequency and DOA versus pulse density for different receiver measurement times.

Figure 2.9 shows the probability of valid measurement of PW versus pulse density for different average background pulse widths.

Figure 2.10 shows the probability of measurement error of frequency and DOA versus pulse density for different measurement times.

The average pulse width W2 is taken as 1μs, and W1 as 1μs in the above figures and the receiver dead time assumed

FIG. 2.8 PROB. OF VALID FREQ. OR DOA MEASUREMENT

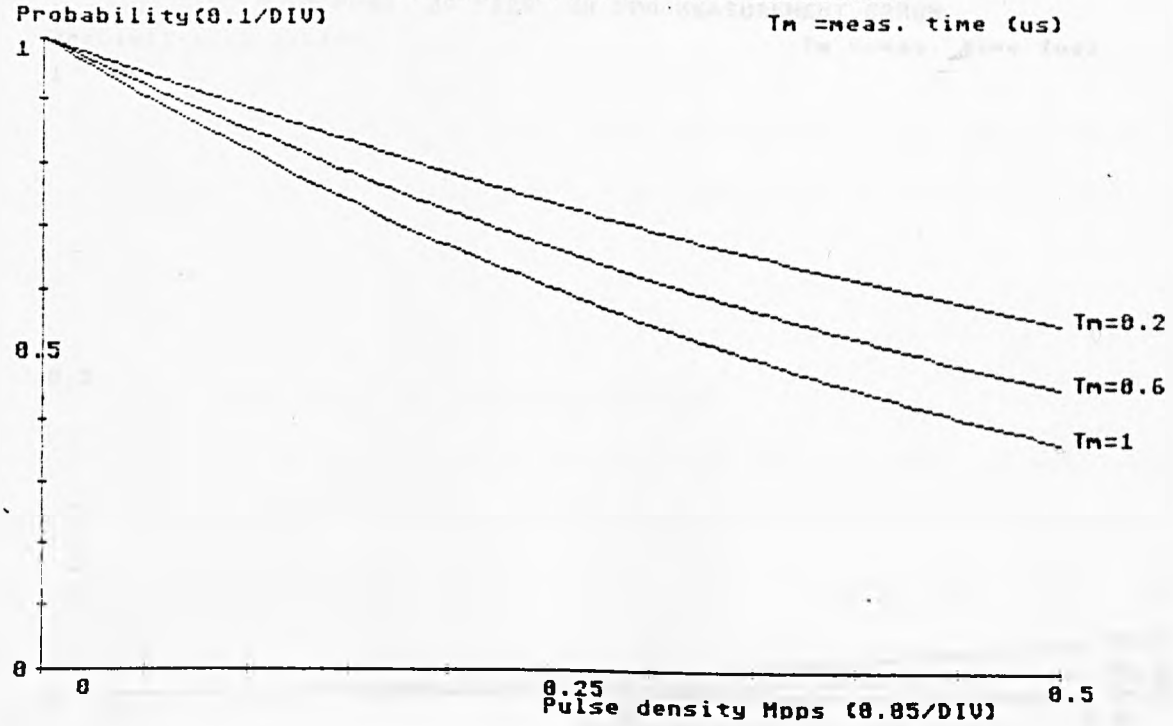

FIG. 2.9 PROB. OF VALID PW MEASUREMENT

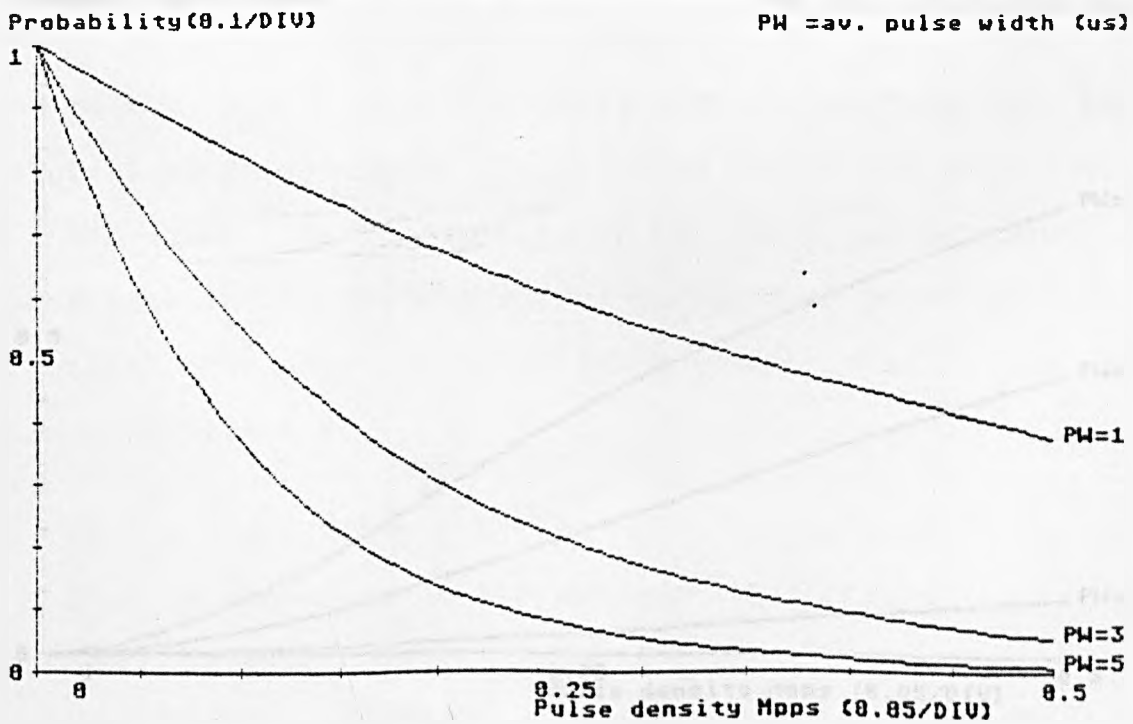

FIG. 2.10 PROB. OF FREQ. OR DOA MEASUREMENT ERROR

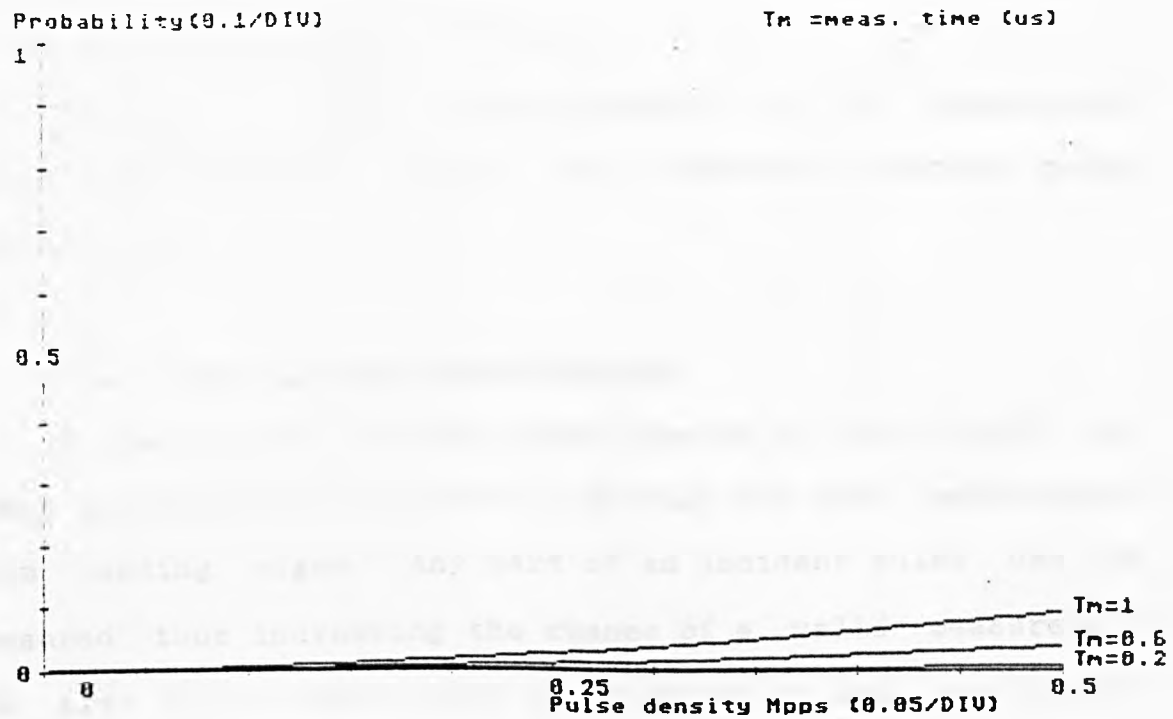

FIG. 2.11 PROB. OF PW MEASUREMENT ERROR

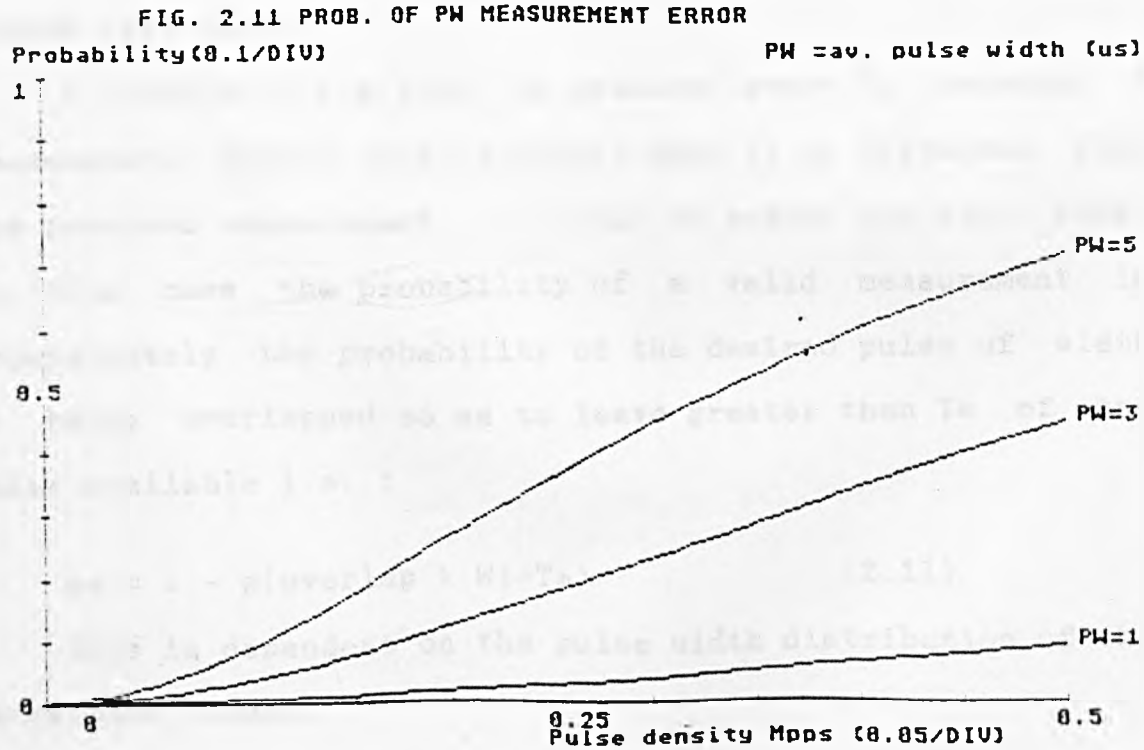

to be zero(in Fig. 2.9 W1 = 1,3,5 μs).

Figure 2.11 shows the probability of PW measurement error versus pulse density for different average pulse widths.

2.2.2 Sampled measurement system

A measurement system where samples of the input are taken continuously [7] gives a greater POI than measurement from leading edges. Any part of an incident pulse can be measured thus increasing the chance of a valid measurement and also allows measurement of pulses which are overlapped. This will give valid measurement if the relative signal strengths are sufficiently different. However as any overlap can cause a measurement error, the sampled system will produce a greater number of errors. Also TOA measurement errors will occur.

A sample of the input is measured every T_m seconds. A measurement should only be output when it is different from the previous measurement, in order to reduce the data rate. In this case the probability of a valid measurement is approximately the probability of the desired pulse of width W_1 being overlapped so as to leave greater than T_m of the pulse available i.e. :

$$p_m = 1 - p(\text{overlap} > W_1 - T_m) \qquad (2.11)$$

This is dependent on the pulse width distribution of the background pulses.

The radar is desired to be identified from a background of high pulse density. This can be assumed to be a large number of radars combining to give a random distribution.

The desired pulse train has an average pulse width of W_1 and an average PRI of T_1. The background pulses have an average pulse width W_2 and an average PRI of T_2.

The work of Stein and Johannsen [13] can be applied to give a description of the coincidences between the two pulse trains assuming the two are independent.

A statistical function $q(x)$ is defined where :

$q(x)dx$ = expected number of pulses per unit time whose length is in the range $(x, x+dx)$

The cumulative function $Q(x)$ is also defined where :

$$Q(x) = \int_x^\infty q(x)dx \qquad (2.12)$$

= expected number of pulses per unit time, whose length exceeds x.

It is shown that in general for n pulse trains the distribution of the overlaps is :

$$Q_o(\tau) = \prod_{i=1}^{n} \int_\tau^\infty Q_i(x)dx \cdot \sum_{i=1}^{n} \frac{Q_i(\tau)}{\int_\tau^\infty Q_i(x)dx} \qquad (2.13)$$

τ = pulse overlap duration

For two pulse trains described by $Q_1(x)$ and $Q_2(x)$ this gives ,

$$Q_o(\tau) = Q_1(\tau)\int_\tau^\infty Q_2(x)dx + Q_2(\tau)\int_\tau^\infty Q_1(x)dx \qquad (2.14)$$

The desired pulse train can be assumed to have a constant pulse width of W_1. The distribution of this train is then described by :

$$q_1(x) = \frac{1}{T_1} \qquad \text{when } x = W_1$$

$$= 0 \qquad \text{otherwise}$$

$$Q_1(x) = \int_x^{\infty} \frac{\delta(x-W_1)}{T_1} dx$$

$$= \frac{1}{T_1} \qquad \text{when } 0 < x < W_1 \qquad (2.15)$$

$$= 0 \qquad x > W_1$$

The pulse width distribution of the background pulse train will be over a range of pulse widths W_{lo} to W_{hi}. If the pulses are assumed to have been generated by radars with similar duty cycles (D) then the probability of short pulses is higher than long pulses i.e.

$$q_2(x) = \frac{D}{xT_2} \left(\int_0^{\infty} \frac{D}{x} dx \right)^{-1}$$

$$= \frac{1}{xT_2(\ln W_{hi} - \ln W_{lo})} \qquad W_{lo} < x < W_{hi}$$

$$= \frac{1}{xT_2 \ln(R)} \qquad \text{where } R = \frac{W_{hi}}{W_{lo}} \qquad (2.16)$$

$$Q_2(x) = \frac{1}{T_2} \qquad x < W_{lo}$$

$$= \frac{\ln(W_{hi}) - \ln(x)}{T_2 \ln(R)} \qquad W_{lo} < x < W_{hi} \qquad (2.17)$$

$$= 0 \qquad x > W_{hi}$$

also the average pulse width is

$$W_2 = \int_0^{\infty} x.p(x)dx = \int_0^{\infty} x.\frac{1}{x\ \ln(R)}.dx$$

$$= \frac{W_{hi} - W_{lo}}{\ln(R)} \qquad (2.18)$$

The integral of the cumulative functions are

$$\int_{\tau}^{\infty} Q_1(x)dx = \left[\frac{x}{T_1}\right]_{\tau}^{W_1}$$

$$= \frac{W_1 - \tau}{T_1} \qquad \tau < W_1 \qquad (2.19)$$

$$= 0 \qquad \tau > W_1$$

$$\int_{\tau}^{W_{lo}} Q_2(x)dx = \frac{W_{lo} - \tau}{T_2} \qquad \tau < W_{lo}$$

$$\int_{\tau}^{\infty} Q_2(x)dx = \frac{1}{T_2\ \ln(R)} \cdot \left[x\ \ln(W_{hi}) - x\ \ln(x) + x\right]_{\tau}^{W_{hi}}$$

$$W_{lo} < \tau < W_{hi}$$

$$= \frac{1}{T_2\ \ln(R)} \cdot \left[W_{hi} - \tau + \tau\ \ln\left(\frac{\tau}{W_{hi}}\right)\right] \qquad (2.20)$$

therefore substituting into equation 2.14, the overlap distribution is :

$$Q_o(\tau) = \frac{1}{T_1T_2\ln(R)}\left[(W_1-2\tau).\ln\left(\frac{W_{hi}}{\tau}\right) + W_{hi} - \tau\right] \qquad (2.21)$$

$$W_{lo} < \tau < W_1$$

thus the probability of an overlap greater than τ on the desired pulse train

$$p(ovlp > \tau) = T_1Q_o(\tau) \qquad (2.22)$$

and substituting the average pulse width in the background gives :

$$p(ovlp>\tau) = \frac{W_2}{T_2(W_{hi}-W_{lo})} \cdot \left[(W_1-2\tau).\ln\left(\frac{W_{hi}}{\tau}\right) + W_{hi} - \tau \right]$$

$$W_{lo} < \tau < W_1 \qquad (2.23)$$

This gives a probability of a valid measurement of frequency and DOA of :

$$p_m = 1 - p(ovlp > W_1-T_m)$$

$$= 1 - \frac{W_2}{T_2(W_{hi}-W_{lo})} \cdot \left[(2T_m-W_1).\ln\left(\frac{W_{hi}}{W_1-T_m}\right) + W_{hi} + T_m - W_1 \right]$$

$$W_1-T_m > W_{lo} \qquad (2.24)$$

Any overlap will cause an error in the PW measurement. Thus the probability of a valid PW measurement from 2.20 and 2.22 is :

$$p_m = 1 - p(ovlp > 0)$$

$$= 1 - \frac{W_1 + W_2}{T_2} \qquad (2.25)$$

The measurement error rate for a sampled measurement can be approximated by the probability of two random background trains interfering. This gives an overlap rate of :

$$Q_o(0) = \frac{W_2}{2T_2^2} \qquad (2.26)$$

when $\tau = 0$

and T_2 = the overall average pulse period

therefore the probability of measurement error is:

$$p_e = T_2Q_o(T_m) = \frac{W_2}{2T_2} \qquad (2.27)$$

The probability is given more accurately by equation 2.10, though equation 2.27 gives a simple estimate.

Figure 2.12 plots the probability of valid frequency and DOA measurements as a function of pulse density, for different measurement times.

Figure 2.13 plots the probability of valid PW measurement as a function of pulse density, for different pulse widths. The desired PW is 1us and the average background pulse width is 1us.

Figure 2.14 plots the probability of measurement error as a function of pulse density for different average pulse widths (it is independent of measurement time).

2.2.3 Amplitude

The effect of the amplitude of pulse trains on the measurement error rate is dependent on the measurement system. The amplitude of a given background pulse is assumed to be independent of the pulse width, though in reality it can be related and may vary according to scan pattern. The measurement error and blocking rates calculated above can now simply be multiplied by the probability that the desired pulse has sufficiently greater amplitude than the interfering pulse.

A random distribution of amplitudes within the dynamic range of the system is assumed giving the probability of a interfering pulse having amplitude α greater than A :

$$p(\alpha > A) = \frac{Ah - A}{Ah - Al} \qquad (2.28)$$

where A_h = high end of range, A_l = low end of range, A = threshold of measurement all in dB scale.

FIG. 2.12 PROB. OF VALID FREQ. OR DOA MEASUREMENT

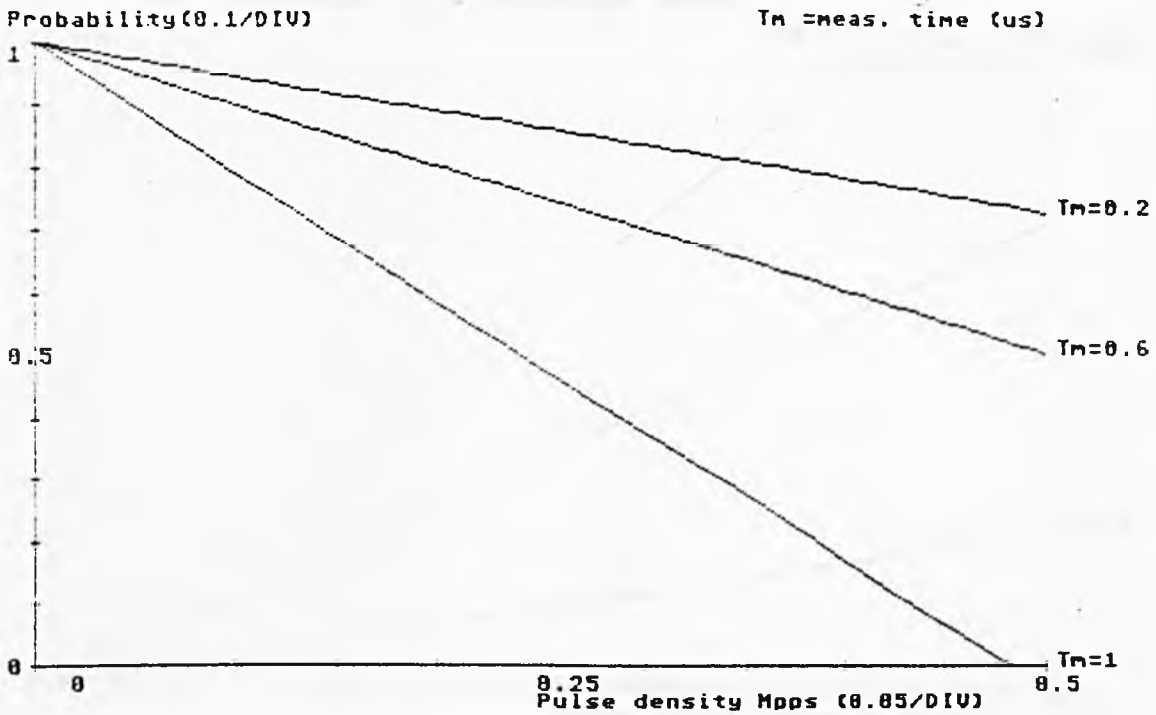

FIG. 2.13 PROB. OF VALID PW MEASUREMENT

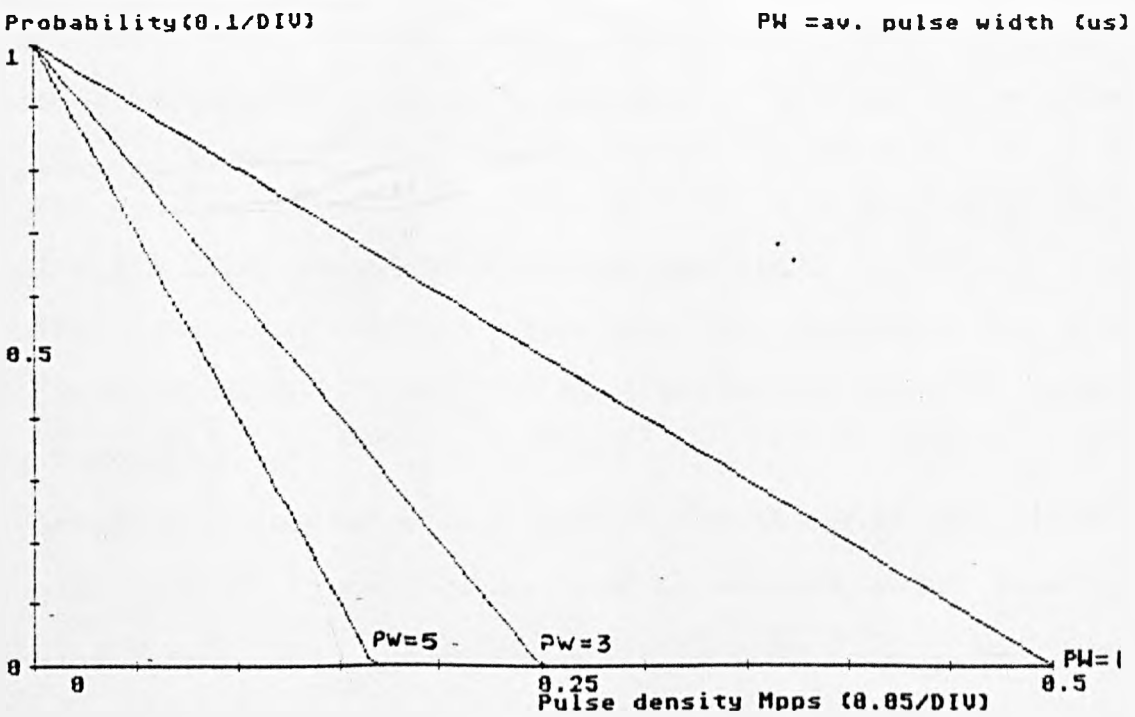

FIG. 2.14 PROB. OF A MEASUREMENT ERROR

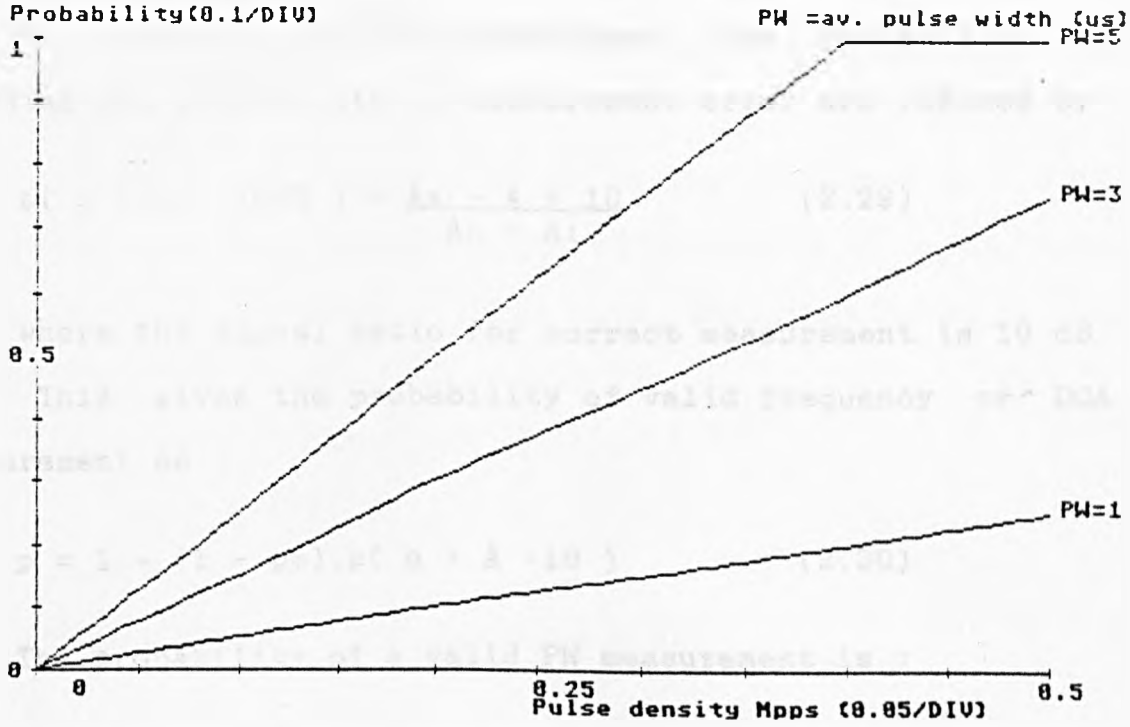

Thus if the desired pulse train has an average amplitude A, for frequency and DOA measurement the probability of blocking and probability of measurement error are reduced by

$$p(\alpha > A - 10dB) = \frac{Ah - A + 10}{Ah - Al} \qquad (2.29)$$

where the signal ratio for correct measurement is 10 dB

This gives the probability of valid frequency or DOA measurement as :

$$p = 1 - (1 - pm).p(\alpha > A - 10) \qquad (2.30)$$

The probability of a valid PW measurement is :

$$p = 1 - (1 - pm).p(\alpha > A - 3) \qquad (2.31)$$

Thus by monitoring the amplitude, PW and pulse density in the environment, thresholds can be determined to match the statistics of the environment rather than using one set of values regardless of conditions. Thus the probability of detecting corrupted signals is increased whilst minimising the false alarm rate.

2.2.4 Evaluation of measurement receivers

The above statistics can now be applied to the specific measurement systems to show the performance in high pulse densities.

Assuming a receiver is required for the 6GHz to 18GHz band with a 60 dB dynamic range, and an average pulse density of 500,000 pps. Let the measurement time be 200ns and the

average pulse width be 1us (assuming a low percentage of surveillance radars). Typical receiver configurations [23] are examined.

For a wide open system giving using an IFM, interferometer DOA and measuring PW between 3 dB points the probability of measuring a pulse with amplitude close to the sensitivity and pulse width (1us) is :

frequency and DOA (from equation 2.7):

p_m = exp(-1.2x0.5)

= 0.55

PW measurement (from equation 2.8):

p_m = exp(-2x0.5)

= 0.37

However unlike frequency or DOA the PW measurement degrades quickly with increasing pulse width e.g the probability of a valid measurement of a 10 us pulse drops to 0.004 . Thus PW is only useful for sorting short PW pulses.

The respective probabilities if the pulse had average amplitude rise to 0.70 for frequency and 0.65 for PW.

For an IFM with 5MHz resolution, an interferometer with 1 degree resolution this gives individual sorting powers for each parameter of :

freq. s.p = 2400x0.55 = 1320 (stable freq. radars)

= 60x0.55 = 33 (agile freq. radars)

DOA s.p = 360x0.55 = 198 (all radars)

PRI s.p = 1000x0.55 = 550 (stable PRI radars)

PW s.p = $\frac{1}{0.1}$ x0.37 = 4 (stable PW radars)

This gives a receiver sorting power of

Receiver s.p = 1320x198x550x4 = 6 x 10^8

Thus relative to the ideal receiver the relative sorting power is 0.1 %. A table of results is given in figure 2.15.

If the band was split into two with identical receivers in each band, such that the pulse density in each is half the total i.e. 250,000 pps then the probability of valid measurements becomes :

p_f = exp(-1.2x0.25) = 0.74

p_{pw}= 0.61

The relative sorting power becomes 1 %.

Thus for this conventional receiver, the DOA and PRI are the best parameters for sorting. Frequency is excellent for sorting non agile radars but poor otherwise and PW measurement is the least useful due to pulse overlap, and is very poor on medium to long pulse widths.

This can be compared with a superhet ESM receiver. A typical configuration is a bank of four superhets of 200 MHz bandwidth, used to downconvert the spectrum, combined with narrowband Frequency measurement and with a amplitude DOA comparision. To gain the advantage of filtering on DOA measurement the receivers must be duplicated on each antenna.

YIG based superhets will sweep at only 100MHz/ms which would give a very low POI. Fast VCOs can give rates of 1 MHz / ns. Each receiver is assumed to sweep 4 GHz, with a frequency resolution of 10 MHz, and DOA resolution of 5

degrees.

The sweep rate is less than the maximum realisable for a 200 MHz filter thus the sweep time is simply 4us. This gives a POI of 0.25 to pulses of average width (1us).

The pulse density, R, is assumed to reduce linearly with bandwidth i.e.

$$R\ (0.2GHz) = R(12GHz) \times \frac{0.2}{12}$$

$$= 500000 \times \frac{0.2}{12} = 8330 \text{ pps}$$

This gives the probability of valid measurement of frequency or DOA as 0.99. The PW measurement is not valid for a swept system. A frequency resolution of 10MHz and DOA of 5 degrees is assumed.

Thus relative to the ideal receiver the sorting power is only 3×10^{-4} percent (figure 2.15).

Now this can be compared with a possible channelised receiver configuration. In order to cover such a large bandwidth, the pulses are downconverted into three filter banks. A typical filter bank covers 2 to 6 GHz with 16, 250 MHz bandwidth channels, each followed by detectors. DOA can be determined by amplitude comparison on 4 or 6 antennas. Without additional frequency measurement this gives a frequency resolution of 250 MHz.

The receiver sorting power relative to ideal is 0.07 %. This has reliable PW measurement and better performance against frequency agile radars than the previous

Receiver Configuration	meas. prob. f.D.T	meas. prob. PW	freq s.p	DOA s.p	TOA s.p	PW s.p	Rec. s.p
IDEAL (agile) see pp33,34	1	1	6000 (60)	720	1000	100	4.10^{11} 4.10^{8}
WIDE OPEN	0.55	0.37	1320 (33)	198	550	4	5.10^{8} 1.10^{7}
2-BAND WIDE OPEN	0.74	0.61	1776 (44)	266	740	12	4.10^{9} 1.10^{8}
3 BAND SUPERHET	0.25	-	300 (15)	20	250	-	2.10^{6} 8.10^{4}
3 BAND CHANNELISER	0.99	0.98	48 (30)	71	990	98	3.10^{8} 2.10^{8}

FIG. 2.15 TABLE OF MEASUREMENT RECEIVER SORTING ABILITY

configurations (figure 2.15).

Finally a hybrid receiver is postulated. This could consist of the wide open receiver described above, combined with a scanning VCO to allow downconversion of a small part of the spectrum. Ideally this should be tracked by a tunable bandstop filter, thus allowing a high density portion of the band to be removed and analysed separately. The VCO can downconvert into a compressive type spectrum analyser (possibly SAW). This would provide high resolution (1 MHz) measurement over a bandwidth of 400 MHz (i.e greater than the frequency agility). This would give sorting by frequency and TOA of simultaneous signals (as DOA is not available) and assuming a constant pulse density across the band gives an additional sorting power of 4.10^6. This would have greater effect when the pulse density is concentrated into frequency bands.

3.0 PROCESSING TECHNIQUES

3.1 The Processor architecture

The processor identifies the radars present in the environment by processing the measured pulse parameters. Identification is required of many complex radar types active simultaneously in the presence of noise and measurement errors, while the number of false identifications must be low. The high pulse densities require high processing rates [14].

The primary sorting parameters are frequency, DOA, TOA and PW, with varying degrees of accuracy and resolution as discussed in the previous chapter. The processor associates pulses into chains of similar pulses within the measurement tolerances. This requires searching and matching data in real time, to process all the data.

Conventional ESM processing falls into two methods. The first is called "pigeonhole" sorting and the second "time-slice" sorting[14]. In the first case "pigeonholes" are defined corresponding to a combination of some of the parameters. Thus each pulse is put into a pigeonhole with other matching pulses. This has been relied on to provide all of the deinterleaving and is followed by a TOA analysis on each pigeonhole assuming only one radar exists. This provided fast sorting of stable radars when high resolution measurement was available. However radar agility and the number of radars with similar parameters in the current radar environment will not be sorted by this fixed pigeonholing.

"Time slice " sorting takes a sample of pulses and searches through the sample for pulses with similar characteristics within defined bounds, and attempts to form a sequence. The bounds can be successively increased to allow for agility and the search continued until all the pulses have been sorted. This provides sorting by all parameters simultaneously. This is however very intensive when there is a high pulse density and is further complicated by radars which have agile PRI.

The approach proposed is to divide the processor into two sub-processes as shown in fig. 3.1 [15]. The first is a flexible, adaptive pigeonholing technique to provide fast grouping of pulses, which provides sorting of stable and agile radars. This separates pulses into groups with similar parameters using DOA, frequency and PW. Each group may contain several radars. This is the grouping process. The pulses in each group can then be deinterleaved according to the PRI which is derived by comparing the TOA differences of the pulses. This deinterleaving process extracts pulses which fit into a repetitive pattern in time and therefore characterises the individual radars. In addition, the pulse to pulse variations of a radar can be examined, and the DOA can be averaged for a more accurate measurement.

For a pulse density of 500,000 pps the avalilable mean processing time for each pulse is 2 μs. The processor requires special hardware to achieve the high data rates

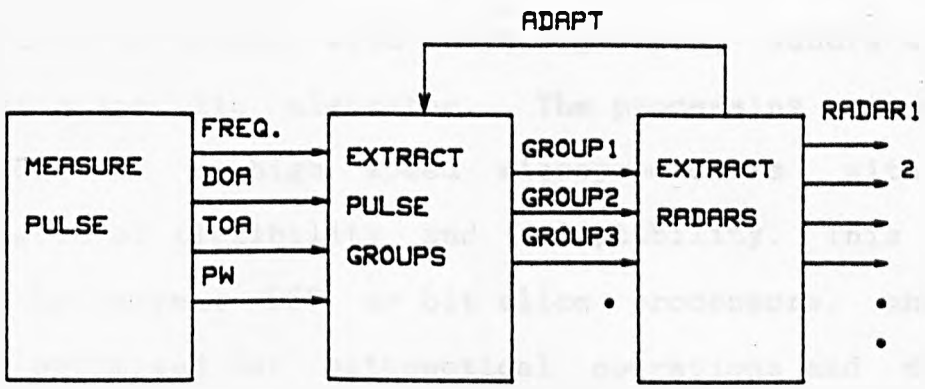

FIG. 3.1 RECEIVER ARCHITECTURE

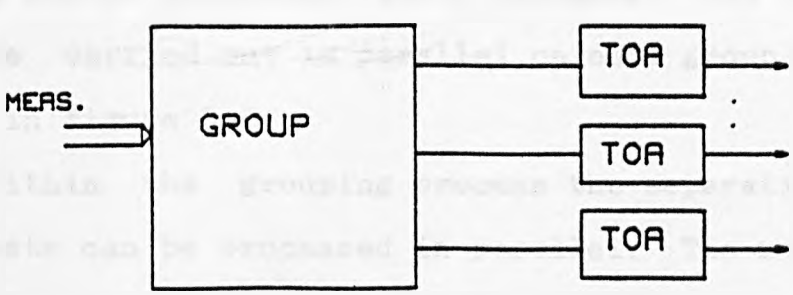

FIG. 3.2 PARALLEL TOA PROCESSING

required. This can be dedicated hardware consisting of fast ROM or RAM look up tables, with shift registers, adders etc. to implement a specific algorithm. The processing rate can also be achieved by high speed microprocessors with a greater degree of flexibility and adaptability. This is fulfilled by current DSP or bit slice processors, which have been optimised for mathematical operations and data manipulation. To maximise the throughput, a parallel architecture is considered. This must allow interaction between the parallel processes. Furthermore the use of intelligent algorithms will allow the receiver to adapt to the environment to gain full utilisation of the receiver. This is able to provide the necessary processing power to meet increasing requirements of the processor.

Parallel processing can be employed where there is parallelism in the processing algorithms. Grouping will normally be necessary before TOA deinterleaving can be applied due to the high pulse densities, though high PRF radars may be extracted before grouping. TOA deinterleaving can be carried out in parallel on each group of pulses as shown in figure 3.2.

Within the grouping process the separation of pulses into sets can be processed in parallel. The measured data is presented as a datastream to all processors and each processor associates data which falls within its prescribed windows and rejecting all other data (fig. 3.4). The processing load is allocated and monitored by the controller.

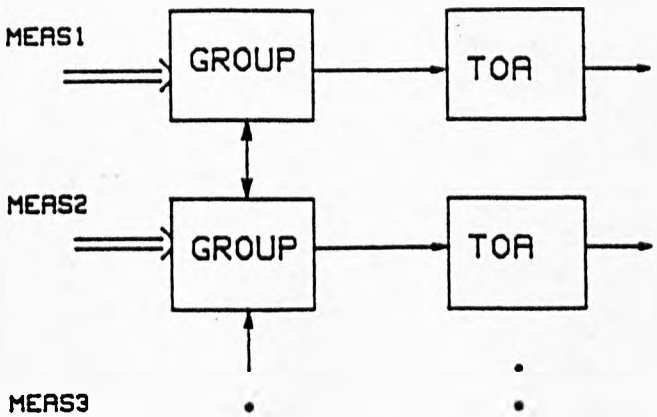

FIG. 3.3 CHANNELISED RX ARCHITECTURE

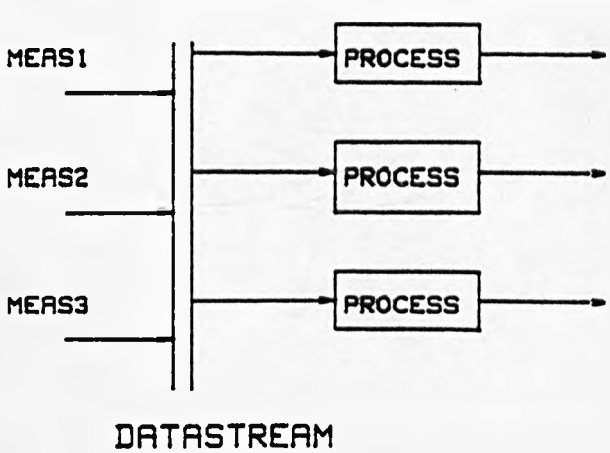

FIG. 3.4 FULLY PARALLEL ARCHITECTURE

Once the data has been reduced into groups, each group can be deinterleaved in parallel to determine the individual radars and PRIs.

Agility or incorrect group assignment will cause pulses not to be sequenced and these residual pulses are present at the output of the TOA deinterleaver. These are combined and the grouping and TOA deinterleaving processes are applied again with larger error bounds to allow for agility.

Within the deinterleaving process stable PRIs should be extracted intially, followed by agile PRIs and scanned PRIs, as the stable PRIs can be removed with greater confidence and once removed, this simplifies further extraction. Thus this process will be largely sequential, though potential PRIs can be searched for in parallel.

The above processor architecture can be applied directly to a channelised measurement system where grouping by one parameter is performed by the measurement (fig. 3.3). The processing of the residue will deal with radar signals crossing the channel boundaries. Fast scanning or wide open systems produce a similar datastream and can be sorted in the same manner, with error bounds changed accordingly. For a hybrid measurement system incorporating a wide open system and a superhet, the superhet can be used to resolve areas of high pulse density, by presenting a reduced group to the processor when a heavy processing load is encountered.

The grouping and TOA sorting algorithms are discussed below.

3.2 Pulse Grouping

Each radar transmits pulses with similar characteristics. The first stage of deinterleaving is to separate the pulse measurements into groups with similar parameters. The aim is for each group to contain a large percentage of pulses from only one radar type. This could be easily achieved if very high accuracy measurement was available such that each radar had a unique characteristic. Measurement errors and radar agility however will cause a spread of measured values and overlaps in the radar characteristics. The radars may overlap in one or more parameters but as more parameters are examined the greater is the likelihood of being able to separate the radars by grouping. Thus for maximum sorting power the data needs to be clustered in n dimensions of the n measured characteristics for an undefined number and size of clusters.

The resolution of the measurements determines the ability of resolving two radars with similar parameters. The grouping technique must draw the line between fragmenting pulses from the same radar into different groups and combining pulses into very large groups. Either of these would prevent the deinterleaver from identifying the pulse sequence. Large groups with a large spread of values will pass the sorting problem to the TOA deinterleaver.

The general subject of clustering and pattern recognition is well covered and algorithms have been developed [16]. It is attempted to apply and optimise these

algorithms for the specific case of the ESM processor, exploiting properties of the data set.

A grouping algorithm is required that is computationally efficient and particularly that the processing time should not increase dramatically for a greater number of parameters. This will then be applicable to both high and low resolution measurement systems.

The grouping should cluster the pulse measurements in at least two dimensions of frequency and DOA, or three including pulse width if the corruption rate is low (or in general n dimensions). A representation of the histogram of various radars against two parameters is shown in fig. 3.5 [17].

The sample of N pulses with measured parameters x,y and z can be described as a set of subgroups :

$$\{ \text{pulses} \} = \sum_{i=1}^{n} (x_i, y_i, z_i) = \sum_{j=1}^{m} \{ S_j \} \qquad (3.1)$$

where S is a subgroup of the sample containing pulses within the expected value of the variation of each parameter:

$$\{S_j\} = \{ \sum_{i=1}^{n} (|x_i - x_j| < E(x), |y_i - y_j| < E(y), |z_i - z_j| < E(z))\} \qquad (3.2)$$

The first point to be noted is that the measurements are digitised and this quantisation leads to a space composed of "minor" cells which are with dimensions of the resolution of the measurements (hypercuboids). Within a given time sample any of these minor cells will contain a

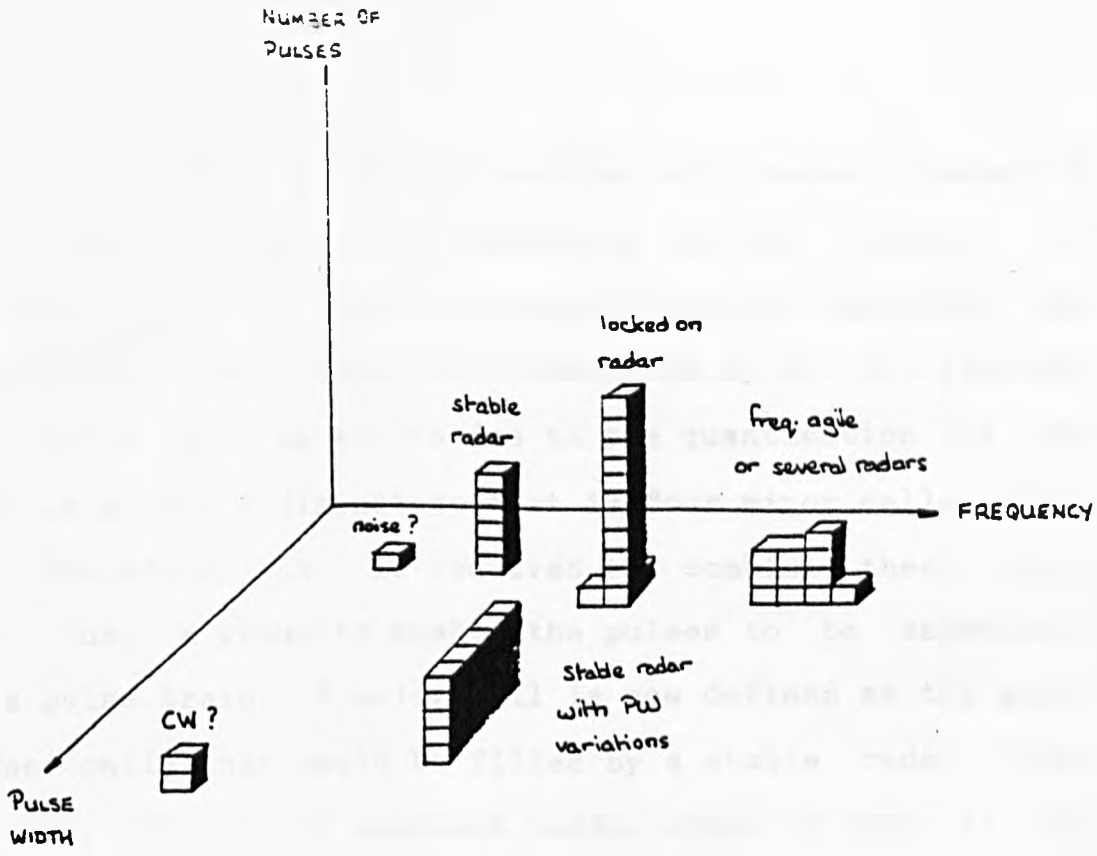

FIG. 3.5 THREE DIMENSION HISTOGRAM

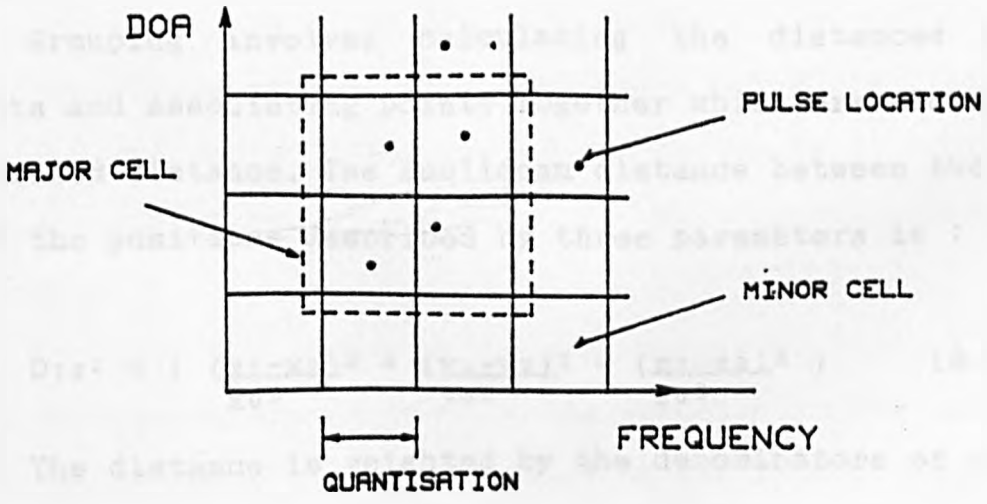

FIG. 3.6 PULSE GROUPS

number of pulses. A stable emitter will cause a number of minor cells to be filled depending on the quality of the measurement. If the measurement error is less than the quantisation level then in n dimensions up to 2^n adjacent minor cells will be active due to the quantisation of the result (e.g. for 2 dimensions that is four minor cells - fig. 3.6). Therefore it is required to combine these minor cells into a group to enable the pulses to be associated with a pulse train. A major cell is now defined as the group of minor cells that could be filled by a stable radar. Thus the major cell is the smallest useful group as shown in fig 3.6.

The total number of minor cells in this array is the product of the resolution of the parameters on each of the axes e.g for 10bit frequency, 8 bit DOA resolution there would be 260,000 unique minor cells to be examined.

Grouping involves calculating the distances between points and associating points together which are closer than a defined distance. The Euclidean distance between two points with the positions described by three parameters is :

$$D_{12}^2 = \left(\frac{(x_1-x_2)^2}{x_0^2} + \frac{(y_1-y_2)^2}{y_0^2} + \frac{(z_1-z_2)^2}{z_0^2} \right) \qquad (3.3)$$

The distance is weighted by the denominators of each of the parameters which reflects the resolving power of the particular characteristic. As DOA is not an agile parameter it is a powerful sorting parameter, whereas the PW parameter

is poor in high density environments and is therefore given less weighting.

Another important quantity in the grouping process is the cluster centre which is defined as the mean value of each of the parameters of all the points within the cluster.

3.2.1 Hardware based grouping

The fastest implementation of the grouping process is the direct allocation of groups by lookup tables and hardwired logic. Lookup tables provide an instantaneous transformation from the digitised pulse measurement to a cell assignment. This can be achieved using high density Random Access Memory (RAM) where the address lines are the measurement words (i.e frequency, DOA etc.) and the contents of the memory are the assignments for each unique combination of measurements.

In the case of an RWR the map can be predefined from prior knowledge of the radar parameters and variations. Thus received pulses will be grouped automatically if they fall within the prescribed areas in the map and rejected otherwise.

In the ESM receiver new radars must be identified and thus the groups are defined during operation. The procedure would be to apply the measurements to the lookup table which is intially empty i.e. no groups have been assigned. A cell number is assigned to the measurement if the cell is unassigned. The cells within a specified distance are

examined. If any of these have been assigned then this cell is assigned the same number otherwise it is assigned a new number. This can be achieved most efficiently by setting the cell spacing equal to the clustering distance, by using the appropriate word length, then clustering will only be required with adjacent cells (fig. 3.6).

Thus the map will be built up and each pulse assigned to a group. The mapping can now be adaptively altered according to the results of the deinterleaving process. Groups which have been processed can be blanked, combined or split dependent on the success of the sorting. This technique is not new and is outlined by Andrews [18].

The advantage of hardware grouping is speed but the disadvantage is the lack of flexibility. Thus separate hardware is required to handle agile radars (with greater distance). The instant pulse grouping also has the disadvantage that pulses are grouped in order of time of arrival and may not be centered on the cluster centre and thus may cause splitting of pulse trains.

Where the pulse descriptors have high resolution the memory size will be large as every permutation has a unique cell allocated. The memory size can be reduced by premapping the pulse descriptors to smaller words using the redundancy in the possible words assuming that every value of the pulse descriptor is not used e.g. a 12 bit word can be mapped to an 8 bit word if less than 256 values occur within the sample.

3.2.2 Grouping software

An efficient algorithm is required to cluster a stored sample of pulse measurements. There is an optimum sample size to allow sufficient pulses for deinterleaving while minimising the processing. A simple one pass through a sample of n pulses in x parameters will require processing in the order :

$$\text{steps} = x \sum_{i=1}^{n} i = \frac{n^2 x}{2}$$

A sample size of 5000 pulses i.e typically several milliseconds of the environment, requires processing rates in excess of 1000 MIPs. This can be greatly reduced by noting that the pulses can only fall into a smaller number of minor cells due to the quantisation. Thus the active minor cells and the number of pulses in each minor cell are monitored, and clustering applied to the minor cells. This active cell list and pulse count can quickly and simply be achieved by the look-up table memory discussed previously. After grouping the minor cells, the pulses are allocated to their respective groups.

Fast clustering algorithms in the class of quick partition are of two forms - sorting and leader [16]. Sorting based algorithms form groups of similar data points by ordering the data in ascendency on each parameter in turn and then the metric can be applied sequentially through the data, (as opposed to a metric between every data point) followed by a tree search to determine the size of the cluster. This

algorithm requires as many passes through the data as there are variables. Thus for a small number of parameters it is fast, providing a fast ordering process is available . The clusters are rectangular in shape which can cause splitting of pulse sequences.

Leader algorithms operate with only a single pass through the data. By clustering points within the defined distance of an arbitrary leader point, and creating new leaders if the point is outside the distance, fixed radius clusters are produced. Processing reduction is therefore achieved by only comparing the distance between each point and the leaders. These algorithms are very fast but the effectiveness is dependent on the order the data points are in, and the choice of cluster size. Where a large number of data points is required to be grouped it is always efficient to apply a leader algorithm to reduce the sample size to a smaller number of clusters [16].

A form of sorting algorithm was proposed by Wilkinson and Watson [19]. This operates by reordering the sample into groups of similar DOA, followed by a search for large gaps in the frequency distribution to determine the clusters. Groups may have been split by the initial separation by DOA therefore a final clustering is necessary which is formed by calculating the metric (leader type). This produces variable size clusters quickly if the size of the DOA buckets is large. This has the disadvantage of being more inefficient for a greater number of variables and also producing large

cluster sizes in dense environments or where agile radars are present. The number of computations where the DOA buckets is d is of the order of:

$$d.n + \frac{n^2}{d}$$

The leader algorithm type is very applicable to the ESM case where the clusters are required to be of a defined size. The disadvantage of clustering around arbitrary centres is that points on the edges of clusters may be selected as centres thus potentially splitting a group and the algorithm is more efficient if cluster leaders are found initially. A modified density led leader algorithm is proposed to solve this. This is based on the Leader algorithm but with the improvement that the leaders are not chosen arbitrarily but are chosen on the basis of high pulse density (i.e. the pulse count in the minor cell). This forms groups around points of high pulse density which reduces the chance of splitting pulse sequences. The list of minor cells is reordered such that cells containing above a threshold pulse density are at the beginning of the list. The standard leader algorithm can then be applied. This produces fast and accurate grouping.

The end result of partitioning is a small number of fixed radius clusters. These clusters may be within the specified clustering distance of each other and thus if the full size clusters are required a metric can be applied

between every cluster, as there will now be a relatively small number of clusters. The size of the cluster can be limited by density, to the optimum number of pulses that can be deinterleaved by the TOA algorithm, or by distance to that expected for measurement spread (agility plus error). This algorithm is efficient for multidimensional clustering as only one extra term is required in the metric for each extra dimension (as opposed to the sorting algorithm which requires a complete pass through the data for each dimension). This requires in the order of :

$$C.(N - \frac{C}{2}) \qquad \text{instructions}$$

where C= number of clusters and N= the number of minor cells to be clustered.

Thus agile and stable radars are optimally sorted and separated into groups for TOA analysis. After the first grouping pass, the lookup table can be reassigned to directly group the pulses and the grouping software has now only to deal with newly active cells and with periodically resetting inactive cells. This gives the algorithm a learning curve such that the efficiency increases with time. Additionally feedback can be implemented from the TOA deinterleaver such that large clusters that cannot be deinterleaved can be split down and small clusters that cannot be deinterleaved can be combined. Unwanted or processed cells can be masked to reduce the processing load.

Software has been developed and simulated on a

microcomputer and sample results are shown in fig. 3.7. A sample of pulses from seven radars with overlapping frequency or DOA was generated. Measurement errors were imposed on the radar parameters. Figure 3.7a shows the active cells in the frequency / DOA map, these cells contain a number of radar pulses. Thus the algorithm groups the cells around high density cells, within stable radar distance i.e into major cells as shown in Figure 3.7b. Finally, a tree search clusters the adjacent major cells to give the grouping shown in figure 3.7c. This means that pulses with a frequency and DOA within the groups shown in figure 3.7c will be clustered into one of the four groups. This mapping now provides instant sorting of subsequent pulses unless they have a different frequency and DOA.

This software has also been implemented in the ESM receiver design in chapter 5 and results of the full system simulation are presented. The efficiency is such that with a single, integer, high speed processor with high speed memory, real time grouping is feasible.

If more parameters are used for grouping then further aspects of pattern recognition can be applied to identify new types of agile signal. The cluster shapes will be distinctive for these radars and can be used for extraction.

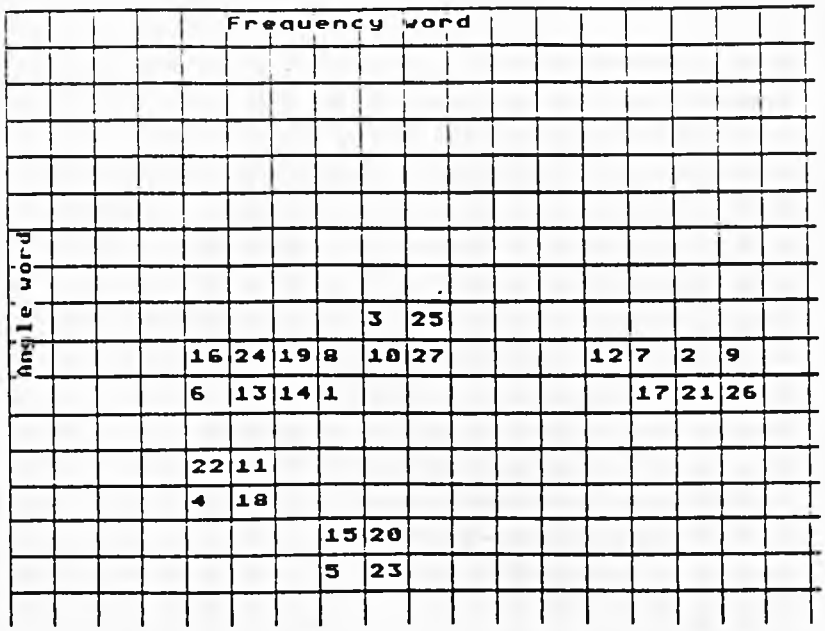

FIG. 3.7 a

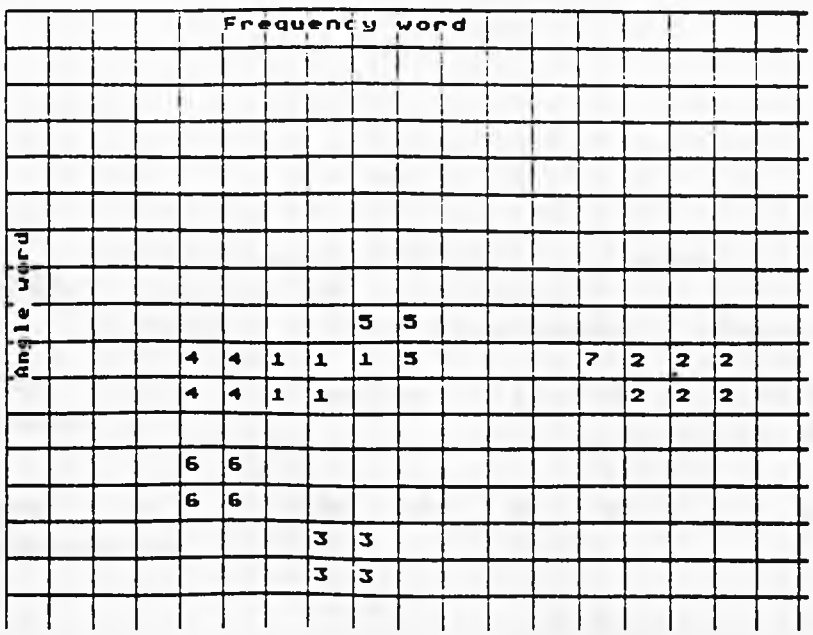

FIG. 3.7bCLUSTERING TRANSFORMATION

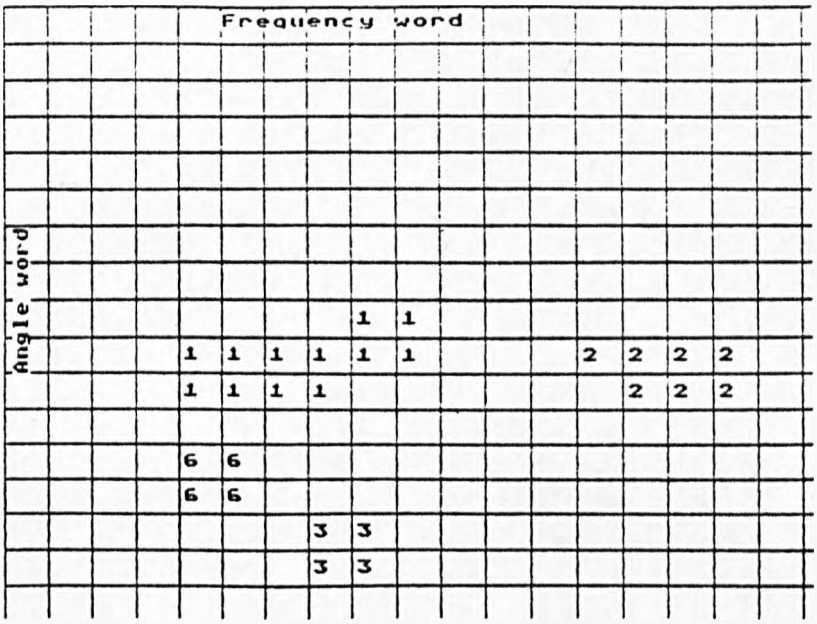

FIG. 3.7 c CLUSTERING TRANSFORMATION

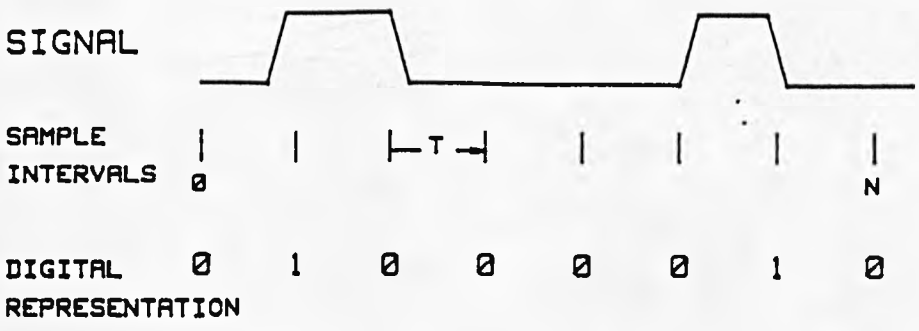

FIG. 3.8 SAMPLED PULSE TRAIN

3.3 TOA Deinterleaving

TOA deinterleaving is a vital part of the ESM receiver. Determination of PRI is essential to separate the pulses of a given radar from the background of pulses, for identification of the radar, and for ECM purposes [17]. The parameters associated with the extracted pulses can then be further processed to determine parameter variations e.g. scan pattern or to refine measurements e.g averaging the DOA.

The input to the TOA deinterleaver is the result of superimposing several, repetitively pulsed signals. The required outputs are the separated pulse sequences. A signal can be characterised by a pattern of pulse intervals that repeats in time, with a given phase or start time. In the simplest case the PRI is constant and the pulses are separated by one, fixed interval time. Jittered radar signals have pulses separated by a interval with a variation (which may be pseudo- random) which is the jitter level. Staggered radars have a frame containing several different intervals, but the frame is repeated continuously. The stagger ratio is the ratio of the smallest interval to the largest, and the number of different intervals defined as the stagger positions.

Conventionally, pulse trains have been extracted by audio analysis, audio filtering or by the use of digital shift registers. However, the range and complexity of modern radar signals, many of which are now generated by DSP, is more suitable for extraction by DSP.

High pulse densities and complex radar signals require more powerful algorithms. The high pulse corruption probabilities mean that it is not possible to guarantee reliable and unambiguous identification. Thus, techniques are presented that test for the best fit and give identification with an indication of confidence level. The algorithms identify particular patterns and reject randomness in the data.

The sample of pulses for PRI sorting has already been separated into a group of pulses of similar frequency, PW, and DOA, as TOA sorting is difficult with a large number of pulses. This group may contain only one radar, however it may contain several unsorted radars. The PRI analysis separates these radars using the TOA information of each pulse.

The PW and amplitude information is not useful at this stage and is discarded. However both pulse density and PW determine the number of missed pulses and measurement errors as discussed in chapter 2. This affects decision thresholds in the deinterleaver. Pulses may also be missing due to splitting of pulse chains at the grouping stage.

The TOA is measured digitally from the leading edge of the pulse. The resolution of the TOA measurement has two implications. Firstly, the resolution determines the minimum separation of pulses that can be measured. This resolution is ideally equal to or better than the measurement system dead time. The digital measurement causes a

quantisation error bounded by the resolution. Secondly, extrapolation of pulse sequences is required when pulses are missing and the PRI error accumulates with projection. The resolution has an impact on both the storage space and the word size for calculations (and therefore the speed of processing).

A stable radar pulse with a start time t_s, a PRI of I, and pulse width W has the function :

$$f(t) = A \quad \text{when} \quad t_s + a.I < t < t_s + W + a.I \qquad (3.4)$$

$$= 0 \quad \text{otherwise}$$

where a = positive integer

Only the TOA information is required and the amplitude and PW information discarded and thus the signal representation becomes a series of impulses.

$$s(t) = \sum_{a=0}^{\infty} \delta(t - t_s - a.I) \qquad (3.5)$$

The sample interval k (s.i.) is defined as the TOA resolution and the sample length defined as N sampling intervals. The presence of a pulse is represented by a logic "1" at the sample interval corresponding to the TOA, otherwise the sample intervals are logic "0" (fig. 3.8). The time of arrival is measured in integer multiples of the sampling interval. The i th stable pulse train with a pulse interval of m (s.i.) and start time of q (s.i.) can be written :

$$S_i = \sum_{r=0}^{\infty} s_i(r.k) \qquad (3.6)$$

where $s_i(t)=1$ when $t = a.I_i + t_{si}$

i.e. $r = a.m_i + q_i$

and $s_i(t)=0$ otherwise

where a,m,q are positive integers

The sample of pulses to be sorted is the result of superposition of several pulse trains . However, it differs from a simple addition of signals in that pulse overlaps are only known as the presence of one pulse at that instant, and thus the resultant pulse sample is the logical "OR" of the x individual pulse sequences. This can be written :

$$P = \sum_{i=1}^{x} S_i = \sum_{r=0}^{N} (s_1(r.k)+s_2(r.k)+ \ldots s_x(r.k)) \qquad (3.7)$$

$$= \sum_{r=0}^{N} p(r.k)$$

and $0 < a < \frac{N - q_i}{m_i} = n_i$

3.4 TOA ALGORITHMS

3.4.1 The TOA difference histogram (ADIF)

TOA sorting of a large number of pulses, with a large range of PRIs requires large processing power and thus algorithms have tended to be simple, relying on the initial grouping process to provide the bulk of the sorting.

The simplest TOA deinterleaver is the TOA difference histogram. The histogram is formed by subtracting the TOA of each pulse from every subsequent pulse and counting the number of pulses at each TOA difference value [20].

Applying this technique to a single constant PRI sequence causes a peak to occur at the repetition interval and at multiples of this PRI, in the histogram. The confidence level is determined by the sample length taken, i.e the greater the number of samples the greater the accuracy and the PRF range of the histogram. The processing time increases with the square of pulses in the sample, The number of computations is in the order of :

$$\sum_{i=1}^{P} i = \frac{P^2}{2}$$

Though a correct output is given, outputs also occur at every multiple of the fundamental interval. Thus when several signals are present, multiples and sum and difference intervals produce an unclear picture (fig. 3.9). The histogram can only be clarified by first extracting the smallest interval that exceeds a difference

threshold and either calculating the harmonics and subtracting their effect, or removing the pulses that correspond to that frequency and recompiling the histogram. The difference histogram is an autocorrelation of the pulse sample as can be seen by applying a delay of d s.i. to the signal (equation 3.7) and correlating :

$$\int_0^T p(t).p(t-d.k).dt = \sum_{r=0}^{N} p(r.k).p((r-d).k)) \qquad (3.8)$$

Thus for each delay d i.e each cell in the histogram a count is found when :

$$q_i+km_i = q_j+lm_j+d \qquad i,j = 1 \text{ to } x \qquad (3.9)$$

Thus at the PRI of the i th radar a minimum count of the n_i pulses is found :

$$n_i = \frac{N - q_i}{m_i} - 1 \qquad \text{when } d = m_i \text{ and } m_i=m_j \text{ , } q_i=q_j$$

False detection of harmonics of this PRI can be seen as equation (3.9) is also solved when :

$$d = h.m_i \qquad \text{count} = \frac{N - q_i}{h.m_i} - 1 = \frac{n_i}{h} - 1$$

The histogram destroys the time domain information, and thus does not identify the pulses that form the sequences.

If no pulses were missed, then histogram count would be as calculated above. However as pulse density, PW and the combination of radar signals vary, the count varies. The

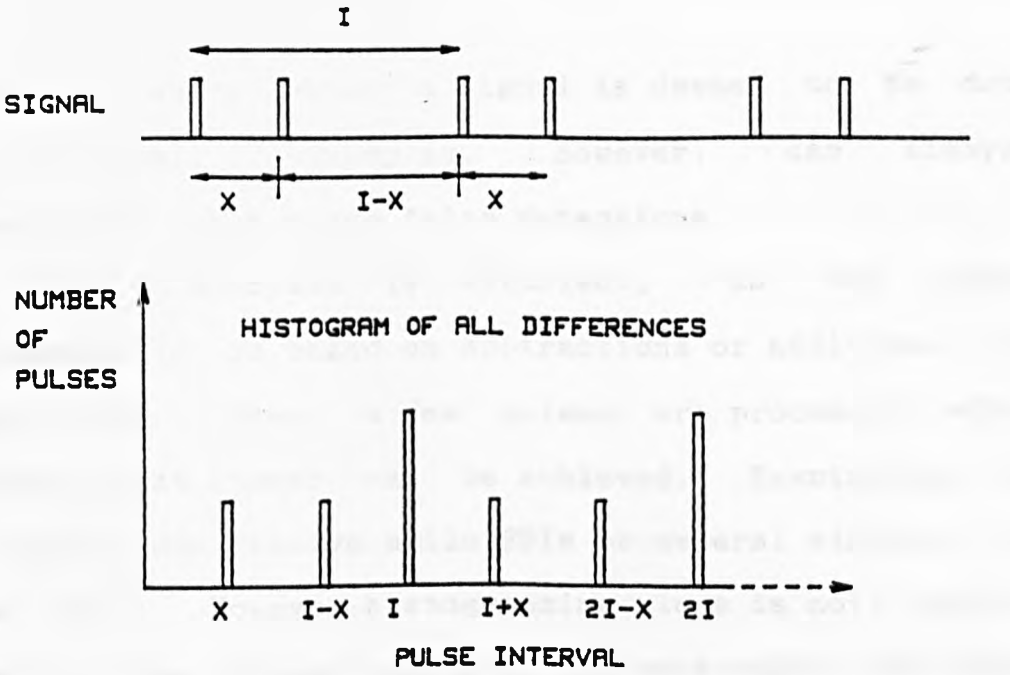

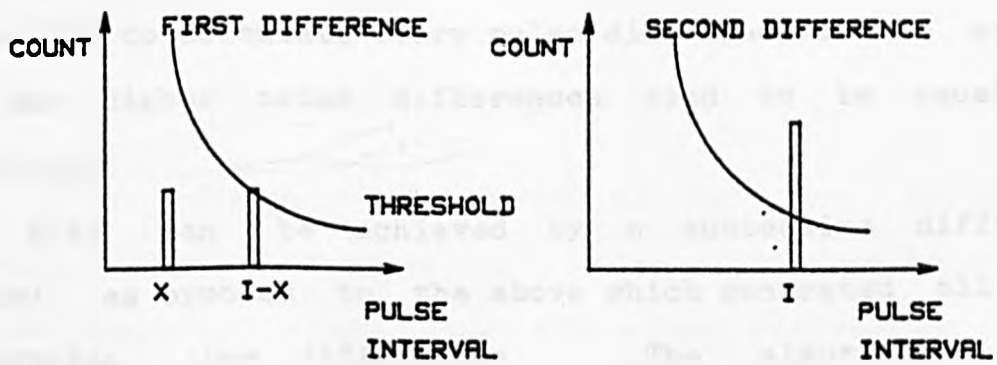

FIG. 3.9 TOA HISTOGRAMS

threshold above which a signal is deemed to be detected is critical. Examples, however, can always be constructed that cause false detections.

This approach is efficient, as the algorithm predominantly is based on subtractions or additions of the pulse TOAs. When a few pulses are processed with few radars a fast answer can be achieved. Examination of the histogram can resolve agile PRIs or several signals of the same PRI. However histogramming alone is not sufficient when the data becomes corrupted and more radars are present, as an unacceptable rate of false alarms occurs.

3.4.2 Successive Difference Histogram (SDIF)

In order to minimise the harmonic and sum and difference terms that appear in the histogram a method that removes highest frequency terms i.e smallest interval is required. Greater efficiency is possible as it is not necessary to calculate every pulse difference in the sample, as the higher order differences tend to be caused by harmonics.

This can be achieved by a successive difference method, as opposed to the above which generated all the interpulse time differences. The algorithm first generates a histogram of differences between adjacent pulses only. This is the first difference. The count at each pulse interval is compared with a threshold value. If a radar is detected then the pulses can be deleted and the

algorithm restarted. If no radar is detected, the second difference i.e the TOA difference between each pulse and the next but one, is calculated and the difference level increased until detection occurs or until the pulses are exhausted (fig. 3.9).

A simple pulse sequence identification and deletion algorithm was developed. This searches sequentially for pulse pairs separated by the required interval. The first pulse pair in the sample separated by this interval is found and the position of the next pulse anticipated. If there is no pulse at this position the next pulse pair is found. The number of pulses found in this manner is counted and compared with the expected value. If sufficient pulses are found, the sequence is deemed to exist at that PRI and the pulses are deleted. The successive difference histogram is recompiled from the first difference level on the remaining pulses. This provides a quick validation and extraction of a sequence, though under certain circumstances this is not accurate (especially when a staggered PRI is present).

This difference method relies on the probability distribution of "interfering" pulses between the required radar pulses. When there are a high proportion of the radar pulses separated by z interfering pulses, a high count will appear on the (z+1)th difference level. This count can be less than the total number of pulse intervals from that radar.

A pulse train of PRI I has N/I pulses. The probability

of one interfering pulse falling in one particular interval is :

$$p = \frac{I}{N}$$

Assuming y random interfering pulses then the average number of pulses in each interval is :

$$\mu = \frac{yI}{N} \qquad (3.10)$$

and the standard deviation according to the binomial theorem :

$$\sigma = \sqrt{(yp(1-p))} \approx \sqrt{(\mu)} \qquad \text{if } p << 1 \qquad (3.11)$$

The peak count is detected at the mean number of interfering pulses, however the peak becomes broader and the count falls with increasing pulse densities.

This algorithm can be illustrated by taking a simple example of two radars with the same PRI of I sample intervals. The start time of the two radars is different by T s.i. (fig 3.9). Thus the first difference generates two counts at T and (I-T). The value of these counts with no missing pulses will be (N/I-1). Now the value of the threshold again is critical - a typical value might be N/2I. Thus dependent on the value of T (i.e the start times) one or two false alarms occur. If the second difference is examined then a count of 2N/I is measured only at interval I. This gives a clear answer of two radars with interval I.

If there are P pulses and x pulse trains then the number of computations is of the order :

x.P

This method can be more efficient than the ADIF algorithm as the difference level is only as large as is necessary and it can be easily recalculated after pulses have been removed from the sample. The spurious outputs are much reduced, however the threshold for detection is more difficult to determine.

3.4.3 Cumulative difference histogram (CDIF)

A cumulative difference histogram is proposed. This is compiled one difference level at a time as in SDIF, but the histogram is accumulated from each difference level until a threshold is exceeded. Thus only the optimum difference level is taken, the probability of detection is increased and the threshold is easier to determine. This is more reliable than the SDIF histogram in higher pulse densities.

3.4.4 Sequence Search

Sequences of pulses with unknown PRI and unknown starting points are to be extracted from the sample. To associate the pulses with a sequence, the PRI and the phase must be found. The histogram does not use sequential information. The search algorithm proposed uses this information giving greater tolerance to interfering pulses and rejection of intermodulations, at the expense of greater processing. To appreciate the processing task a

"sledgehammer" approach can be examined. If all the possible pulse intervals at all the different start points are generated and compared in turn with the data sample, a match can be found for these signals in the sample.

The signal postulated is :

$$Se = \sum_{r=0}^{N} se(r.k) \qquad (3.12)$$

This signal can be multiplied with the sample, p(t), (equation 3.7) and integrated to provide the correlation function :

$$\int_0^T se(t).p(t)dt = \sum_{r=0}^{N} [\ se(rk).(s_1(rk)+s_2(rk)\ldots)\ ] \qquad (3.13)$$

This yields a count of pulses equal to the number of solutions to:

$$q_e+jm_e = q_i+km_i \qquad \text{for } i= 1 \text{ to } x \qquad (3.14)$$

j,k positive integers

Thus the maximum count is n_e when all the pulse TOAs in the postulated train exist in the sample.

At a PRI of I s.i. there are I possible starting times and N/I pulses to be correlated. Assume the PRI of signals can be from 1 to N then number of computations in a search for all possible sequences is of the order of :

$$N.\frac{N}{I}.I = N^2$$

However, if a signal postulated has a PRI which is an integer multiple of a PRI that exists within the sample i.e.

$q_e = q_i$ and $m_e = h.m_i$ $\quad h = 2,3,4 \ldots$ (3.15)

then equation 3.14 is solved for

$$j = \frac{k}{h}$$

The expected count and sequence is found at this subharmonic and detection of the wrong PRI occurs.

Thus the search must start from the smallest interval to prevent matches on subharmonics of a signal. Furthermore, the detected pulse sequence must then be deleted. In a dense environment pulses will be missing from the sequences and therefore a threshold has to be set to determine the count that constitutes a sequence. It can also be seen that there is a finite probability of a random set of pulse trains producing another apparent pulse train.

The search will find signals that have PRIs which are an integer multiple of the sample interval (i.e. $m = j.k$). However take the case where the PRI is (I + 0.5) s.i. Successive pulses are separated by I,(I+1),I ... and so on. Thus a match must be allowed with either of two positions in the sample - at I or (I+1). However this possible error increases with time and the error bound becomes increasingly large i.e after several intervals a sequence from a signal with PRI of I is well separated

from a signal with PRI of (I+0.5).

Now, the actual PRIs and phases in the sample will be a small subset of all the possible combinations. Therefore the search should be limited to the possible phases and PRIs in the sample.

One solution is to anticipate the position of the next pulse based on projecting a short sequence found in the sample, and calculating the average PRI in the sequence. As the sequence is lengthened the PRI can be calculated with greater accuracy.

An algorithm of this type is presented by Davies and Holland [14] where the interval between the first pair is taken and the position of subsequent pulses calculated using that interval and checked against the sample. As pulses can be missing, the projection has to be taken forward till the next pulse is found. The error bound increases, and the probability of an incorrect match increases.

If a sufficient match is not found, the interval between the first and third pulses is calculated and projected and so forth. This process is repeated on the second pulse, third pulse etc. When a pulse train is found the pulse sequence is deleted to simplify further deinterleaving.

This has the advantage of only searching for PRI values within the sample, but many unsuccessful searches will occur, especially when several pulse trains or interfering pulses are present. The efficiency of this technique is critically dependent on the choice of the pulse

pair.

Assuming a set of P random pulses (where P << N) containing no stable pulse sequences, the number of computations required to determine this condition is of the order of :

$$\sum_{i=1}^{P} i + \sum_{i=1}^{P-1} i + \ldots \sum_{1}^{2} i = \sum_{1}^{P} i^2 = \frac{P^3}{3} \qquad (3.16)$$

The Watkins Johnson algorithm [20] also uses the above approach. This projects from the central pulse in the sample, with a PRI of the interval between adjacent pulses. The hypothesized pulse train is compared with the sample. If sufficient correlation is not found, the interval between the centre pulse and the next but one pulse is taken and projected. This process is repeated until a match has been found or the pulses have been exhausted in which case the 25 percentile pulse is taken and the algorithm repeated.

This approach has the disadvantage of requiring many computations if the abritrary starting pulse chosen was an error, or where many PRIs are present, as every PRI within the sample may require to be searched, projected and correlated. The projection of the PRI from a single measured interval suggested by WJ can lead to a divergence from the actual PRI, due to measurement errors. This will prevent detection even if jitter tolerance is allowed for. Thus a more robust technique is required.

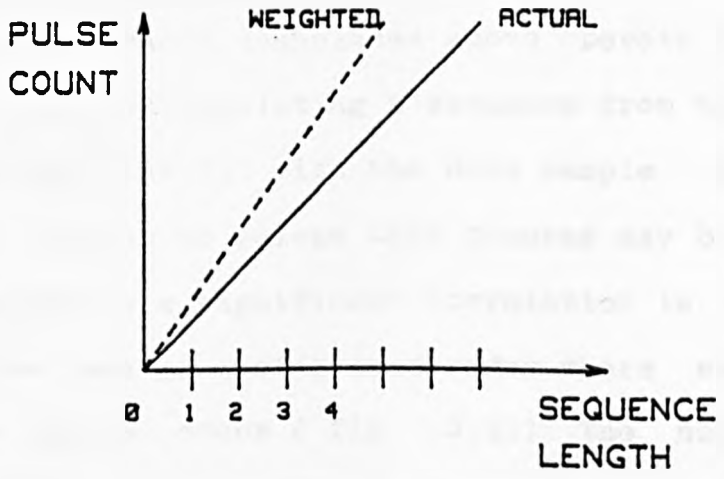

FIG. 3.10 A COUNT WEIGHTING FUNCTION

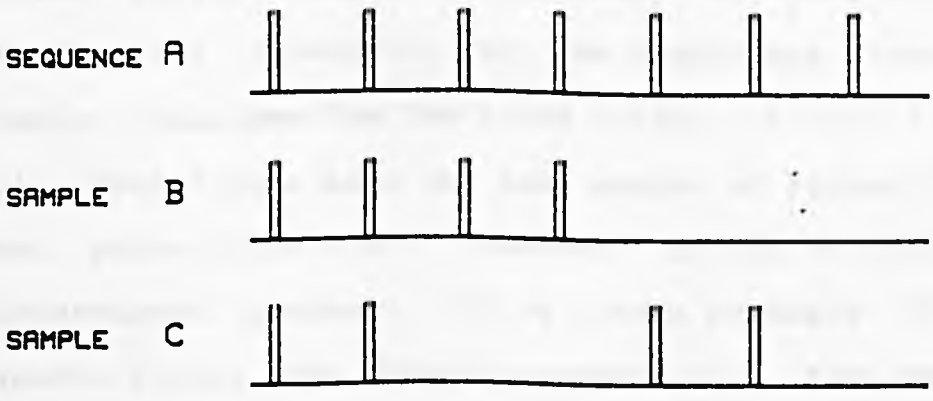

FIG. 3.11 PULSE SEQUENCES

3.4.5 The weighted search algorithm

The search techniques above operate by taking a pulse pair and extrapolating a sequence from the pulse pair and examining the fit with the data sample. Where there are a large number of pulses this process may be repeated several times before a significant correlation is found, especially in the case of a staggered radar where several unsequenced pulse pairs occur (fig. 3.11). The number of succesive iterations can be reduced substantially by selecting a longer sequence to prime the search. In high pulse densities a long uncorrupted sequence may not occur therefore either of two sequences containing three pulses have been chosen as the primer (fig. 3.12). This will reject sub intervals of a staggered radar or random pulse pairs thus reducing the processing time and also providing a more accurate PRI for projection (averaged over the sequence).

An evaluation of the fit of a sequence of pulses with several pulses missing is required, in order to determine the decision thresholds and the confidence level . For example, consider the two pulse trains (B and C) in figure 3.11. Both trains have the same number of pulses fitting the ideal pulse train (A). However, it can be seen that the uninterrupted sequence (B) is a more probable fit to the sequence A than the broken sequence (C). Also sample C may be a better fit a different type of signal e.g. a staggered PRI.

Thus, weighting the pulse sequence length (as in fig.

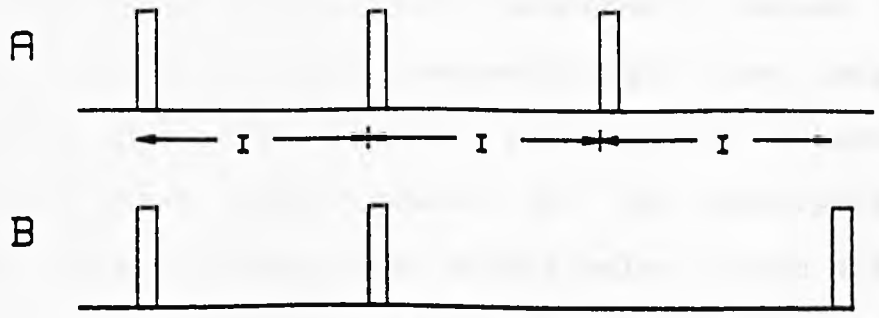

FIG. 3.12 STARTING SEQUENCES

3.10) is proposed, such that a sequence of pulses produces a greater count than two sequences of half the length. The decision threshold should discriminate between an apparent pulse train caused by the superposition of several pulse trains and an actual pulse train with pulses missing. The threshold is dependent on pulse density as discussed in chapter 2. The weighting function should make the decision more reliable.

A simple weighting function is proposed where the count is the sum of the number of pulses fitting the sequence plus the number of pulse pairs separated by the searched interval.

An alternative weighting function that gives greater enhancement of sequences is based on the probability of an uninterrupted sequence of y pulses occuring. If the average pulse density is R pulses per sample interval and the PRI is I (s.i.) then the probability of a sequence of y intervals being found is :

$$p(y) = (1 - \frac{1}{I})^{RIy} \approx (1-R)^{y} \qquad \text{if } I >> 1 \text{ and } R < 1 \qquad (3.17)$$

Thus, for each sequence of pulses this factor reciprocates is added to the count. This enhances detection of sequences in high pulse densities.

When several radars are present, the number of overlapping pulses can become high. Under these conditions deleting detected pulse chains can leave a small residue of pulses even when further longer PRI chains still exist,

but few pulses remain from the sequence. A method of applying "fuzzy" logic has been examined.

When a sequence is detected, the number of pulses in the sequence is counted. When this weighted count is greater than the threshold, the constituent pulses are not removed but given a smaller weighting factor. Thus the pulses that could have been overlaps are still available to detect the longer PRI radars. By giving a lower weighting and applying the rule that sequences may not start on a pulse with low weighting, the redetection of harmonics is avoided.

The "fuzzy" pulses represent blocking of another pulse due to measurement dead time or overlapping pulse width. This feature could be used to enhance processing in high density environments, by detecting pulse overlap and measurement errors and allowing the processor to use these occurences as "wild" pulses which can be assigned to several radars if it increases the pulse sequence fit.

3.4.6 Two-pass TOA deinterleaving

The histogramming methods while detecting the PRIs quickly, have the drawback of generating false alarms and not identifying pulse sequences. The sequence search techniques are very accurate but relatively slow. Thus a two pass approach is presented combining the advantages of the two techniques. This provides an efficient sorting method with a high confidence level.

The histogram quickly determines the likely PRI values within the sample. The sequence search provides validation and deletion of the PRIs indicated. This is analagous to the human ESM operator who makes an estimate by inspection and then follows with a more detailed analysis.

3.4.7 Deinterleaving of agile signals

The above algorithms are suitable for the identification of simple, stable PRI signals (and the rejection of agile signals). Further processing is required to extract the more complex signals which are in three types - staggered, jittered and scanning. In the presence of several signals, the agile signal can be difficult to identify, therefore the first stage of deinterleaving is the extraction of stable signals from the sample.

If sufficient samples are taken to contain several frames of a staggered PRI, it is found as several pulse trains. They have the same PRI as the stagger frame rate and are separated in time by the stagger intervals. Thus by examining the stable PRIs found in the sample, the staggered radars can be identified simply.

Short emissions from scanning radars with stable PRIs are extracted next using the same algorithms with lower thresholds to identify the short sequences (typically ten pulses). The sequence search is modified to extract only bursts of pulses to prevent detecting a sequence spread over the sample.

The jittered radar is more difficult to extract reliably

due to the random or pseudo-random factor on the pulse interval (unless the jitter level is less than one sample interval when it will appear as a stable radar). Therefore the jittered extraction is performed on the residue of the previous searches. The same histogramming technique is used, however groups of histogram entries are summed with the size of the group increased proportionately to the PRI to allow for the variation in PRI. When the summed count exceeds the threshold the search algorithm is again used, however the PRI variation is allowed to be greater and the threshold is made higher due to the greater likelihood of false alarms. This process is repeated for various jitter levels (10 percent, 20 percent etc.).

The final residue is accumulated to extract longer PRIs using the same algorithms. The residue is also available to the frequency agile grouping process for recombination followed by another pass through the TOA deinterleaver, to extract frequency agile signals.

3.4.8 The pulse sample size

The choice of sample length and sample interval determine the maximum and minimum PRI that can be detected and the minimum separation of two radar signals. As PRFs can be from a few hundred Hz to hundreds of kHz there is a 1000:1 range.

The greater the number of pulses in a sequence the greater the confidence level of detection, the minimum

acceptable number being five pulses. Thus a sample length of 10 ms would be required to cover the full range of radars in a single sample. A sample interval of less than five microseconds would be required for high PRF radars. Thus the sample could potentially contain thousands of pulses (the number of pulses must be much less than the number of sampling intervals to allow TOA deinterleaving) though many of these pulses may be sorted by the grouping stage. The majority of the above techniques are efficient on small samples (100-200 pulses) as the number of computations is proportional to the square of the number of pulses.

This suggests reducing the sample lengths and extracting high PRF radars and then combining the residue from several such samples and extracting low PRF radars. The algorithm can use prior knowledge of PRFs to search and extract the known radars, thus reducing processing in the histogramming stages. Thus the sample size is traded off with the maximum PRI detectable in one sample to enable real time processing.

3.5 Test results

Test programs have been written to test the algorithms on stable sequences and results with various data samples have been produced for comparative analysis. The data for several signals is generated by a simulator program and the samples are common to each algorithm. These five algorithms have been implemented in high level language (compiled BASIC) on a microcomputer. Code Fragments are contained in appendix A.3. The three tests contain several interleaved sequences with identical PRIs, harmonic PRIs and non integer PRIs.

The results (figure 3.13) show the percentage of correct identifications, false reports and calculated number of computations. This table shows that the SDIF2 algorithm gives best performance for low to medium pulse densities. For deinterleaving in very high densities the CDIF and sequence search algorithms become more efficient and accurate, as the processing overheads become a smaller proportion of the computation.

The calculated number of computations required to sort x radars using the SDIF/deletion algorithm (allowing for x false alarms from the histogram) with a sample of P pulses is in the order of :

insts. = 5.x.P

Each computation requires typically four microprocessor level instructions (read number A, read number B, add/subtract A and B, store result) and one microprocessor

add instruction is taken as the measure of the processing power (IPs). Integer multiplication typically requires 20 cycles unless a dedicated multiplier is used, and division tends to take more cycles.

For a pulse density D, containing x radars, and a sample length containing P pulses to be deinterleaved, the processing rate required by the SDIF/deletion algorithm is :

$$\text{Process rate} = 30.\ \frac{Dx}{G}$$ where G= number of groups

For example, a pulse density of 500,000 pulses per second, containing 100 radars, with a sample of 2500 pulses (5ms sample time) the initial process rate is less than 45 MIPs. This reduces with time as the learning process occurs.

In the case where the processing power does not meet the initial peak demand, the TOA deinterleaving must be reduced. This can be achieved by deinterleaving groups in order of priority, thus the unsorted groups would be of lowest priority. Alternatively, the sorting could be applied to a short sample of the data, discarding the remaining pulses, thus providing extraction of signals, but at lower confidence levels.

These algorithms should be written in a low level language such as assembler or "C" to obtain maximum speed. The algorithms can achieve high processing rates, as only integer arithmetic is necessary rather than floating point, and multiplication and division has been minimised.

The results indicate that real time TOA deinterleaving in dense pulse environments with high accuracy is possible with available microprocessors (such as the Inmos Transputer, Motorola 68020) and a parallel architecture.

The CDIF/sequence algorithm is extended to extract agile PRI signals in the complete ESM processor design in chapter 5.

FIGURE 3.13. TOA SORTING ALGORITHM PERFORMANCE

ALGORITHM	TEST1 RATE / SUCC (MIPS)/ (%)	TEST2	TEST3
SDIF1	40/ 80	70/ 100	125/ 33
SDIF2	30/ 100	70/ 100	120 / 67
ADIF	85/ 100	75/ 100	200 / 50
CDIF	50/ 100	40/ 100	100 / 78
SEARCH	50/ 100	50/ 100	90 / 78
CDIF+SEQUENCE	80/ 100	85/ 100	200 / 90

TEST1 400 samples at 11,13,17,19,23 us PRI (280,000 pulses/sec)

TEST2 300 samples at 13.6,23,23,23,23,23 us PRI (270,000 pulses/sec)

TEST3 400 samples at 15,17.5,19,21,23,26.5,26.5,29,29 (350,000 pulses/sec)

4.0 SIMULATION

To test the performance of a system and compare algorithms it is necessary to provide conditions that are realistic for the environment for which the system has been designed. Physical realisation of several different emitters with different signal types from different locations is difficult to achieve. Therefore software modelling and simulation is a valuable tool for the assessment of a system under complex conditions [22].

This allows flexibility and repeatability. The simulation closely models the physical conditions i.e the simulation must not abstract the model to the ideal case. The simulation does not need to be in real time.

The simulation can be split into two parts :

1. The signal environment
2. The ESM system

4.1 The signal simulator

The signal simulation generates an environment consisting of several radars. The frequency, PW, PRI, signal strength and DOA and variations of these parameters, of each radar are described. The simulator should be capable of simulating agile radars, scanning and CW radars. Simultaneous or overlapping signals must be generated.

Computer simulation is time consuming and thus certain details must be omitted, providing care is taken to simulate events which do affect receiver systems. The simulation objective is to determine how the system performs under

varying signal mixes, how pulse overlaps affect the system, and the performance of the system under overload situations.

Thus the simulation does not need to be at the level of RF cycles. Movement of emitters or of the receiver can be regarded as a longer term function. Pulse shape need only be simulated if it is used as a sorting parameter. Multipath has only been modelled as a random effect on pulse width and TOA parameters at the receiver as opposed to the mechanics of the RF propagation and modelling the terrain.

The signal simulator that has been written takes a library of emitter descriptions and produces a sample of the RF environment in terms of time and pulse parameters at the receiver. This library can be altered. Though real time operation is not required, fast simulation is desirable. A compiled, high level language was used.

The simulator assigns a random start time to each radar and then calculates the position of the successive pulses according to the PRI and the agility. Random variations within defined limits can be put on all the pulse parameters to represent propagation or radar variations. If other parameters are agile they are also varied from pulse to pulse according to agility type (hopping or scanning). Frequency agility and PRI agility have been modelled. The output is formatted to drive the system simulator program. The accuracy of all the parameters is greater than

that of the measurement system.

The choice of signals and parameter variations is subject to known information on the EW environments. This indicates the combinations of radars for which the system is tested. This includes generation of scenarios where problems are expected in the receiver e.g very high pulse densities or multiple radars of one type from the same direction. Specific scenario information is classified secret therefore potential scenarios have been devised from published information.

A pulse environment for simulation of the RWR and ESM designs is generated in chapter 5 and details are given in appendix A.4.

4.2 System simulator

The system simulator is designed to simulate different receiver configurations, which can be tested with the data from the environment simulator.

An ESM system comprises of antennas, measurement units, preprocessor, processor and output modules. There are many possible realisations of each module. Therefore a generalised framework was designed, based on modules whose specific functions can be defined as required. This framework provides the background utilities and overall operation of the modules.

The modules have a standard "black box" definition to interface directly into the framework. The modules are defined by inputs, outputs and the user defined function. An interconnection list connects the modules together into the required configuration. This allows the internal operation of a module to be defined to any appropriate detail. Thus the system can be modelled containing several different hierarchical levels.

The function has to be defined carefully to realistically model the subsystem. Simplifying assumptions may prevent certain effects or errors from being seen, thus giving a false simulation.

The simulator is based on a state - machine approach. Each of the modules is operated after small, discrete time intervals. The function is performed on the inputs to the module and the outputs updated. Propagation delays in

terms of multiples of the simulation time step can be built into each module. Thus critical paths can be examined. Thus for a module i, with inputs x and outputs Y (y representing the previous state of the output).

$$[Y_{i1}, Y_{i2}, \ldots Y_{in}] = f_i[(x_{i1}, x_{i2}, \ldots x_{im}),(y_{i1}, y_{i2} \ldots y_{in})] \quad (4.1)$$

During simulation any module can be monitored. Parameters within modules can be altered to examine their effect on the performance of the receiver.

Simulation of the receiver hardware requires software modelling to the appropriate accuracy. Due to the sheer amount of data to be processed, simplifications have been made. The spiral antennae field patterns have been defined by simple exponential functions of direction. The model can be refined to include frequency effects of beamwidth and gain or gain variations due to non ideal siting. An RF amplifier has been defined with a fixed gain and perfect limiting characteristic above a defined power level. Again gain variations with frequency could be modelled. Harmonic generation on limiting can also be modelled.

The simulation of the processor could be done to machine cycle level, however the operation of the processor can be modelled at a higher hierarchical level. This allows a high level representation of the software to be operated in a block, where the block size is determined by interaction with hardware. This allows simpler implementation of algorithms. Timing of the algorithm

has to be calculated within the algorithm, by counting the equivalent number of machine cycles that would be necessary for each operation. By assigning deadlines for each process, overload situations can be examined.

The simulator is used to compare and evaluate receiver designs in chapter 5.

The simulation of 1 second using a 250 ns step size requires the entire system to be simulated at 4 million points. On the microcomputer used, simulation at each point averaged at half a second, thus only a relatively short simulation time can be examined.

5. RECEIVER DESIGN

Two receivers have been designed incorporating the previously discussed techniques. A complete RWR design is presented including the prototype hardware and actual test data. A paper design is presented for an adaptive ESM receiver. Both receivers have been simulated in software to demonstrate the performance and feasibility of these configurations.

5.1 THE RADAR WARNING RECEIVER DESIGN

Description

A radar warning receiver gives an indication of the presence of specific threat radars with known characteristics. This role allows the RWR to be simpler than the ESM receiver though it operates in the same radar environments. The RWR is used on small aircraft or vehicles and is required to be physically small. Thus a simple architecture was adopted, to gain a high pulse throughput from a small amount of hardware.

The system (figure 5.1) consists of four spiral antennas each connected in turn, via a four way switch, to a Digital Amplitude and Frequency Measurement unit (DAFM). This outputs measurements on each pulse received as a digital word. This word is transmitted to the processor via a high speed link.

The processor consists of a CPU, an output interface and a fast hardware front end containing look-up tables to identify radars from the frequency and PW measurements.

The look-up tables are programmable by library data which is generated separately on a microcomputer. Fig. 5.1 shows the schematic diagram of the RWR.

5.1.1 The measurement subsystem

The cost and size of the RWR is largely dictated by the microwave front end. As the threat radars cover a large band, broadband components, specifically 6 to 18 GHz, are used to give overall coverage with the same hardware. Thus broadband spiral antennas are used for interception. DOA measurement can be achieved by comparison of the signal amplitudes in each of four antennas. Amplitude measurement is performed by detection, amplification and digitisation of the signal. A video logarithmic amplifier (DLVA) provides a large dynamic range of measurement (40 dB).

An IFM can be used to measure the signal frequency, however RWR cost considerations lead to a choice between either instantaneous frequency measurement or instantaneous direction. The system presented has a single IFM which is shared between the four antennas by a microwave switch. This has been chosen because frequency, in addition to a sorting parameter, is an important radar identifier, and is therefore vital for the RWR role. The DOA of a radar can still be measured but it must be derived after one complete scan of the antennas and cannot be used for deinterleaving. The DOA is still useful as an indication of the direction of the threat radar.

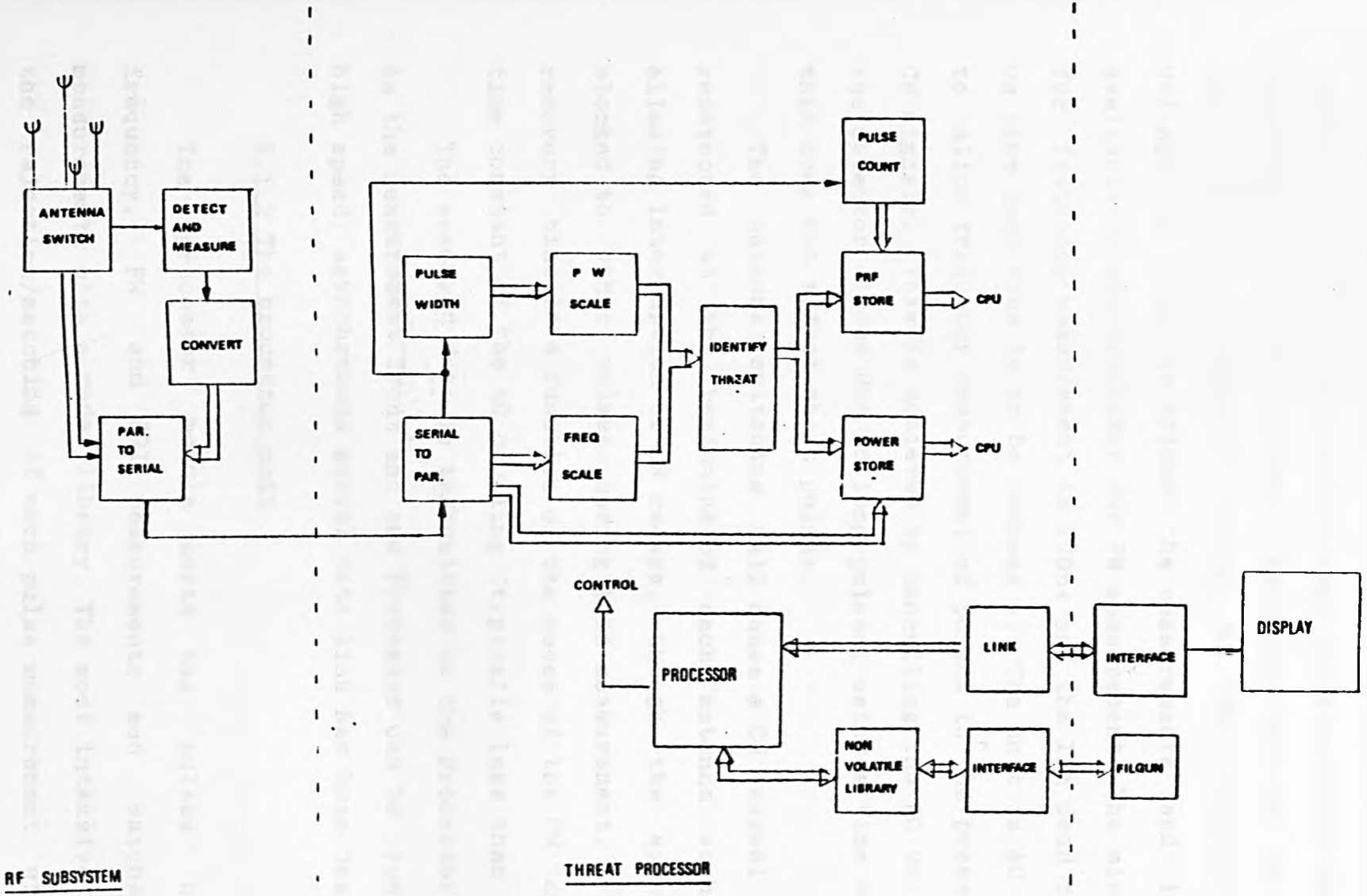

FIG. 5.1 RWR SYSTEM

The IFM unit used provides 8 bit measurement of frequency over the 6 to 18 GHz range and also 6 bit amplitude measurement over 30 dB range. This unit operates in a wide open mode as discussed in chapter 2. The detected video voltage is used to trigger the measurements and is also available to the processor for PW measurement. The minimum PW for frequency measurement is 100ns and the IFM dead time 10 us (the dead time is to be reduced). The unit is AC coupled to allow frequency measurement of pulses in the presence of CW signals. This is achieved by cancelling the DC voltage on the detector diodes due to long pulses, using a time constant that does not affect short pulses.

The antenna switching will cause a CW signal to be redetected at the beginning of each antenna scan, thus allowing interception of CW radars, though the system is blocked to other pulses during this measurement. The CW recovery time is a function of the power of the CW and the time constant of the AC coupling (typically less than 1ms).

The measured data is transmitted to the Processor unit. As the measurement front end and Processor can be remote, a high speed, asynchronous serial data link has been designed.

5.1.2 The processor unit

The processor module sorts the pulses by the frequency, PW and PRI measurements and matches the measurements with a radar library. The most intensive task is the rejection/matching of each pulse measurement with the

library radars. The design aim was to operate in environments with several hundred thousand pps. A low cost processor would not be able to compare each pulse descriptor with each library entry at this rate. Thus a fast, hardwired front end sorts the pulses into separate radar types. This reduces the processing demand on the processor, which performs the final deinterleaving and control functions.

The front end processor is simply implemented with high speed memory, used as lookup tables. The lookup tables are preprogrammed to output the number of the radar corresponding to the pulse measurements on the input. This achieves instant separation of these radar types from the background of pulses which do not fit into these groups.

This provides two dimensional pulse grouping on the basis of frequency and PW. A lookup table to perform this on an 8 bit frequency word and 10 bit PW word would require to be 256,000 entries long. This can be dramatically reduced by noting that the library characteristics will not use every frequency or PW word and also that the PW measurement is far less accurate (chapter 2). Thus both the frequency and PW measurements can be mapped onto a smaller set of numbers (figure 5.2).

The frequency look-up table is generated by entering a unique number against the frequency of each radar in the library. This number is also assigned to the frequency error bounds to account for measurement error. Similarily the pulse width is mapped to a width number.

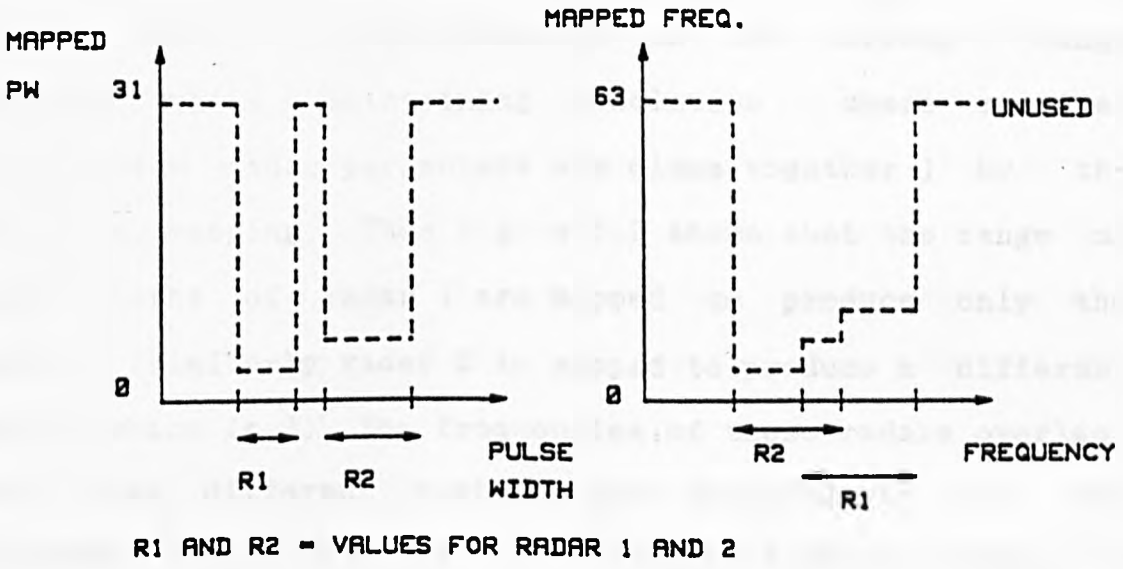

FIG. 5.2 NON LINEAR MAPPING

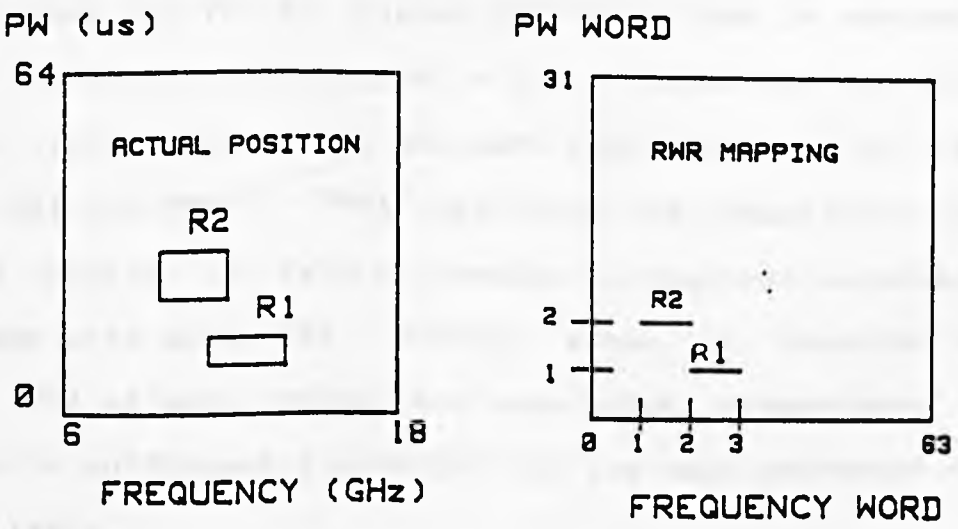

FIG. 5.3 PW / FREQ. MAP FOR RWR

This achieves a large reduction in the mapping range required while maintaining resolution where required (i.e where radar parameters are close together) by the non linear mapping. Thus figure 5.2 shows that the range of pulse widths of radar 1 are mapped to produce only the number 1 (similarly radar 2 is mapped to produce a different number, which is 2). The frequencies of these radars overlap. Thus three different numbers are assigned to the the frequency range, because the overlapped frequency range is given a unique number.

A further lookup table maps the frequency and pulse width numbers to the radar number (fig. 5.3). This shows that in the two dimensional mapping the two radars do not overlap and pulses are separated correctly for each radar. However only one radar can be recognised per frequency/PW combination. Thus if two (or more) radars overlap in both frequency and PW the higher priority radar is assumed.

Each pulse is assigned a radar number and can be sorted into pulse groups with the same radar number, to calculate the PRI and DOA. TOA algorithms can potentially give the best results but fast processing is required especially for radars with agile PRI. Storage space is required to store the TOA of each pulse and associated parameters. At the time a sufficiently powerful but low cost processor was not available.

For the simplest implementation the pulse count and average amplitude is stored in RAM for each radar number and

antenna. The processor only calculates the average PRI based on the frequency/PW combinations being unique i.e an interfering radar does not exist within the same bounds as the radar to be detected. Errors occur when radars overlap on both these pulse parameters and when the pulse density is high causing pulse blocking. Therefore the PRI measurement is not accurate but works equally for stable, staggered or jittered PRI radars.

This method achieves a very high throughput -capable of half a million pulses per second. Radars can only be recognised if they are within the library. The number of radars in the library is limited by storage space and the size of the architecture which has been chosen to be 8 bit given the availability of VLSI ICs (8 bit gives 256 radar modes).

The library is generated on a microcomputer. Software processes the library information and includes measurement error bounds and radar priority, which minimises extra processing required by the RWR.

The Z80 based CPU examines the radar stores and resets them for the next scan. The memory is duplicated giving access alternately every scan to the front end and the CPU. The CPU calculates the DOA by comparing the average amplitude measured in the four antenna, for each radar within one scan. This is used to give DOA to better than 45 degrees. Again, if simultaneous radars of the same type are present errors can occur e.g a radar at 0 degrees and the same type

at 90 degrees can be indicated as one radar at 45 degrees. If radars of the same type are clustered, then the correct DOA will be indicated with a greater PRF.

The scan time has been chosen as 40ms which allows a pulse count from 500Hz to 25kHz to be stored in 8 bit architecture while still having an acceptable intercept time. The processor accumulates the counts of each radar to allow low PRF or scanning radars to be intercepted. Two PRI modes are allowed for each radar - search mode and locked on mode. The search mode will give a lower count than the locked on mode. Locked on radars are given maximum priority.

ELINT categories (Electronic Intelligence) can also be defined. Frequency and PW ranges are defined. The frequency and PRI of the first radar to fall within these bands of interest is recorded. This allows a limited ESM capability.

Radar blanking is used to reduce the extent of own radar transmissions interfering with the RWR. This is achieved by isolating the DAFM from the antennas.

5.1.3 Hardware design

The processor unit has been designed as four boards communicating via a backplane (figure 5.4). These are the DAFM link board, the mapping board, the threat processor board and the CPU board. The processor unit sends the description of the detected radars to the display or RS232 interface modules. A solid state cartridge has been designed to transfer the library from the microcomputer to the RWR. The processor and display modules have been prototyped

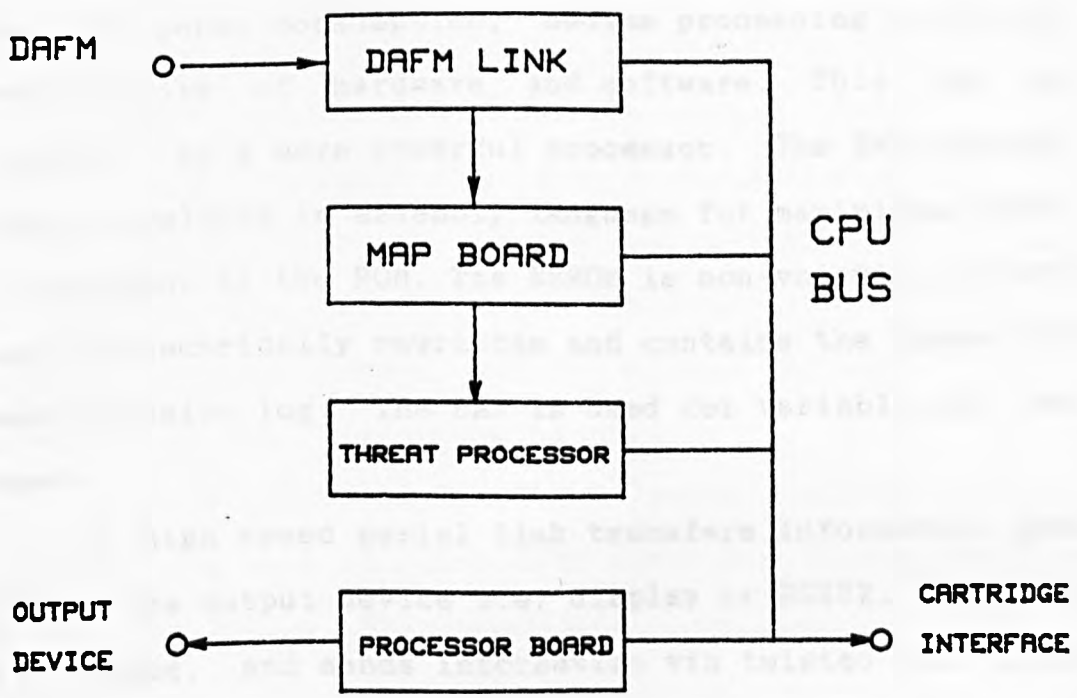

FIG. 5.4 RWR PROCESSOR CONFIGURATION

on Multibus boards.

The CPU board

The CPU board is based on a Z80A microprocessor with 2K RAM, 4K ROM and 8K EEROM. The Z80 operates at 4MHz and has a processing rate of 0.5 MIPs. The Z80 was chosen because of the low power consumption, medium processing power and the availability of hardware and software. This can now be replaced by a more powerful processor. The RWR program has been developed in assembly language for maximimum speed and is resident in the ROM. The EEROM is non-volatile memory that can be electrically rewritten and contains the threat library and a mission log. The RAM is used for variable and pointer space.

A high speed serial link transfers information from the CPU to the output device i.e. display or RS232. This operates at 2 Mbaud, and sends information via twisted pair lines via differential drive for noise immunity. To minimise the transfer time, DMA is used.

A cartridge interface allows loading or unloading of a radar library from an external cartridge through the CPU bus.

Address buffering and decoding is provided for the control of the boards within the module via the CPU bus. Programmable Array Logic (PAL) and low power Schottky TTL have been used to implement the glue logic.

The processor receives an interrupt every 40 ms which synchronises the software to the antenna scan and hardware

changeovers. Thus the CPU must complete processing within one scan time.

The DAFM link

This board provides a high speed link to the microwave module and also timing signals. A stable crystal oscillator at 16 MHz provides clock signals for the processor unit. A 25 Hz signal is also derived which controls the antenna switch, interrupts the Z80 and toggles the memory. The four antennas are scanned in turn for 10 ms with guard spaces on the switching transitions. The antenna switch can be isolated completely from the antennas. This is also used for radar blanking via an external control signal corresponding to the waveform of the radar to be blanked.

The datalink is 4 Mbaud serial asynchronous, and receives 14 bits of pulse data from the measurement module i.e. the pulse frequency and amplitude. False start prevention circuitry and differential drive provide noise immunity.

The mapping board

This board matches each pulse to a radar type in the library or rejects the pulse. This is done on a pulse by pulse basis and is achieved by fast look up tables as shown in figure 5.5.

The pulse width of the detected signal is measured by a counter giving a 10 bit word with 60ns resolution. The PW word and the 8 bit frequency word address two high speed RAMS

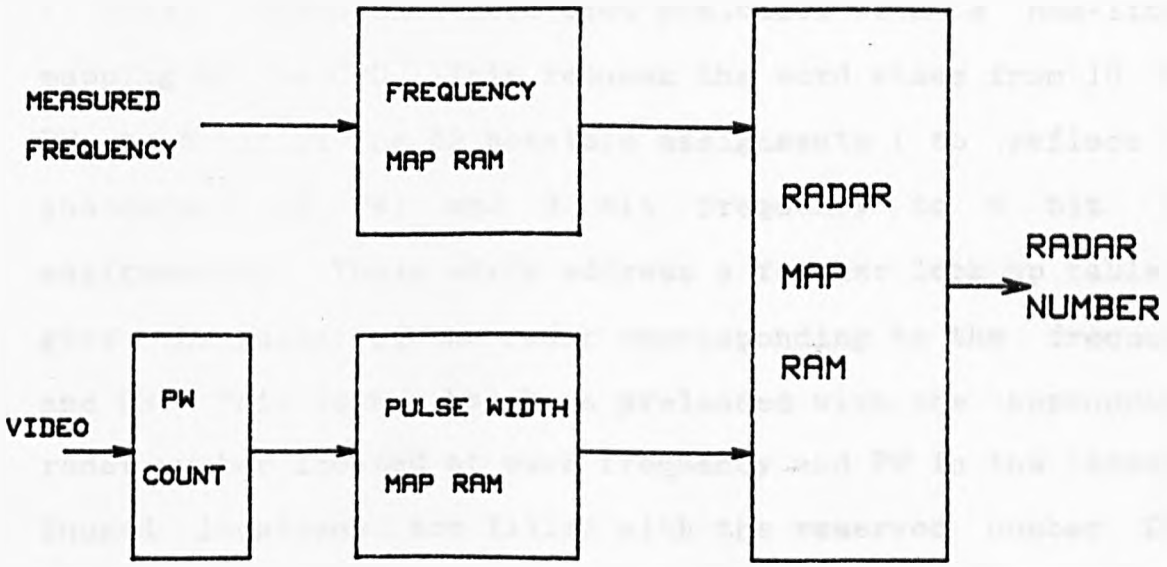

FIG. 5.5 MAPPING BOARD SCHEMATIC

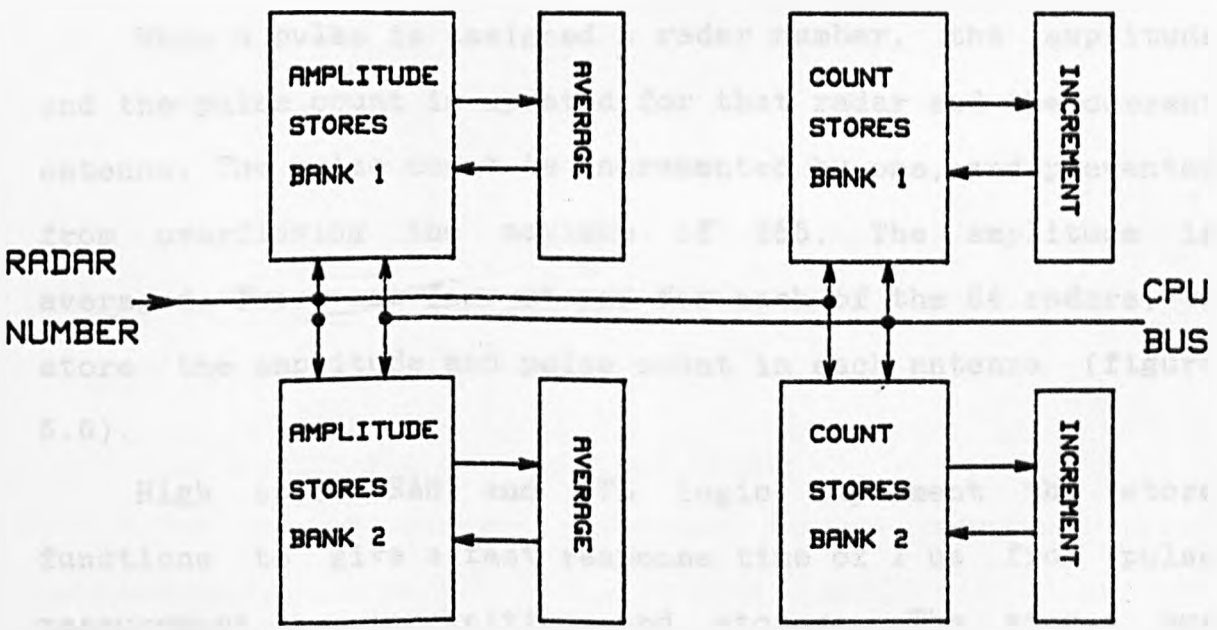

FIG. 5.6 THREAT PROCESSOR SCHEMATIC

(70ns). These RAMs have been preloaded with a non-linear mapping by the CPU. This reduces the word sizes from 10 bit PW to 5 bit giving 32 possible assignments (to reflect the inaccuracy of PW) and 8 bit frequency to 6 bit (64 assignments). These words address a further look up table to give the number of the radar corresponding to the frequency and PW. This lookup has been preloaded with the appropriate radar number located at each frequency and PW in the library. Unused locations are filled with the reserved number 255. Thus pulses which do not fit the library automatically produce the number 255 and a "PULSE REJECT" indication is given which inhibits further processing. The radar number is output onto the bus.

The threat processor board

When a pulse is assigned a radar number, the amplitude and the pulse count is updated for that radar and the current antenna. The pulse count is incremented by one, and prevented from overflowing the maximum of 255. The amplitude is averaged. There are four stores for each of the 64 radars, to store the amplitude and pulse count in each antenna (figure 5.6).

High speed RAM and TTL logic implement the store functions to give a fast response time of 1 us from pulse measurement to recognition and storage. The stores are duplicated and have multiplexed address and data lines. The Z80 accesses and resets one set whilst the other set is available to the front end. The stores are interchanged every

40 ms.

The display module

The display gives a quick warning of radar threats to a pilot or operator. It consists of three rows of four LED characters. This displays three letter library names for the three highest priority threats identified and an arrow representing the direction of the radar to within 45 degrees.

The display and keys are controlled by a Z80 microprocessor via a Peripheral I/O device (Intel 8255). A high speed serial link communicates with the processor unit to allow the display of detected radars.

RS232 interface module

An RS232 standard interface was designed around a Z80 and Motorola 6850 interface IC. This was for the dual purpose of providing a detailed output of detected radar characteristics and providing an interface between the microcomputer and the cartridge. The module contains a high speed serial interface and a cartridge interface. This unit allows the RWR to output onto a printer.

The ground station computer system

The ground station computer system consists of a microcomputer with VDU, disk drives, RS232 interface and cartridge programmer. Menu driven software has been written to allow entry of radar libraries and programming of cartridges. Radar libraries can be edited and stored on disk.

Radar parameter ranges are entered, highest priority first. The software automatically adds error bounds. A map of frequency versus PW shows the position of all the radars. The software formats the information and programs the cartridge via the RS232 interface.

5.1.4 Test results

This system has been built and tested to examine its performance. Sample test results are shown in figure 5.7. These show the RWR ouput when irradiated by test signals operating over the full RWR parameter ranges. The radar library consists of radars with overlapping parameters either in frequency or PW and radars with similar parameters (appendix A.2).

The testing has shown that the RWR can identify many emitters, including agile radars, with DOA accuracy to 45 degree sectors. The RWR, however, has poor performance when several radars are present which overlap in both frequency and PW. This occurs when more than one radar of the same type is present. A significant improvement can be gained by implementing TOA deinterleaving . This would be able to resolve overlaps by PRI determination and also improve the DOA accuracy by rejecting pulses that are not part of the pulse sequence.

This can be implemented simply by replacing the pulse count and amplitude stores with a larger memory. The TOA and amplitude of every pulse is stored for each radar number in each antenna. This would require a faster processor, which is

		TEST SIGNAL						
		1	2	3	4	5	6	7
IDENTIFIED	1	80	-	-	-	-	-	-
SIGNAL	2	-	100	-	-	-	-	-
(% TIME)	3	20	-	100	4	-	-	-
	4	-	-	-	96	-	-	-
	5	-	-	-	-	100	-	-
	6	-	-	-	-	-	100	-
	7	-	-	-	-	-	-	100

SIGNAL	FREQ. RANGE (GHz)	PW (us)	PRI (kHz)	TYPE
1	6 - 6.1	0.1	30	
2	17.9 - 18	64	0.2	
3	6.2 - 6.3	0.1	1	
4	6.2 - 6.3	2	1	
5	10.3 - 11	-	-	CW
6	8 - 8.1	15	1	Scanning
7	9 - 9.2	30	-	ELINT

FIG 5.7 TABLE OF MEASURED RWR TEST RESULTS

now feasible with the advent of high speed 16 bit processors such as the Motorola 68000 and the Inmos Transputer. This configuration has been designed incorporating the SDIF2 deinterleaving algorithm (appendix A.3). Both configurations have been simulated and the improved results are given below. This shows the ability to resolve similar radars or radars whose parameters overlap, in real time with a fast response time.

Simulation with Scenario 1

The simple RWR was simulated using the environment generated in appendix A.4.

The environment contains eleven radars including identical radars at different relative directions as shown in figure 5.8 (e.g TR1) with a total pulse density of 70,000 pulses/sec. The RWR system has a measurement dead time of 10 us i.e a maximum pulse processing density of 100,000 pulses/sec. The antenna scan time is 40 ms with a 10ms dwell on each antenna.

The radar library was programmed to detect ten of the radars, using the ground station software program. The library includes an ELINT entry and non locked / locked PRI modes. This library was loaded into the RWR simulation (as in practice on the real system).

The result of 40ms of simulation time in figure 5.9 shows the detected radars. All the radar types but TR6 were detected. TR6 is not detected as the pulse count on this scan is below the detection threshold.

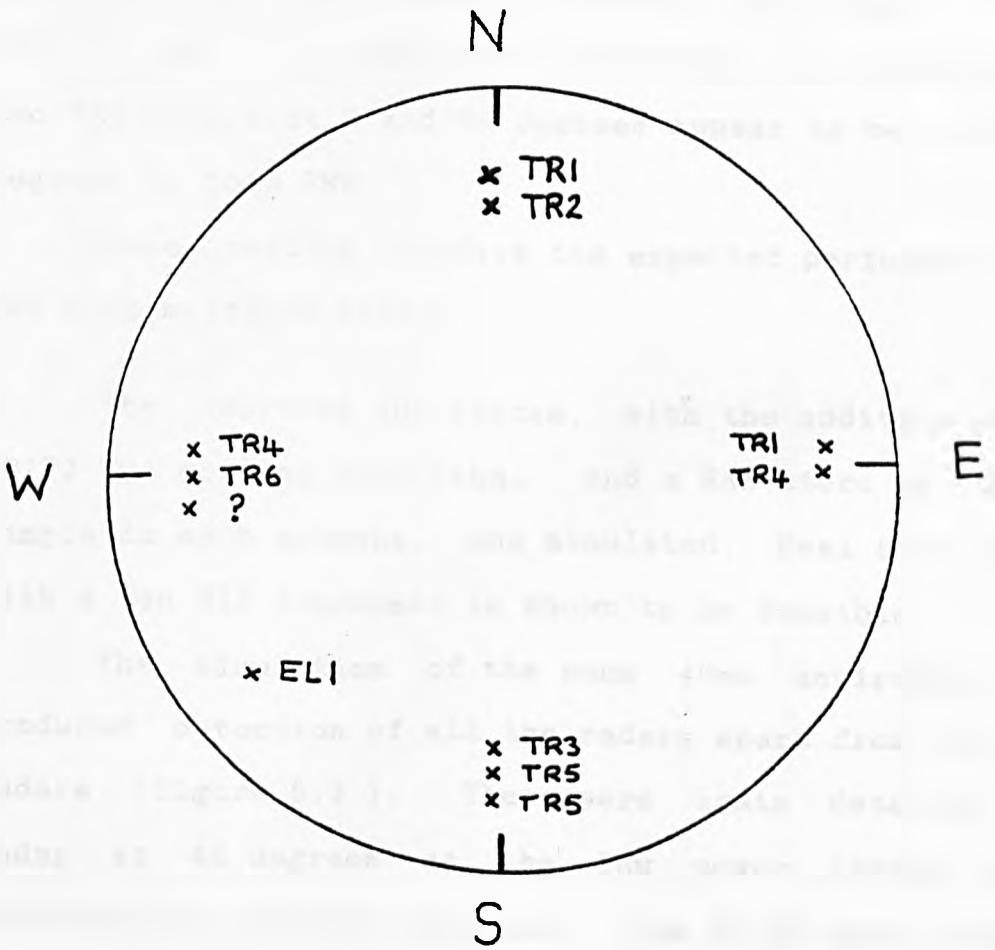

FIG. 5.8 MAP OF THE SIMULATED RADARS

The RWR was designed to only detect one of each radar type, due to the limitations of antenna switching. Thus for TR1,TR4 and TR5 only one of each radar is displayed. The two TR1 radars at 0 and 90 degrees appear to be one TR1 at 45 degrees to this RWR.

These results confirm the expected performance of the RWR with multiple radars.

The improved RWR system, with the addition of the SDIF2 TOA sorting algorithm, and a RAM store of the pulse sample in each antenna, was simulated. Real time operation with a ten MIP processor is shown to be feasible.

The simulation of the same 40ms environment sample produced detection of all the radars apart from the two TR1 radars (figure 5.9). These were again detected as one radar at 45 degrees as the low power levels prevented detection in adjacent antennas. The ELINT radar entry was detected at half the PRF in the West antenna due to excessive missing pulses. Thus it was not combined with the detection in the South antenna to give the correct DOA.

The PRI accuracy is very high especially when compared with the pulse counting method. The simulation demonstrates the substantial improvement in performance achieved by the TOA sorting algorithm.

The RWR outputs from each scan would be averaged over 5 to 10 scans to give greater confidence levels and this would remove certain errors in the RWR output over single scans as

Radar Type (Direction)	TR1 (N)	TR1 (E)	TR2	TR3	TR4 (E)	TR4 (W)	TR5 (S)	TR5 (S)	TR6	EL1
RWR 1	Y	N	Y	Y	Y	N	Y	N	N	Y
RWR 2 (TOA sorting)	Y	N	Y	Y	Y	Y	Y	Y	Y	Y
ESM Receiver	Y	Y	Y	Y	Y	Y	Y	Y	Y	Y

Y = identification of radar
N = incorrect or no identification of radar

FIG 5.9 TABLE OF RESULTS WITH SIMULATION SCENARIO 1

above. This was not practical on the simulation due to the speed and size restrictions of the microcomputer.

5.2 The ESM Receiver

The design of an ESM receiver to operate in high pulse density environments is presented with particular emphasis on the processor. The design incorporates algorithms and architectures discussed in the previous chapters.

The requirements of an advanced ESM receiver were detailed in chapter 2. The measurement system will clearly be based on instantaneous measurement of high resolution frequency and DOA. The measurement system will be channelised in frequency such that the pulse density in any given channel will not cause excessive errors e.g. 2-6 GHz, 6-10 GHz, 10-14GHz, 14-18 GHz. Channelisation in this way is assumed to reduce the pulse density to the order of 250,000 pps average and 500,000 pps peak.

The IFM is most suitable for wideband high resolution frequency measurement, and bandfolding or switching may be used to minimise the hardware. A broadband interferometer or multiport (6 or 8) antenna amplitude comparison will provide high resolution, instantaneous DOA. A fast measurement time is required to minimise pulse blocking i.e. in the order of 200 ns. The measurement system should also incorporate intelligent RF processors such as a superhet or switched multiplexer and a device to measure CW signals,however these are outside the scope of this research.

A very high speed link (parallel or serial optical) transmits the frequency, DOA, TOA and PW measurements to the processor. The processor uses frequency, DOA and TOA as the

main sorting parameters. The processor presented essentially comprises high speed, high density RAM and software algorithms operating on high speed microprocessors.

Separate processors are dedicated to grouping, to TOA deinterleaving and to the final classification. The data is pipelined through the hardware to minimise the dead time and can be made similar to the measurement system dead time (200ns).

It is proposed that the processor is simple so that several units can be paralleled (i.e one per channel) to achieve very high throughput. The Inmos Transputer microprocessor is well suited due to the parallel processing capability. One processor will be required for the grouping process and a cluster of four processors for TOA sorting.

Figure 5.10 shows the basic processor design.

The first processing stage is mapping of the frequency/DOA values. PW is not used as it has been shown to be unreliable in high pulse densities. The cell map (RAM) begins empty. As each pulse accesses the map, a cell number is written to empty locations and the cell counter incremented. Subsequent pulses with the same frequency and DOA will automatically give the same cell number. A cell memory is formed giving the frequency, DOA and pulse count corresponding to each cell number used. A pulse memory lists the cell number, frequency, DOA, PW, TOA and amplitude of each pulse.

The grouping processor has access to the map, the cell

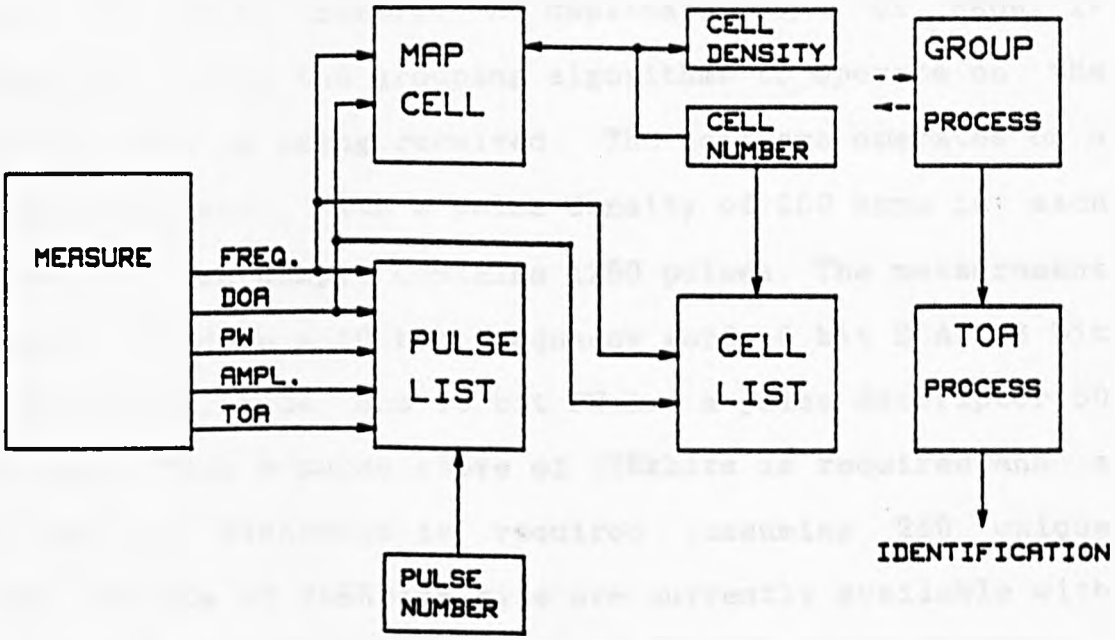

FIG. 5.10ESM RECEIVER SCHEMATIC

memory and pulse memory. A duplicate bank of RAMs is necessary to allow the grouping algorithms to operate on the map while data is being received. The software operates on a sample of pulses. With a pulse density of 250 kpps in each sub-band a 5 ms sample contains 1250 pulses. The measurement system can produce a 10 bit frequency word, 8 bit DOA, 16 bit TOA, 6 bit amplitude, and 10 bit PW i.e a pulse descriptor 50 bits long. Thus a pulse store of 128kbits is required and a cell map of 256Kbytes is required (assuming 256 unique cells). RAM ICs of 256Kbits size are currently available with 100ns access time. Hardware mapping on each pulse provides a considerable saving in software processing, by reducing the amount of searching needed to match the pulses.

The density-led grouping algorithm, developed in chapter 3 forms clusters of cells in the map within measurement tolerance (the cells are themselves groups of pulses). The pulses are separated into their respective clusters and the pulse list reassembled in TOA order by the grouping processor. The blocks of pulses are transferred to the TOA processors via high speed memory.

The grouping process changes the cell numbers in the map to reflect the cell clusters (as shown previously in fig. 3.7) and thus subsequent pulses are automatically clustered by the mapping. Grouping needs only to be carried out on newly activated cells. By noting the number of cells, the new cells are known. The constituent cells and centre of gravity of each cluster is stored and new cells are grouped against

these existing clusters. Thus the processing load reduces considerably with time. Cells with zero count can be deleted after a given time to free the cell store. This achieves adaptive clustering of the radar pulses.

The TOA processor deinterleaves the pulse sequences within each of the clusters and determines the PRI. This is very intensive as every pulse must be processed as opposed to every cell in the grouping process. The TOA algorithm CDIF/SEQUENCE developed in chapter 3 is proposed for accurate, real time deinterleaving. This sequentially extracts stable PRI sequences, followed by staggered, scanning and jittered with residual pulses being passed through each stage. Finally any residue is passed to a frequency agile grouping process. This uses the same grouping algorithm but combines pulses within frequency agile distance. These recombined pulses are passed though the TOA deinterleaver. If a sequence is found the TOA process instructs the grouping process to reassign the cluster map, providing automatic agile grouping of subsequent pulses. This two pass grouping process is proposed in favour of clustering at frequency agile level initially. This is to prevent forming clusters which are too large for TOA sorting or for detection of fixed frequency radars.

Learning is used within the TOA deinterleaver. Pulse groups where radars have previously been found are searched for the same sequences before applying the full algorithm. This provides a substantial reduction in processing and a

higher detection probability. The algorithm has been optimised by the use of a common histogram and common procedures for the stable and agile PRI deinterleaving. When a search for a particular PRI has been unsuccessful, further searching for that PRI in the sample is inhibited. Integer arithmetic, especially addition or subtraction, has been used wherever possible.

The average value and the variance of the pulse parameters in the sorted pulse trains are calculated. These values (f, DOA, TOA, PRI, PW, and Amplitude) are passed onto the final process. This process joins chains together and performs further analysis to classify the radars against library information e.g scan analysis. The detection can then be output and used to prime an ECM system or recorded for library intelligence.

5.2.1 Test results

This receiver has been simulated with the relatively simple environment used to test the RWR (scenario 1, 68,000pulses). This has shown full, accurate identification (figure 5.9). However, the high duty cycles and the lack of spatial filtering due to instantaneous 360 DOA coverage gives a missing pulse ratio of 41%, causing detection of two PRI harmonics. These would be corrected over several scans. The sorting algorithms are efficient, requiring a simulated processing rate of 25 MIPs including agile searches and using no prior ESM knowledge unlike the RWR.

Simulation of ESM receiver with Scenario 2

This scenario is more complex than Scenario 1, with an average pulse density of 140,000 pulses/s from 10 radars. The radars include frequency agile, scanning, high PRF, staggered PRI and jittered PRI radars (appendix A.4). Several radars have similar characteristics.

Initially, the frequency agile radars and the jittered PRI radar caused unforeseen problems for the TOA deinterleaver. The frequency agile signal crosses cluster boundaries at a regular interval causing a regular pattern in the split clusters. This gave detection and deletion of harmonics of the actual PRI. This was solved by an algorithm that recombines sequences at the agile grouping stage with the same PRI or harmonic PRI if they fit a into a lower PRI sequence. This was achieved efficiently by comparison of the sequence start times.

The jittered radar has a large number of PRI values due to its random nature. This will cause problems to most TOA deinterleavers as many unsuccessful searches will be required before it is decided that no stable sequence exists. The two level histogram/search TOA algorithm is less prone to this. By raising the histogram decision thresholds when searching for jittered signals the number of wasted searches was reduced.

The ten radars were deinterleaved and identified correctly (figure 5.11). The results of four consecutive

RADAR	Detected	Freq.	DOA	PRI	TYPE	Description -error
1	YYYY	YYYY	YYYY	YYYY	YYYY	STABLE
2	YYYY	YYYY	YYYY	YYYY	YYYY	FREQ. AGILE
3	YYYY	YYYY	YYYY	YYYY	YYYY	STABLE
4	YYYY	YYYY	YYYY	YYYY	YYNN	3 STAGGER- 2 found
5	YYYY	YYYY	YYYY	YYNY	YYYY	JITTERED -harmonic
6	YYYY	YYYY	YYYY	YYYY	YYYY	STABLE
7	Y---	Y---	Y---	Y---	Y---	SCANNING
8	YYYY	YYYY	YYYY	YYYY	YYYY	STABLE
9	NYYY	-YYY	-YYY	-YYY	-YYY	STABLE -not found
10	YYYY	YYYY	YYYY	YYYY	YYYY	FREQ. AGILE

The results for 4 samples are indicated by :

Y = Correct identification
N = Incorrect or no identification
- = Not applicable

5.11 TABLE OF ESM SIMULATION WITH SCENARIO 2

samples are shown. Reliable detection occurs. The small proportion of errors as indicated (lack of detection due to missing pulses) in single samples can be removed over the set of samples.

The increasing efficiency due to the adaptive algorithms was also shown. For a 2.5ms sample with 1us sample interval the grouping process required real time processing at 1 MIP, dropping to 0.5 MIPs and the TOA deinterleaving 60 MIPs both dropping to 20 MIPs with time (i.e. with learning). This can be reduced by a further factor of 2 by optimising the histogram clearing process.

Simulation with scenario 3

A high PRF, 100 kHz radar was added to the above scenario giving an overall pulse density of 250 kpps. This was simulated and the results are shown in figure 5.12. The greater blocking rate (33% of pulses are missing) causes a greater number of missing detections, however all the radars are detected and identified over two samples. A small increase in processing time also occurs.

For a 2.5ms sample with 1us sample interval the grouping process required real time processing at 1.5 MIP, dropping to 1 MIP and the TOA deinterleaving 60 MIPs both dropping to 25 MIPs with time (i.e. with learning).

In practice, a larger number (50) lower PRF radars can be expected with a pulse density of 250kpulses/s. This would require approximately 15 MIPs for grouping and 50 MIPs for

RADAR	Detected	Freq.	DOA	PRI	TYPE	Description -error
1	YY	YY	YY	YY	YY	STABLE
2	YY	YY	YY	YY	YY	FREQ. AGILE
3	YY	YY	YY	YY	YY	STABLE
4	YY	YY	YY	YY	NY	3 STAGGER- 2 found
5	NY	-Y	-Y	-Y	-Y	JITTERED
6	YY	YY	YY	YY	YY	STABLE
7	Y-	Y-	Y-	N-	Y-	SCANNING- harmonic
8	YY	YY	YY	YY	YY	STABLE
9	NY	-Y	-Y	-Y	-Y	STABLE -not found
10	YN	Y-	Y-	Y-	Y-	FREQ.AGILE- " "
11	YY	YY	YY	YY	YY	PULSE DOPPLER

The results for two scans are indicated by :

Y = Correct identification
N = Incorrect or no identification
- = Not applicable

5.12 TABLE OF ESM SIMULATION WITH SCENARIO 3

TOA deinterleaving initially dropping to less than 8 MIPs and 15 MIPs respectively in the steady state as estimated below:

$$\text{Rate for grouping} \approx 8.(C.4 + \frac{C^2}{4} + 2.P).400$$

$$\text{Rate for TOA deint.} \approx G\left(8.\frac{N}{G} + 2N + \frac{R}{G}.(30\frac{N}{G} + \frac{N}{2}) \right).400$$

where C = no. of active cells, P = no. of pulses

G = no. of groups , R = no. of emitters

N = sample length

and assuming

$$C \approx 3.R \qquad \text{and} \qquad G \approx \frac{R}{3}$$

6.0 Conclusions

ESM receivers have been inadequate to meet the increasing pulse densities and complexity of radar environments. The high pulse densities have been shown to cause unacceptable error rates in the wide open type ESM receiver: Architectures have been compared for ESM in these conditions. A quantitative method is given for evaluating a front end measurement system and statistics presented to allow estimates of error rates and pulse blocking in order to determine the acceptable pulse density and the approach required for deinterleaving. This has shown that direction and time of arrival are the most powerful sorting paramters. Frequency is very powerful but only for the decreasing proportion of non frequency agile signals. Pulse width information is only useful in low pulse densities.

New approaches to deinterleaving complex signals have been presented, in the form of adaptive and pattern recognition algorithms. Algorithms are presented which give high accuracy, real time processing in high pulse densities. Reduction in processing has been achieved by extracting the simpler signals followed by the complex signals, and also by learning from previous information.

Complete receiver designs are presented. A Radar Warning Receiver has been built and tested. Receivers incorporating the algorithms and adaptive techniques are presented and simulation results given. These demonstrate that these

techniques combined with a simple architecture give better performance in high pulse densities than conventional ESM processors.

Further work

The conceptual design of an advanced ESM receiver has been presented. A prototype receiver can be built from this design , and ideally, tested with a real radar environment if feasible. At minimum, a Transputer based ESM processor can be built and tested with the simulation signals of an actual scenario, in order to prove that the algorithms and adaptive techniques work in these conditions.

Further work can be undertaken on applying intelligent techniques to minimise the effects of simultaneous signal errors, by indication from the measurement system and processing as opposed to discarding the measurement errors.

As new techniques emerge, new types of radar with different agilities will be used. Thus the measurement architectures and deinterleaving algorithms must be extended to cope with new problems. This will require measurement of more parameters (such as modulation within pulse) and sorting by these parameters can be added using the n- dimensional grouping algorithms developed.

New technologies such as acousto-optic analysers and SAW channelisers will also produce better measurement devices with higher resolution and simultaneous signal performance for a given size and cost and these can be encompassed in the receiver design. Fast superhets and switchable channelisers

will allow direct manipulation of the pulse environment at RF, with the ESM processor giving intelligent allocation of the measurement resources. Thus the concept of adaptivity can be extended from the processor to the complete receiver.

APPENDICES

Appendix A.1 DOA accuracy calculation

The DOA is determined by amplitude comparison of the logged, detected power received from two adjacent antenna, orientated at different angles [21].

The voltage pattern of a spiral antenna is approximately Gaussian in shape i.e.

$$G_1(\theta) = A_1 \exp\left(-k^2 \frac{(\theta-\alpha)^2}{\theta_B^2} \right)$$

$$G_2(\theta) = A_2 \exp\left(-k^2 \frac{(\theta+\alpha)^2}{\theta_B^2} \right) \qquad \text{(A1.1)}$$

where

$G(\theta)$ = offset gain pattern

A^2 = boresight antenna gain

α = squint angle (half the angle between antenna boresights)

θ_B = the 3dB beamwidth

$k^2 = \ln(4)$ as $G^2\left(\frac{\theta_B}{2}\right) = 0.5\, G^2(0)$

The ratio of powers in adjacent antennas determines the DOA

$$R\ (dB) = 10 \log \frac{G_1^2(\theta)}{G_2^2(\theta)} = 20 \log \frac{A_1}{A_2} + 20 \log e . \frac{k^2}{\theta_B^2} . 4.\theta\alpha \qquad \text{(A1.2)}$$

The slope of relative power with DOA is

$$\frac{\delta R}{\delta \theta} = 20\ (\log e\ ).4k^2 \frac{\alpha}{\theta_B^2} \qquad \text{(A1.3)}$$

The measured amplitudes in each antenna is dependent on the signal to noise ratios (SNR) :

$$\frac{\delta A^2}{A^2} = \frac{1}{2.SNR}$$

therefore

$$\delta R = 20\ (\log e).\left(\frac{\delta A_1}{A_1} + \frac{\delta A_2}{A_2} \right) \qquad (A1.4)$$

Assuming uncorrelated noise, the r.m.s error in measuring the relative power is :

$$\sigma_R = 20\ (\log e).\sqrt{\left(\frac{1}{2.SNR_1} + \frac{1}{2.SNR_2} \right)} \qquad (A1.5)$$

The SNR in each channel is itself a function of DOA

$$SNR_1(\theta) = SNR_0 - 20\ (\log e).\frac{k^2}{\theta_B{}^2}.(\theta-\alpha)^2 \qquad (A1.6)$$

where SNR_0 = SNR at the antenna boresight

Thus the r.m.s. angle error is

$$\sigma_\theta = \sigma_R \Big/ \frac{\delta R}{\delta \theta} = \sqrt{\left(\frac{1}{2.SNR_1} + \frac{1}{2.SNR_2} \right)}.\ \frac{\theta_B{}^2}{4k^2\alpha} \qquad (A1.7)$$

Thus at the antenna crossovers $\theta = 0$

$$\sigma_0 = \frac{\theta_B{}^2}{4\ln(4)\alpha}.\sqrt{\left(\frac{1}{SNR_0 - 20(\log e)\left(\frac{k\alpha}{\theta_B}\right)^2} \right)} \qquad (A1.8)$$

and at the antenna boresights $\theta = \alpha$

$$\sigma_\alpha = \frac{\theta_B{}^2}{4\ln(4)\alpha}.\sqrt{\left(\frac{1}{2.SNR_0} + \frac{1}{2.SNR_0 - 160(\log e)\left(\frac{k\alpha}{\theta_B}\right)} \right)} \qquad (A1.9)$$

Thus the following results are obtained with a 30dB SNR

TABLE A1.1 DOA accuracy for amplitude comparision

	4 port θ_B= 75		6 port θ_B=75		6 port θ_B=50	
	θ=0	θ=α	θ=0	θ=α	θ=0	θ=α
SLOPE (dB/deg)	0.38		0.26		0.58	
σ SNR r.m.s	7.2	4.6	6.9	6.3	4.6	3.1
σ RIPPLE(1dB)	5	5	7.7	7.7	3.5	3.5
σ QUANT(.5dB)	2.6	2.6	3.8	3.8	1.7	1.7
TOTAL DOA error r.m.s	9.1	7.3	11	10.6	6.0	4.9

The following results show the DOA error caused by a signal being detected close to the amplitude measurement threshold. Due to attenuation, the power in the adjacent channel will be below the detection threshold at certain angles of arrival and thus the relative power cannot be measured.

TABLE A1.2 DOA accuracy versus power

	SIGNAL POWER ABOVE THRESHOLD (dB)	BORESIGHT ERROR deg.r.m.s	TOTAL ERROR deg.r.m.s
4 port	20	8	16
θ_B =75	10	32	40
6 port	20	5	10
θ_B =50	10	20	25

Appendix A.2 RWR test results

The RWR system described in chapter 5 was tested, using an RF oscillator, pulse modulator and horn antenna to generate test signals.

A range of RF frequencies, pulse widths, and PRIs were generated with the RWR loaded with a library containing a set of test radar parameters covering the RWR operating range. The library also contains ELINT, scanning and CW radars. The radars cover similar values in each parameter to test the sorting ability of the RWR.

The printout shows the RWR output when the antennas are illuminated by the test source. The identifier, averaged radar parameters, signal strength, DOA, locked on indication (corresponding to the second PRI entry in the library), and time of detection are displayed.

The low power signals caused an incorrect DOA reading (due to antenna attenuation, as discussed in chapter 2.1). A single programmable test source was used and the signals were intercepted though some false reports of similar radars occured.

The RWR was also tested with multiple signals (three sources) and showed the ability to identify them simultaneously.

```
NUMBER OF THREATS  6

THREAT NUMBER 0
THREAT NAME FAS
RADAR TYPE <N>ORMAL,<S>CANNING OR <C>W
FREQUENCY BAND LOWER,UPPER (6-18 GHZ)   6    6.1
PW BAND (62-64000 NS)          100            100
PRR BAND (0-30 KHZ)            30             0

THREAT NUMBER 1
THREAT NAME SLO
RADAR TYPE <N>ORMAL,<S>CANNING OR <C>W
FREQUENCY BAND LOWER,UPPER (6-18 GHZ)   17.9                  18
PW BAND (62-64000 NS)          64000          64000
PRR BAND (0-30 KHZ)            .2             0

THREAT NUMBER 2
THREAT NAME TR1
RADAR TYPE <N>ORMAL,<S>CANNING OR <C>W
FREQUENCY BAND LOWER,UPPER (6-18 GHZ)   6.2                   6.3
PW BAND (62-64000 NS)          100            100
PRR BAND (0-30 KHZ)            1              5

THREAT NUMBER 3
THREAT NAME TR2
RADAR TYPE <N>ORMAL,<S>CANNING OR <C>W
FREQUENCY BAND LOWER,UPPER (6-18 GHZ)   6.2                   6.3
PW BAND (62-64000 NS)          2000           2000
PRR BAND (0-30 KHZ)            1              5

THREAT NUMBER 4
THREAT NAME CWR
RADAR TYPE <N>ORMAL,<S>CANNING OR <C>W C
FREQUENCY BAND LOWER,UPPER (6-18 GHZ)   10.3                  11
PW BAND (62-64000 NS)          65000          66000
PRR BAND (0-30 KHZ)            0              0

THREAT NUMBER 5
THREAT NAME SCN
RADAR TYPE <N>ORMAL,<S>CANNING OR <C>W S
SCAN TIME (SECS)  1
FREQUENCY BAND LOWER,UPPER (6-18 GHZ)   8    8.100001
PW BAND (62-64000 NS)          15000          15000
PRR BAND (0-30 KHZ)            1              0

NO. OF ELINTS 1

THREAT NUMBER 6
THREAT NAME EL1
FREQUENCY BAND LOWER,UPPER (6-18 GHZ)   9    9.2
PW BAND (62-64000 NS)          30000          30000
PRR BAND (0-30 KHZ)            0              0
```

FIG. A.2.1 RWR TEST RADAR LIBRARY

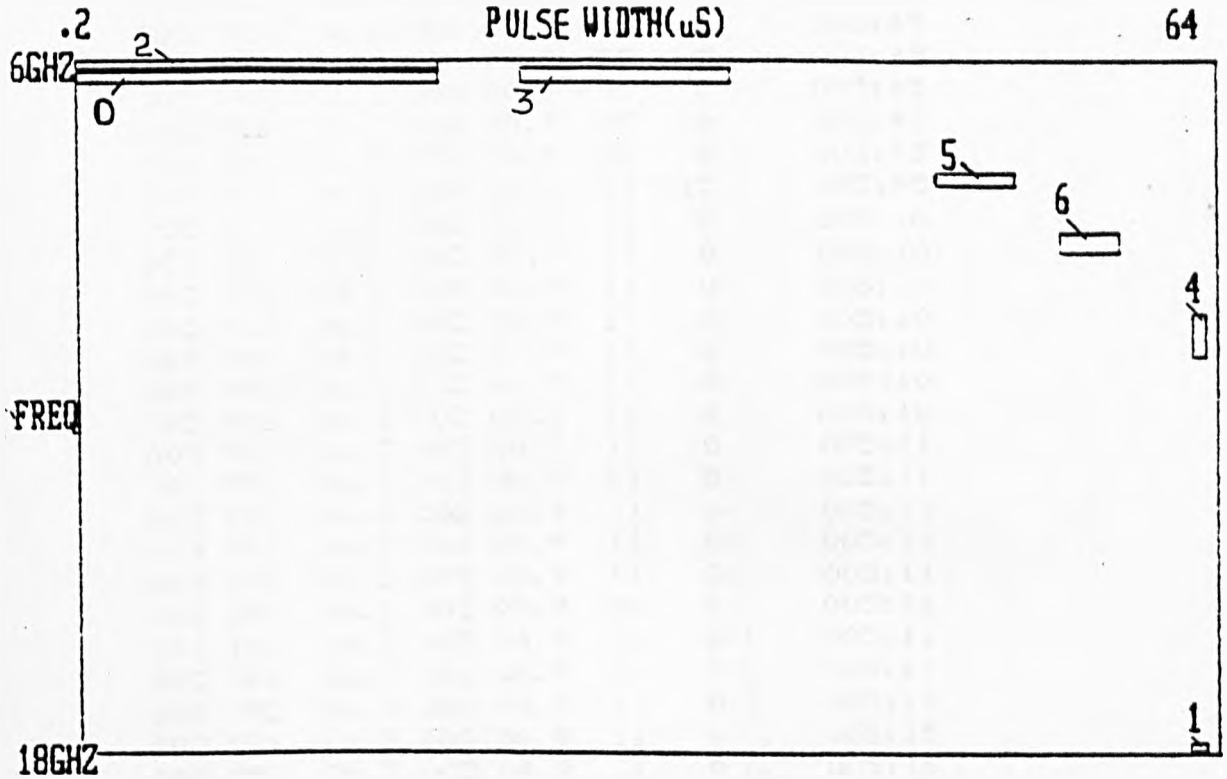

FIG. A.2.2 RWR FREQUENCY/PW MAP

NO	CODE	FREQ GHZ	PW US	PRI KHZ	AMP DBM	DIR DEG	LOCK Y/N	TIME MMM:SS
002	TR1	06.3	000	00.9	-05	0		003:45
002	TR1	06.3	000	00.9	-05	0		003:45
002	TR1	06.3	000	00.9	-05	0		003:45
002	TR1	06.3	000	00.9	-05	0		003:45
002	TR1	06.3	000	00.9	-05	0		003:45
002	TR1	06.3	000	00.9	-05	0		003:45
002	TR1	06.3	000	00.9	-05	0		003:45
002	TR1	06.3	000	00.9	-27	315		003:45
003	TR2	06.3	002	00.9	11	0		005:10
003	TR2	06.3	002	00.9	11	0		005:10
003	TR2	06.3	002	00.9	11	0		005:10
003	TR2	06.3	002	00.9	11	0		005:10
003	TR2	06.3	002	00.9	11	0		005:10
003	TR2	06.3	002	00.9	11	0		005:10
003	TR2	06.3	002	00.9	11	0		005:10
003	TR2	06.3	002	00.9	11	0		005:11
003	TR2	06.3	002	00.9	11	0		005:11
003	TR2	06.3	002	00.9	11	0		005:11
003	TR2	06.3	002	00.9	11	0		005:11
003	TR2	06.3	002	00.9	11	0		005:11
003	TR2	06.3	002	00.9	11	0		005:11
003	TR2	06.3	002	04.9	11	0	L	005:11
003	TR2	06.3	002	04.9	11	0	L	005:11
003	TR2	06.3	002	04.9	11	0	L	005:11
002	TR1	06.3	000	00.9	11	0		005:15
003	TR2	06.3	002	04.9	11	0	L	005:18
003	TR2	06.3	002	04.9	11	0	L	005:18
003	TR2	06.3	002	04.9	11	0	L	005:18
003	TR2	06.3	002	04.9	11	0	L	005:18
003	TR2	06.3	002	04.9	11	0	L	005:18
003	TR2	06.3	002	04.9	11	0	L	005:18
003	TR2	06.3	002	04.9	-28	0	L	005:18
004	CWR	10.7	061	00.1	-25	315		006:59
004	CWR	10.7	061	00.1	-25	315		006:59
004	CWR	10.7	061	00.1	-28	225		007:22
004	CWR	10.7	061	00.1	-24	315		007:24
004	CWR	10.7	061	00.1	-25	315		007:24
004	CWR	10.7	061	00.1	-25	315		007:25
004	CWR	10.7	061	00.1	-27	315		007:25
000	FAS	06.1	000	25.0	-03	45		012:29
000	FAS	06.1	000	25.0	-03	0		012:30
000	FAS	06.1	000	25.0	-03	45		012:30
000	FAS	06.1	000	25.0	-03	45		012:30
002	TR1	06.3	000	00.9	-04	0		012:30
000	FAS	06.1	000	25.0	-03	45		012:30
002	TR1	06.3	000	00.9	-07	0		012:30
000	FAS	06.1	000	25.0	-03	0		012:30
000	FAS	06.1	000	25.0	-03	0		012:30
005	SCN	08.1	016	00.4	00	0		013:19
005	SCN	08.1	016	00.4	-28	0		013:19
005	SCN	08.1	016	00.4	-28	0		013:19
005	SCN	08.1	016	00.4	-28	0		013:19
005	SCN	08.1	016	00.4	-28	0		013:19
005	SCN	08.1	016	00.4	-28	225		013:19
005	SCN	08.1	016	00.4	-28	225		013:19
005	SCN	08.1	016	00.4	-28	225		013:19

FIG. A.2.3 RWR TEST OUTPUT

```
006 EL1   09.1 031 00.0 -28 315      019:58
006 EL1   09.1 031 00.0 -28 315      020:02
006 EL1   09.1 031 00.0 -28 315      020:02
006 EL1   09.1 031 00.0 -28 315      020:06
006 EL1   09.1 031 00.0 -28 315      020:06
006 EL1   09.1 031 00.0 -28 315      020:06
006 EL1   09.1 031 00.0 -28 315      020:09
006 EL1   09.1 031 00.0 -28 315      020:09
006 EL1   09.1 031 00.0 -28 315      020:09
006 EL1   09.1 031 00.0 -28 315      020:09
006 EL1   09.1 031 00.0 -28 315      020:09
006 EL1   09.1 031 00.0 -28 315      020:09
006 EL1   09.1 031 00.0 -28 315      020:09
006 EL1   09.1 031 00.0 -28 315      020:10
006 EL1   09.1 031 00.0 -28 315      020:10
006 EL1   09.1 031 00.0 -28 315      020:10
006 EL1   09.1 031 00.0 -28 315      020:10
006 EL1   09.1 031 00.0 -28 315      020:10
006 EL1   09.1 031 00.0 -28 315      020:10
006 EL1   09.1 031 00.0 -28 315      020:10
006 EL1   09.1 031 00.0 -28 315      020:10
006 EL1   09.1 031 00.0 -28 315      020:10
006 EL1   09.1 031 00.0 -28 315      020:10
006 EL1   09.1 031 00.0 -28 315      020:10
006 EL1   09.1 031 00.0 -28 315      020:10
006 EL1   09.1 031 00.0 -28 315      020:10
006 EL1   09.1 031 00.0 -28 315      020:10
006 EL1   09.1 031 00.0 -28 315      020:10
006 EL1   09.1 031 00.0 -28   0 L    020:10
006 EL1   09.1 031 00.0 -28   0 L    020:10
006 EL1   09.1 031 00.0 -28   0 L    020:10
006 EL1   09.1 031 00.0 -28 135      020:10
006 EL1   09.1 031 00.0 -28 180      020:48
006 EL1   09.1 031 00.0 -28 180      020:48
006 EL1   09.1 031 00.0 -28  45      020:48
006 EL1   09.1 031 00.0 -28 315 L    020:48
006 EL1   09.1 031 00.0 -28 315 L    020:48
006 EL1   09.1 031 00.0 -28  45      020:48
006 EL1   09.1 031 00.0 -28   0      020:48
001 SLO   18.0 061 00.1 -15 315      027:48
001 SLO   18.0 061 00.1 -15 315      027:48
001 SLO   18.0 061 00.1 -15 315      027:48
001 SLO   18.0 061 00.1 -15 315      027:48
001 SLO   18.0 061 00.1 -15 315      027:48
001 SLO   18.0 061 00.1 -15 315      027:48
001 SLO   18.0 061 00.1 -15 315      027:48
001 SLO   18.0 061 00.1 -15 315      027:48
001 SLO   18.0 061 00.1 -15 315      027:49
001 SLO   18.0 061 00.1 -15 315      027:49
```

FIG. A.2.3 RWR TEST OUTPUT

Appendix A.3 TOA algorithms

Simplified representations of the algorithms are given below to describe the principle of operation.

The algorithms operate on a sample of P pulses, stored during a time slice of N sampling intervals. The TOAs of each pulse i is stored in an array TOA(i). In the algorithms using weighting functions each pulse i has an associated weighting, stored in the array WEIGHT(i). The histograms contain pulse counts at each interval I and is stored in the array HIST(I).

The threshold constants are determined by pulse densities and pulse corruption rates. In the algorithms the following constants were used :

thresh1 = 0.5 x

thresh2 = 2.5

thresh3 = 0.8 x

thresh4 = 0.7 x

where x = 1 - P/N

A3.1 SDIF (successive difference histogram)

This algorithm performs histogramming at each difference level combined with the PAIR routine to identify the sequences. The commands contained in square brackets [] are ignored for SDIF1 but are used in SDIF2, where fuzzy logic is used.

```
·DEFPROC sdif
    diff_level = 1
    FOR pulse = 1 TO P
     WEIGHT(pulse)=1
    NEXT pulse
ITERATE: PROC zero histogram
    FOR pulse = 1 TO ( P - diff_level)
      [  IF  WEIGHT(pulse +  diff_level)+WEIGHT(pulse)  <2
                                          THEN NEXT pulse ]
      interval = TOA( pulse + diff_level ) - TOA( pulse )
      HIST( interval ) = HIST( interval ) +1
    NEXT pulse
    FOR interval = 1 TO N/5
       IF HIST( interval ) > thresh1*N/interval THEN
                            PROC pair( interval )
    NEXT interval
    IF radar_found THEN diff_level = diff_level - 1
                   ELSE diff_level = diff_level + 1
    IF pulses_left < diff_level/5 THEN  STOP
                                  ELSE GOTO  ITERATE
ENDPROC
```

PROCEDURE - PAIR (interval)

```
        /   Finds and deletes a pulse sequence
        /   Partial deletion (fuzzy logic ) algorithm uses
commands in square brackets
    DEFPROC pair(interval)
    count = 0 : pulse_A = 1: pulse_B = 2: wtg = 1
      DO UNTIL pulse_B = P
NEXT:  TOA_diff = TOA (pulse_B) - TOA(pulse_A)
       fuzzy = 1
       [ fuzzy = WEIGHT(pulse_B) + WEIGHT(pulse_A) ]
       IF TOA_diff < interval THEN pulse_B = pulse_B + 1
                                          :GOTO NEXT
       IF TOA_diff > interval THEN pulse_A = pulse_A + 1
                                          :wtg = 1: GOTO NEXT
       [ IF fuzzy = 0 THEN pulse_A = pulse_A +  1
                                          :GOTO NEXT ]
       count = count + wtg : wtg = wtg + fuzzy/2
       pulse_A = pulse_B :pulse_B = pulse_B + 1
    DOEND
    IF  count  >   thresh2*N/interval THEN  radar_found
                                  [ PROC weight sequence  = 0]
                                    PROC average sequence DOA

    PROCEND
```

A3.2 ADIF - All differences histogram

```
DEFPROC adif
  PROC zero histogram
  FOR start_pulse = 1 TO P-1
    FOR end_pulse = (start_pulse + 1) TO P
      interval = TOA(end_pulse) - TOA(start_pulse)
    · HIST(interval) = HIST(interval) + 1
    NEXT end_pulse
  NEXT start_pulse
  FOR interval = 1 TO N/5
    IF HIST(interval) > thresh3*N/interval THEN
                                PROC pair(interval)
  NEXT interval
PROCEND
```

A3.3 CDIF - Cumulative difference histogram

```
DEFPROC cdif
        diff_level = 1
ITERATE: FOR pulse = 1 TO (P - diff_lev)
           interval = TOA(pulse + diff_lev) - TOA(pulse)
           HIST(interval) = HIST(interval) + 1
         NEXT pulse
         FOR interval = 1 TO N/5
           IF HIST(interval) > thresh3*N/interval THEN
                                        PROC  PAIR(interval)
         NEXT interval
         diff_lev = diff_lev + 1
         IF pulses_left < diff_lev/5 THEN END
                                        ELSE GOTO ITERATE
      ENDPROC
```

A3.4 SEARCH - no histogramming

```
DEFPROC search
    FOR interval = 1 TO N/5
       DO UNTIL false_alarm
          PROC pair(interval)
       DOEND
       IF pulses_left < 5 THEN END
    NEXT interval
```

A.3.5 CDIF / SEQUENCE

```
DEFPROC cdif
        diff_level = 1
ITERATE:  FOR pulse = 1 TO (P - diff_lev)
            interval = TOA(pulse + diff_lev) - TOA(pulse)
            HIST(interval) = HIST(interval) + 1
          NEXT pulse
          FOR interval = 1 TO N/5
            IF HIST(interval) > thresh4*N/interval THEN
                                        PROC  SEQUENCE(interval)
          NEXT interval
          diff_lev = diff_lev + 1
          IF pulses_left < diff_lev/5 THEN END
                                        ELSE GOTO ITERATE
        ENDPROC

   / Sequence extrapolation incorporating fuzzy logic
   / Based on three pulse projection
  DEFPROC sequence(interval)
    count=0 : pulse_A = 1 : pulse_B = 2 : wtg = 1
FIRST: TOA_diff = TOA(pulse_B) - TOA(pulse_A)
       fuzzy = WEIGHT(pulse_B) + WEIGHT(pulse_A)
       IF pulse_B > P THEN false = 1: END
       IF TOA_diff < interval THEN pulse_B = pulse_B + 1
                                   :GOTO FIRST
       IF TOA_diff > interval THEN pulse_A = pulse_A+1
                              :pulse_B = pulse_B+1:GOTO FIRST
       IF fuzzy = 0 THEN pulse_A = pulse_A+1: GOTO FIRST
```

```
        pulse_C = pulse_B+1: PRI = TOA_diff
SECOND:TOA_diff = TOA(pulse_C) - TOA(pulse_B)
        IF TOA_diff < interval THEN pulse_C = pulse_C + 1
                                        :GOTO SECOND
        IF TOA_diff > interval THEN pulse_A = pulse_A+1
                                :pulse_B = pulse_B+1:GOTO FIRST

        PRI = PRI + TOA_diff : CNT = 2
        pulse_D = pulse_C + 1 : last_TOA = TOA(pulse_C)
SEQUEN:TOA_diff = TOA(pulse_D) - last_TOA
        IF pulse_D > P THEN  GOTO FINISH
        IF TOA_diff < interval THEN pulse_D = pulse_D + 1
                                        :GOTO SEQUEN
        IF   TOA_diff   >   interval   THEN
                  last_TOA = last_TOA+PRI/CNT:GOTO SEQUEN
        PRI = PRI +TOA_diff: CNT=CNT+1 : last_TOA=TOA(pulse_D)
        weighted_cnt = weighted_cnt + WEIGHT(pulse_D)
FINISH:IF weighted_cnt > thresh5*N/interval THEN radar_found
                            PROC weight sequence(0)
                            PROC average DOA
     ENDPROC
```

APPENDIX A.4 Simulator

A.4.1 Signal simulator

Description

ENTRY: Enter radar descriptions -

Radar type (stable/scanning/agile)

DOA, RF frequency, PW, PRI

Edit description

Enter parameter tolerances

Enter pulse corruption rate

Store library on disk

GENERATE: Assign random start times to each radar

Generate pulses according to PRIs

Corrupt pulses randomly

Inject pulses randomly

Output pulse :

TOA, parameters +/- random variation

Store pulse sample on disk

A.4.2. System Simulator

Description

```
        Set initial system state : Time = 0
RPT:    Read Environment simulator input (TOA, parameters)
        Execute each module within the system :
              OUTPUTS = FUNCTION ( INPUTS,OUTPUTS )
        Read module interconnection list
        Update module inputs
        Display selected module :
              INPUT STATES / OUTPUT STATES
        Select option :
               PRINT  Module list / System schematic
               SELECT module for display
        Next time increment
        GOTO RPT
```

A.4.3. Receiver Simulations

Three environments are generated - Scenario 1, 2 and 3. The details of each environment and the detailed simulation results with the RWR, the improved RWR and the ESM receiver are given in this appendix.

A library of radar signals is shown (fig. A.4.1). This library was generated in order to test the RWR described in chapter 5 and includes identical radars from several directions. This is scenario 1

An example of the signal simulator output is shown, (fig A.4.2) the pulses are in TOA order, with their associated parameters with random variations imposed. The map of the simulated radars (fig. A.4.3) shows their positions relative to the receiving system.

System simulator schematics of the two RWR designs are shown in figures A.4.4 and A.4.5.

The results of testing these receivers (RWR1 and RWR2) are shown in figures A.4.6 and A4.7

The system simulator schematic of the ESM receiver is given in figure A.4.8. The results of simulation with scenario 1 is given in figure A4.9.

The radar signals in scenarios 2 and 3 are shown in figure A.4.10. Scenario 2 does not include the high PRF radar number 11.

The results of simulation of the ESM receiver are shown in figures A.4.11 (four samples) and A.4.12 (two samples) for scenarios 2 and 3 respectively.

```
Number of signals  11

 SIGNAL NUMBER      1

Radar type - Normal
Radio frequency     (GHz)      9
Pulse width         (us)       15
Amplitude           (dB)      -20
Direction           (degree)   0
Pulse interval      (us)       200

 SIGNAL NUMBER      2

Radar type - Normal
Radio frequency     (GHz)      9
Pulse width         (us)       15
Amplitude           (dB)      -20
Direction           (degree)   90
Pulse interval      (us)       200

 SIGNAL NUMBER      3

Radar type - Normal
Radio frequency     (GHz)      9
Pulse width         (us)       30
Amplitude           (dB)      -20
Direction           (degree)   0
Pulse interval      (us)       200

 SIGNAL NUMBER      4

Radar type - Normal
Radio frequency     (GHz)      9.3
Pulse width         (us)       15
Amplitude           (dB)      -17
Direction           (degree)   180
Pulse interval      (us)       170

 SIGNAL NUMBER      5

Radar type - Normal
Radio frequency     (GHz)      10
Pulse width         (us)       5
Amplitude           (dB)      -20
Direction           (degree)   270
Pulse interval      (us)       100

 SIGNAL NUMBER      6

Radar type - Normal
Radio frequency     (GHz)      10
Pulse width         (us)       5
Amplitude           (dB)      -20
Direction           (degree)   90
Pulse interval      (us)       100
```

FIG. A.4.1 SIMULATOR SCENARIO 1

SIGNAL NUMBER 7

Radar type - Normal		
Radio frequency	(GHz)	11
Pulse width	(us)	2
Amplitude	(dB)	-20
Direction	(degree)	180
Pulse interval	(us)	170

SIGNAL NUMBER 8

Radar type - Normal		
Radio frequency	(GHz)	11
Pulse width	(us)	2
Amplitude	(dB)	-21
Direction	(degree)	180
Pulse interval	(us)	172

SIGNAL NUMBER 9

Radar type - Normal		
Radio frequency	(GHz)	9.6
Pulse width	(us)	1
Amplitude	(dB)	-20
Direction	(degree)	270
Pulse interval	(us)	100

SIGNAL NUMBER 10

Radar type - Normal		
Radio frequency	(GHz)	9.7
Pulse width	(us)	1
Amplitude	(dB)	-20
Direction	(degree)	270
Pulse interval	(us)	220

SIGNAL NUMBER 11

Radar type - Normal		
Radio frequency	(GHz)	7.5
Pulse width	(us)	.3
Amplitude	(dB)	-18
Direction	(degree)	242
Pulse interval	(us)	260

FIG. A.4.1 SIMULATOR SCENARIO 1

PULSE SIMULATOR OUPUT

Number of pulses 1366

TOA (us)	RFreq(GHz)	Amp(dB)	DOA(deg)	PW(us)
+3.0	+8.0	-10.0	+20.0	+0.9
+10.0	+7.0	+0.0	+0.0	+2.4
+11.0	+10.0	-10.0	+91.0	+5.0
+13.0	+10.0	+0.0	+90.0	+3.4
+18.0	+11.0	+0.0	+181.0	+7.0
+23.0	+8.0	-11.0	+20.0	+1.1
+37.0	+12.0	+0.0	+269.0	+0.9
+40.0	+10.0	-11.0	+178.0	+1.2
+41.0	+7.0	+0.0	+0.0	+1.7
+47.0	+10.0	+0.0	+91.0	+2.3
+50.0	+8.0	-9.0	+20.0	+1.2
+75.0	+7.0	+0.0	+0.0	+1.6
+76.0	+8.0	-9.0	+20.0	+1.2
+81.0	+10.0	+0.0	+90.0	+2.9
+88.0	+7.0	+0.0	+0.0	+1.8
+91.0	+8.0	-9.0	+20.0	+1.0
+93.0	+8.0	-10.0	+20.0	+0.9
+106.0	+10.0	-10.0	+90.0	+4.4
+115.0	+10.0	+0.0	+90.0	+2.5
+129.0	+8.0	-10.0	+20.0	+0.8
+135.0	+7.1	+0.0	+0.0	+1.9
+140.0	+7.0	+0.0	+0.0	+2.2
+146.0	+10.0	-11.0	+181.0	+1.0
+149.0	+8.0	-10.0	+20.0	+1.1
+165.0	+12.1	+0.0	+272.0	+1.1
+182.0	+7.1	+0.0	+0.0	+2.4
+183.0	+8.0	-11.0	+20.0	+1.1
+199.0	+10.0	-10.0	+181.0	+1.2
+201.0	+10.0	-9.0	+90.0	+5.6
+205.0	+7.0	+0.0	+0.0	+2.2
+217.0	+10.0	+0.0	+89.0	+2.9
+224.0	+8.0	-9.0	+20.0	+1.2
+229.0	+7.2	+0.0	+0.0	+1.5
+235.0	+8.0	-10.0	+20.0	+1.0
+251.0	+10.0	+0.0	+89.0	+2.4
+252.0	+10.0	-10.0	+179.0	+1.1
+255.0	+11.0	+0.0	+179.0	+6.0
+265.0	+8.0	-11.0	+20.0	+0.9
+270.0	+7.0	+0.0	+0.0	+1.7
+273.0	+8.0	-11.0	+20.0	+1.1
+276.0	+7.2	+0.0	+0.0	+1.7
+285.0	+10.0	+0.0	+90.0	+2.0
+288.0	+8.0	-10.0	+20.0	+1.2
+293.0	+12.2	+0.0	+270.0	+0.8
+296.0	+10.0	-10.0	+90.0	+5.7
+305.0	+10.0	-10.0	+180.0	+1.2
+319.0	+10.0	+0.0	+91.0	+2.0
+323.0	+7.0	+0.0	+0.0	+2.0
+335.0	+7.0	+0.0	+0.0	+1.9
+341.0	+8.0	-9.0	+20.0	+0.9

FIG. A.4.2 SIGNAL SIMULATOR SAMPLE

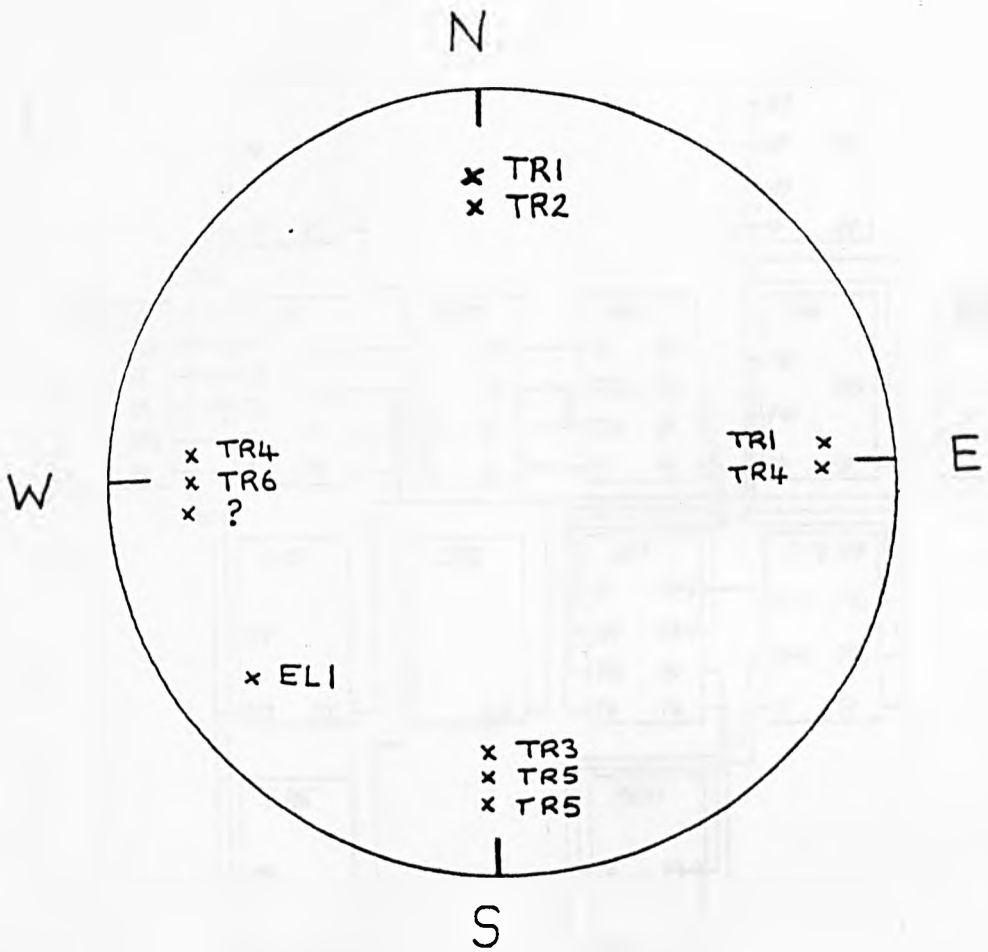

FIG. A.4.3 SIMULATED RADAR MAP

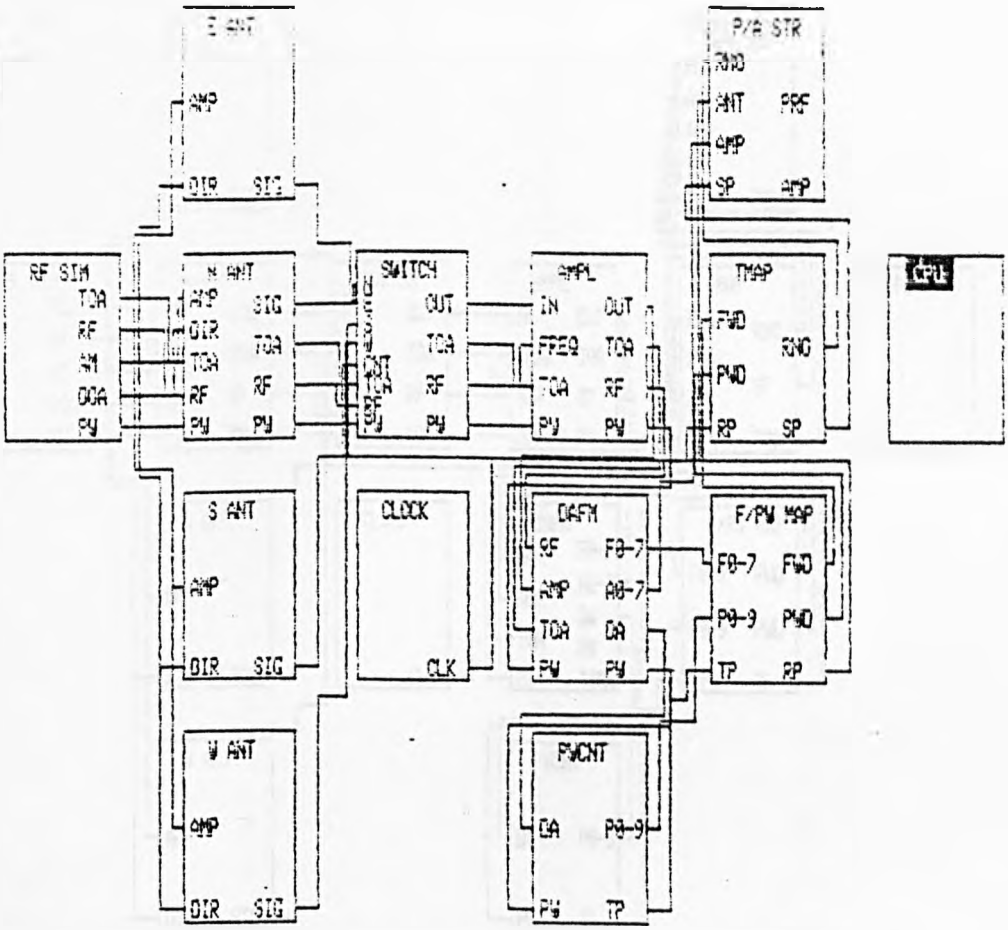

FIG. A.4.4 SIMULATOR SCHEMATIC OF RWR1

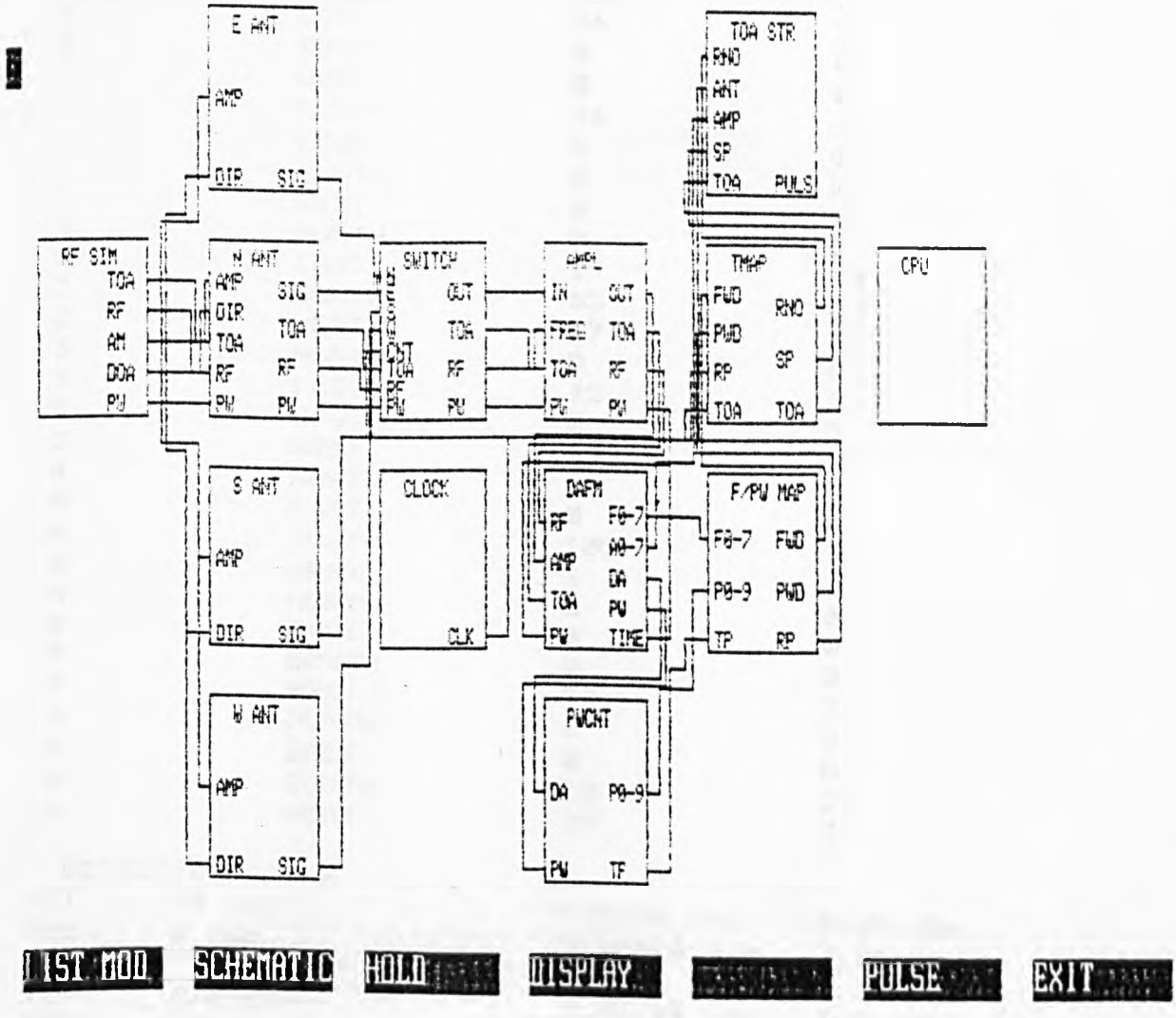

FIG. A.4.5 SIMULATOR SCHEMATIC OF RWR2

RADAR	ANTENNA	PULSES	AMPLITUDE
0	NORTH	45	31
0	EAST	36	26
0	SOUTH	0	0
0	WEST	0	0
1	NORTH	36	31
1	EAST	0	0
1	SOUTH	0	0
1	WEST	0	0
2	NORTH	0	0
2	EAST	19	13
2	SOUTH	55	33
2	WEST	17	12
3	NORTH	0	0
3	EAST	72	30
3	SOUTH	0	0
3	WEST	69	32
4	NORTH	0	0
4	EAST	0	0
4	SOUTH	102	29
4	WEST	1	16
5	NORTH	0	0
5	EAST	0	0
5	SOUTH	0	0
5	WEST	29	31
6	NORTH	0	0
6	EAST	0	0
6	SOUTH	30	21
6	WEST	29	31

DETECTED RADARS

TR1	45 deg.	4.5009 kHz	-4.25 dBm	
TR2	0 deg.	3.60072 kHz	-4.25 dBm	
TR3	180 deg.	5.5011 kHz	-2.75 dBm	
TR4	270 deg.	7.20144 kHz	-3.5 dBm	
TR5	180 deg.	10.20204 kHz	-5.75 dBm	Locked
EL1	225 deg.	3.0006 kHz	-11.75 dBm	

FIG. A.4.6 SIMULATOR OUTPUT FOR RWR1

```
SUCCESSIVE DIFF


THE DETECTED RADARS WERE -
 200          us Amplitude -6    Antenna N    RADAR  0     TR1
 200          us Amplitude -7    Antenna N    RADAR  1     TR2
 200          us Amplitude -6    Antenna E    RADAR  0     TR1
 100          us Amplitude -6    Antenna E    RADAR  3     TR4
 170          us Amplitude -3    Antenna S    RADAR  2     TR3
 170          us Amplitude -6    Antenna S    RADAR  4     TR5
 180          us Amplitude -7    Antenna S    RADAR  4     TR5
 260          us Amplitude -13   Antenna S    RADAR  6     EL1
 100          us Amplitude -6    Antenna W    RADAR  3     TR4
 230          us Amplitude -6    Antenna W    RADAR  5     TR6
 530          us Amplitude -6    Antenna W    RADAR  6     EL1

 6837     INSTRUCTIONS REQUIRED
 1000     SAMPLES WITH    10    us  SAMPLE SIZE
 186  PULSES ORIGINALLY  : 9  PULSES REMAINING
 SIMULATION TIME  40000  us
Antenna W

 0              200  us  -6  dBm  NE        TR1
 1              200  us  -7  dBm  N         TR2
 3              100  us  -6  dBm  E         TR4
 2              170  us  -3  dBm  S         TR3
 4              170  us  -6  dBm  S         TR5
 4              180  us  -7  dBm  S         TR5
 6              260  us  -13  dBm  S        EL1
 3              100  us  -6  dBm  W         TR4
 5              230  us  -6  dBm  W         TR6
 6              530  us  -6  dBm  W         EL1
```

FIG. A.4.7 SIMULATOR OUTPUT FOR RWR2

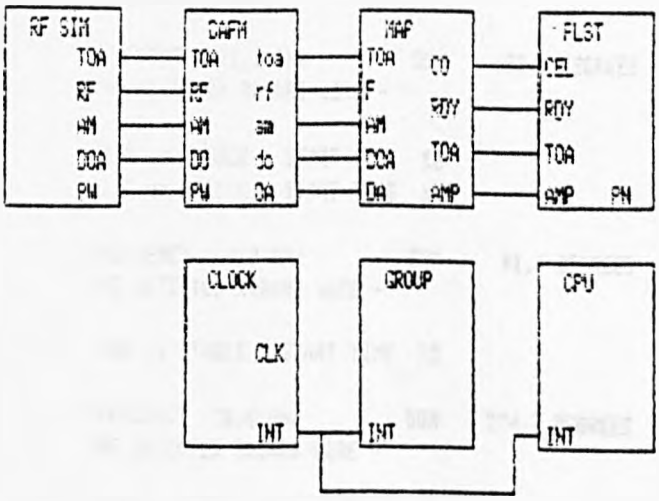

FIG. A.4.8 SIMULATOR SCHEMATIC OF ESM

```
SIMULATION OF ENVIRONMENT 9:RFRIN          08-20-1987
PULSE SORTING PROCESSOR

SUCCESSIVE DIFF

FREQUENCY  11.0 GHz        DOA    182.9 DEGREES
THE DETECTED RADARS WERE -

 170 us STABLE   START TIME  59
 172 us STABLE   START TIME  6

FREQUENCY   9.0 GHz        DOA     91.4 DEGREES
THE DETECTED RADARS WERE -

 200 us STABLE   START TIME  23

FREQUENCY  10.0 GHz        DOA    274.3 DEGREES
THE DETECTED RADARS WERE -

 100 us STABLE   START TIME  39

FREQUENCY   9.0 GHz        DOA      0.0 DEGREES
THE DETECTED RADARS WERE -

 200 us STABLE   START TIME  89
 198 us STABLE   START TIME  65

FREQUENCY   9.3 GHz        DOA    182.9 DEGREES
THE DETECTED RADARS WERE -

 170 us STABLE   START TIME  38

FREQUENCY  10.0 GHz        DOA     91.4 DEGREES
THE DETECTED RADARS WERE -

 200 us STABLE   START TIME  123

FREQUENCY   7.5 GHz        DOA    240.0 DEGREES
THE DETECTED RADARS WERE -

 260 us SCAN   START TIME  6

FREQUENCY   9.7 GHz        DOA    268.6 DEGREES
THE DETECTED RADARS WERE -

 440 us STABLE   START TIME  283


 1561    INSTS. REQUIRED  FOR CLUSTERING
 32295  INSTS. REQUIRED FOR TOA DEINTERLEAVING
 30  INSTS. REQUIRED FOR FREQ. AGILE SORTING
 5000    SAMPLES WITH   1   us  SAMPLE SIZE
 318  PULSES AVAILABLE       201  PULSES MEASURED  :
 SIMULATION TIME  5001  us
```

FIG. A.4.9 SIMULATOR OUTPUT FOR ESM (1)

```
Number of signals  11

 SIGNAL NUMBER      1

Radar type - NORMAL
Radio frequency    (GHz)    7
Pulse width        (us)     2
Amplitude          (dB)     0
Direction          (degree) 0
Pulse interval     (us)     65

 SIGNAL NUMBER      2

Radar type - FREQ. AGILE
Radio frequency    (GHz)    7
Max.freq.      (GHz)  7.2
No. of steps       5
Pulse width        (us)     2
Amplitude          (dB)     0
Direction          (degree) 0
Pulse interval     (us)     47

 SIGNAL NUMBER      3

Radar type - NORMAL
Radio frequency    (GHz)    8
Pulse width        (us)     1
Amplitude          (dB)    -10
Direction          (degree) 20
Pulse interval     (us)     53

 SIGNAL NUMBER      4

Radar type - STAGGERED
Stagger level    (%)  30
No. of stagger posns.    3
Radio frequency    (GHz)    8
Pulse width        (us)     1
Amplitude          (dB)     0
Direction          (degree) 20
Pulse interval     (us)     194

 SIGNAL NUMBER      5

Radar type - JITTERED
Jitter level    (%)  15
Radio frequency    (GHz)    8
Pulse width        (us)     1
Amplitude          (dB)     0
Direction          (degree) 20
Pulse interval     (us)     88

 SIGNAL NUMBER      6

Radar type - NORMAL
Radio frequency    (GHz)    10
Pulse width        (us)     3
Amplitude          (dB)     0
Direction          (degree) 90
Pulse interval     (us)     34
```

FIG. A.4.10 SIMULATOR SCENARIO 2 AND 3

Radar type - SCANNING
Scan time (secs) 20
Radio frequency (GHz) 13
Pulse width (us) 5
Amplitude (dB) -10
Direction (degree) 90
Pulse interval (us) 95

SIGNAL NUMBER 8

Radar type - NORMAL
Radio frequency (GHz) 10
Pulse width (us) 1
Amplitude (dB) -10
Direction (degree) 180
Pulse interval (us) 53

SIGNAL NUMBER 9

Radar type - NORMAL
Radio frequency (GHz) 11
Pulse width (us) 3
Amplitude (dB) 0
Direction (degree) 180
Pulse interval (us) 227

SIGNAL NUMBER 10

Radar type - FREQ. AGILE
Radio frequency (GHz) 12
Max.freq. (GHz) 12.2
No. of steps 2
Pulse width (us) 1
Amplitude (dB) 0
Direction (degree) 270
Pulse interval (us) 123

SIGNAL NUMBER 11

Radar type - NORMAL
Radio frequency (GHz) 9.5
Pulse width (us) 1
Amplitude (dB) 0
Direction (degree) 74
Pulse interval (us) 10.5

```
SIMULATION OF ENVIRONMENT B:RFR3          04-17-1987
PULSE SORTING PROCESSOR

SUCCESSIVE DIFF

FREQUENCY  10.0 GHz         DOA    132.9 DEGREES
THE DETECTED RADARS WERE -

 53 us STABLE   START TIME  19

FREQUENCY  10.0 GHz         DOA     91.4 DEGREES
THE DETECTED RADARS WERE -

 34 us STABLE   START TIME  10
 95 us SCAN   START TIME  25

FREQUENCY   7.1 GHz         DOA      0.0 DEGREES
THE DETECTED RADARS WERE -

 65 us STABLE   START TIME  18
 47 us STABLE   FREQ. AGILE  2 STEPS      START TIME  37
FREQUENCY   8.0 GHz         DOA     22.9 DEGREES
THE DETECTED RADARS WERE -

 53 us STABLE   START TIME  41
 194 us STAGGER    3  POSITION           START TIME  3
 194 us STAGGER    3  POSITION           START TIME  132
 194 us STAGGER    3  POSITION           START TIME  87
 86 us JITTERED    17  % LEVEL           START TIME  26

FREQUENCY   7.2 GHz         DOA      0.0 DEGREES
THE DETECTED RADARS WERE -

FREQUENCY  12.1 GHz         DOA    268.6 DEGREES
THE DETECTED RADARS WERE -

 128 us STABLE   FREQ. AGILE  2 STEPS     START TIME  84


 1897    INSTS. REQUIRED  FOR CLUSTERING
 43939  INSTS. REQUIRED FOR TOA DEINTERLEAVING
 4603  INSTS. REQUIRED FOR FREQ. AGILE SORTING
 2500    SAMPLES WITH   1   us  SAMPLE SIZE
 344  PULSES AVAILABLE       277  PULSES MEASURED  :
 SIMULATION TIME  2501  us
```

FIG. A.4.11 SIMULATOR OUTPUT FOR ESM (2)

```
SIMULATION OF ENVIRONMENT B:RFR3          04-17-1987
PULSE SORTING PROCESSOR

SUCCESSIVE DIFF

FREQUENCY  10.0 GHz        DOA    182.9 DEGREES
THE DETECTED RADARS WERE -

 53 us STABLE   START TIME  10

FREQUENCY  10.0 GHz        DOA     91.4 DEGREES
THE DETECTED RADARS WERE -

 34 us STABLE   START TIME  26

FREQUENCY   7.1 GHz        DOA      0.0 DEGREES
THE DETECTED RADARS WERE -

 65 us STABLE   START TIME  53
 47 us STABLE   START TIME  28

FREQUENCY   8.0 GHz        DOA     22.9 DEGREES
THE DETECTED RADARS WERE -

 53 us STABLE   START TIME  32
 194 us STAGGER    3  POSITION          START TIME  25
 194 us STAGGER    3  POSITION          START TIME  109
 194 us STAGGER    3  POSITION          START TIME  154
 87 us JITTERED    17  % LEVEL          START TIME  47

FREQUENCY   7.1 GHz        DOA      0.0 DEGREES
THE DETECTED RADARS WERE -

FREQUENCY  12.1 GHz        DOA    268.6 DEGREES
THE DETECTED RADARS WERE -

 128 us STABLE   START TIME  16

FREQUENCY  11.0 GHz        DOA    182.9 DEGREES
THE DETECTED RADARS WERE -

 237 us STABLE   START TIME  136


 1224    INSTS. REQUIRED  FOR CLUSTERING
 21473  INSTS. REQUIRED FOR TOA DEINTERLEAVING
 15  INSTS. REQUIRED FOR FREQ. AGILE SORTING
 2500    SAMPLES WITH   1   us  SAMPLE SIZE
 682  PULSES AVAILABLE      287  PULSES MEASURED  :
 SIMULATION TIME  5001  us
```

```
SIMULATION OF ENVIRONMENT 9:RFR3          04-17-1987
PULSE SORTING PROCESSOR

SUCCESSIVE DIFF

FREQUENCY  10.0 GHz          DOA    182.9 DEGREES
THE DETECTED RADARS WERE -

 53 us STABLE   START TIME  1

FREQUENCY  10.0 GHz          DOA     91.4 DEGREES
THE DETECTED RADARS WERE -

 34 us STABLE   START TIME  9

FREQUENCY   7.1 GHz          DOA      0.0 DEGREES
THE DETECTED RADARS WERE -

 65 us STABLE   START TIME  23
 47 us STABLE   START TIME  19

FREQUENCY   8.0 GHz          DOA     22.9 DEGREES
THE DETECTED RADARS WERE -

 53 us STABLE   START TIME  23
 194 us STAGGER    2  POSITION          START TIME  47
 194 us STAGGER    2  POSITION          START TIME  176
 170 us JITTERED    18  % LEVEL         START TIME  155

FREQUENCY   7.1 GHz          DOA      0.0 DEGREES
THE DETECTED RADARS WERE -

FREQUENCY  12.1 GHz          DOA    274.3 DEGREES
THE DETECTED RADARS WERE -

 128 us STABLE   START TIME  76

FREQUENCY  11.0 GHz          DOA    182.9 DEGREES
THE DETECTED RADARS WERE -

 237 us STABLE   START TIME  6


 1171    INSTS. REQUIRED  FOR CLUSTERING
 15939  INSTS. REQUIRED FOR TOA DEINTERLEAVING
 55  INSTS. REQUIRED FOR FREQ. AGILE SORTING
 2500    SAMPLES WITH   1   us  SAMPLE SIZE
 1820  PULSES AVAILABLE      275  PULSES MEASURED  :
 SIMULATION TIME  7501  us
```

```
SIMULATION OF ENVIRONMENT 3:RFR3          04-17-1987
PULSE SORTING PROCESSOR

SUCCESSIVE DIFF

FREQUENCY  10.0 GHz         DOA    182.9 DEGREES
THE DETECTED RADARS WERE -

 53 us STABLE   START TIME  45

FREQUENCY  10.0 GHz         DOA     91.4 DEGREES
THE DETECTED RADARS WERE -

 34 us STABLE   START TIME  24

FREQUENCY   7.1 GHz         DOA      0.0 DEGREES
THE DETECTED RADARS WERE -

 65 us STABLE   START TIME  58
 47 us STABLE   START TIME  10

FREQUENCY   8.0 GHz         DOA     22.9 DEGREES
THE DETECTED RADARS WERE -

 53 us STABLE   START TIME  14
 194 us STAGGER    2  POSITION          START TIME  153
 194 us STAGGER    2  POSITION          START TIME  4
 98 us JITTERED    18  % LEVEL          START TIME  40

FREQUENCY   7.1 GHz         DOA      0.0 DEGREES
THE DETECTED RADARS WERE -

FREQUENCY  12.1 GHz         DOA    274.3 DEGREES
THE DETECTED RADARS WERE -

 128 us SCAN   START TIME  8

FREQUENCY  11.0 GHz         DOA    182.9 DEGREES
THE DETECTED RADARS WERE -

 237 us STABLE   START TIME  113


 1164    INSTS. REQUIRED  FOR CLUSTERING
 18288  INSTS. REQUIRED FOR TOA DEINTERLEAVING
 60  INSTS. REQUIRED FOR FREQ. AGILE SORTING
 2500    SAMPLES WITH   1   us  SAMPLE SIZE
 1356  PULSES AVAILABLE      283  PULSES MEASURED  :
 SIMULATION TIME  10001  us
```

```
SIMULATION OF ENVIRONMENT 8:RFR4          07-19-1987
PULSE SORTING PROCESSOR

SUCCESSIVE DIFF

FREQUENCY  10.0 GHz          DOA     91.4 DEGREES
THE DETECTED RADARS WERE -

 34 us STABLE   START TIME  12
 190 us STABLE   START TIME  42

FREQUENCY   9.5 GHz          DOA     74.3 DEGREES
THE DETECTED RADARS WERE -

 11 us STABLE   START TIME  6

FREQUENCY   8.0 GHz          DOA     22.9 DEGREES
THE DETECTED RADARS WERE -

 53 us STABLE   START TIME  17
 194 us STAGGER    2  POSITION            START TIME  113
 194 us STAGGER    2  POSITION            START TIME  58

FREQUENCY   7.1 GHz          DOA      0.0 DEGREES
THE DETECTED RADARS WERE -

 65 us STABLE   START TIME  14
 47 us STABLE   FREQ. AGILE  2 STEPS      START TIME  85
FREQUENCY  10.0 GHz          DOA    182.9 DEGREES
THE DETECTED RADARS WERE -

 53 us STABLE   START TIME  45

FREQUENCY   7.2 GHz          DOA      0.0 DEGREES
THE DETECTED RADARS WERE -

FREQUENCY  11.0 GHz          DOA    182.9 DEGREES
THE DETECTED RADARS WERE -

 237 us STABLE   START TIME  29

FREQUENCY  12.1 GHz          DOA    268.6 DEGREES
THE DETECTED RADARS WERE -

 129 us SCAN   FREQ. AGILE  2 STEPS      START TIME  11


 2651    INSTS. REQUIRED  FOR CLUSTERING
 42412  INSTS. REQUIRED FOR TOA DEINTERLEAVING
 6674  INSTS. REQUIRED FOR FREQ. AGILE SORTING
 2530    SAMPLES WITH   1   us  SAMPLE SIZE
 539  PULSES AVAILABLE       407  PULSES MEASURED  :
 SIMULATION TIME  2501  us
```

FIG. A.4.12 SIMULATOR OUTPUT FOR ESM (3)

```
SIMULATION OF ENVIRONMENT B:RFR4          07-19-1987
PULSE SORTING PROCESSOR

SUCCESSIVE DIFF

FREQUENCY  10.3 GHz          DOA     91.4 DEGREES
THE DETECTED RADARS WERE -

 34 us STABLE   START TIME  28

FREQUENCY   9.5 GHz          DOA     74.3 DEGREES
THE DETECTED RADARS WERE -

 11 us STABLE   START TIME  3

FREQUENCY   8.0 GHz          DOA     22.9 DEGREES
THE DETECTED RADARS WERE -

 53 us STABLE   START TIME  8
 194 us STAGGER    3  POSITION          START TIME  135
 194 us STAGGER    3  POSITION          START TIME  6
 194 us STAGGER    3  POSITION          START TIME  90
 87 us JITTERED    17  % LEVEL          START TIME  38

FREQUENCY   7.1 GHz          DOA      0.0 DEGREES
THE DETECTED RADARS WERE -

 65 us STABLE   START TIME  49
 47 us STABLE   START TIME  29

FREQUENCY  10.0 GHz          DOA    182.9 DEGREES
THE DETECTED RADARS WERE -

 53 us STABLE   START TIME  36

FREQUENCY   7.1 GHz          DOA      3.3 DEGREES
THE DETECTED RADARS WERE -


 1718    INSTS. REQUIRED  FOR CLUSTERING
 23566  INSTS. REQUIRED FOR TOA DEINTERLEAVING
 74  INSTS. REQUIRED FOR FREQ. AGILE SORTING
 2500    SAMPLES WITH   1   us  SAMPLE SIZE
 1069  PULSES AVAILABLE      437  PULSES MEASURED  :
 SIMULATION TIME  5001  us
```

REFERENCES

[1] P.M.GRANT and PROF.J.H.COLLINS :"Introduction to Electronic Warfare ", IEE Proc.F, Communications Radar and Signal Proc., 1982, vol. 129(3), pp 113-131.

[2] W.C.BAKER :"ESM systems applications ", IEE Proc. F, Communications, Radar and Signal Proc., 1985, vol 132(4), pp 206-211

[3] C.KONIG :"ELINT design melds classic methods", Microwaves and RF, Sept 1984, pp 150-155

[4] R.BOWMAN :"Channelised integrating ESM receivers using a Bragg cell", IEE Proc. F, Comms. Radar and Signal Proc., 1985, 132(4), pp275-279

[5] R.McLENDON and C.TURNER :"Broadband sensors for lethal defense suppression", Microwave Journal, Sept 1983, pp 85-94

[6] J.P.Y.LEE :"Detection of complex and simultaneous signals using an IFM", IEE Proc. F, Comms. Radar and Signal Proc., 1985, 132(4), pp 267-274

[7] P.W.EAST :"Design techniques and performance of the digital IFM ", IEE Proc. F,Comms. Radar and Signal Proc.,June 1982, pp154 -163

[8] R.G.WILEY :" Electronic intelligence: The interception of radar signals", Artech house, 1985, pp 87

[9] A.G.SELF and B.G.SMITH :"Intercept time and its prediction", IEE Proc. F, Comms. Radar and Signal Proc., 1985, 132(4), pp 215-222

[10] D.K.BARTON :"Radar Systems Analysis ", Artech House, 1976, pp 111,199

[11] R.G.WILEY :" Electronic intelligence: The analysis of radar signals", Artech house, 1985

[12] A.MUNDAY and R.FARRAR :"An engineering data book",Macmilan press, 1979, pp 30

[13] S.STEIN and D.JOHANSEN :"A statistical description of coincidences among random pulse trains", IRE Proc., 1958, pp827-830

[14] C.L.DAVIES and P.HOLLANDS :"Automatic processing for ESM", IEE Proc. F, Comms. Radar and Signal Proc., 1982, 129(3), pp164-171

[15] J.A.V.ROGERS :"ESM processor system for high pulse density radar environments", IEE Proc. F, Comms. Radar and Signal Proc., 1985, 132(7), pp621-624

[16] A.K.JAIN :"Pattern recognition", Chapter 3, pp74-86

[17] R.E.LONG :"Advanced EW processing ", 12th annual journal of Old Crows, 1975, pp35-48

[18] R.S.ANDREWS :"ESM processing using 3D memory mapping and adaptive pattern formation algorithms", Military Microwaves Transactions, 1984, pp 27-36

[19] D.R.WILKINSON and A.W.WATSON :"Use of metric techniques in ESM data processing", IEE Proc F, Comms. Radar and Signal Proc., 1985, 132(4), pp 229-232.

[20] J.W.CAMPBELL and S.SAPERSTEIN :"Signal recognition in complex radar environments", Watkins-Johnson Tech-notes, Nov/Dec 1976, vol. 3 no.6.

[21] R.G.WILEY :"Electronic intelligence: The analysis of radar signals ", Artech house, 1982, pp 156-160

[22] P.HOLLANDS :"Use of simulation as a design tool ", IEE Proc. F, Comms. Radar and Signal Proc., 1985, 132(4), pp 292-297

[23] "International Countermeasures Handbook", 11th edition, 1986, Wiseman, pp76, pp306-312